

CHALMERS



Grouting in the Nygård Tunnel: Pre-Grouting Design for Drip Sealing and Evaluation

CHRISTIAN BUTRON
GUNNAR GUSTAFSON
JOHAN FUNEHAG

Department of Civil and Environmental Engineering
Division of GeoEngineering
Engineering Geology Research Group
CHALMERS UNIVERSITY OF TECHNOLOGY
Göteborg, Sweden, 2008
Report No. 2008:2

Report No. 2008:2

Grouting in the Nygård Tunnel:
Pre-Grouting Design for Drip Sealing
and Evaluation

CHRISTIAN BUTRON
GUNNAR GUSTAFSON
JOHAN FUNEHAG

Department of Civil and Environmental Engineering
Division of GeoEngineering
Engineering Geology Research Group
CHALMERS UNIVERSITY OF TECHNOLOGY
GÖTEBORG, SWEDEN, 2008

Grouting in the Nygård Tunnel
Pre-Grouting Design for Drip Sealing and Evaluation
CHRISTIAN JUVENAL BUTRON PERICON
GUNNAR GUSTAFSON
JOHAN FUNEHAG

©CHRISTIAN BUTRON, GUNNAR GUSTAFSON, JOHAN FUNEHAG 2008

Publ. 2008:2
ISSN 1652-9162

Department of Civil and Environmental Engineering
Division of GeoEngineering and Geology
Engineering Geology Research Group
Chalmers University of Technology
SE-412 96 Göteborg
Phone: +46(0)31-772 10 000

Chalmers Reproservice
Göteborg, 2008

PREFACE

I would like to express my thanks to Banverket for financing this field study, especially Lars Jonsson and Behnam Shahriari for their assistance and comments, and Lemcom for their cooperation as contractors.

The design, implementation and evaluation presented in this report have been carried out in Nygård and at Chalmers University of Technology during 2007 under the supervision of Professor Gunnar Gustafson and with help of Johan Funehag.

I am grateful for comments and help given by Åsa Fransson during the progress of this report. I would also wish to express my appreciation to Roger Tjärnlund and Marianne Lindström for their help in the field.

Göteborg, January, 2008.

Christian Butrón

SUMMARY

In underground constructions, ground water control is an important aspect to consider, it consists of much more than just pumping water and sealing leaks. Ground water seepage can be harmful for a tunnel structure or the equipment inside it. Therefore, preparation on potential problems is essential. This study deals with a pre-grouting design in order to avoid dripping of water from the ceiling.

The Nygård tunnel is a railway tunnel located in the south part of Sweden. Approximately 3 km long, this tunnel will connect two communities Nygård and Håltorp, it consists of one main tunnel and one service tunnel. The tunnel is located between 40 to 50 m below ground surface.

The project started with a rock mass characterisation from where the number of fractures per 3 meter section and the transmissivity for the same sections were obtained. With the use of these data, the hydraulic apertures of the fractures were estimated and a Pareto-distribution curve was fitted, and the hydraulic apertures of the fractures were established. At the end, the inflows to the tunnel were estimated. Based on the leakage demands a hydraulic aperture of 0,1 mm was needed to be seal.

The grouting design of this tunnel was based on two different materials, which have different properties and aims. The base and the walls of the tunnel were grouted with cement to reduce the leakage and meet the leakage demands, and the ceiling with silica sol to minimize the dripping. This design has the advantage to use cheap materials and if the target is achieved totally, lining and the use of impermeable membranes could be avoided.

The design was used in 86 m of the tunnel and 5 fans where successfully pre-grouted. Previous data from 4 drilled core-boreholes suggested that the transmissivity was approximately $1.2 \cdot 10^{-6} \text{ m}^2/\text{s}$. Based on log-normal distribution curves, the results after pre-grouting showed a decrease of the leakage where the sum of all median transmissivity values from all 5 fans was reduced to $4.2 \cdot 10^{-7} \text{ m}^2/\text{s}$. Taken into consideration just the ceiling of the tunnel, it is concluded that dripping was minimized in great extent and in the most difficult part of the project the inflow was reduced to 0.06 l/min.

Some other findings made were: water pressure tests conducted in all grout-holes were representative within a radius of 4 m. The volume taken by a grout-hole is very much dependent of the flow system. A generalization of the flow system can not be done, but it can be determined from water pressure tests. The disadvantage found was that the analysis of one parameter, e.g. inflow, is not enough to evaluate the results obtained and several need to be coupled making data availability an important factor.

TABLE OF CONTENTS

PREFACE.....	i
SUMMARY.....	ii
TABLE OF CONTENTS.....	iii
TABLE OF APPENDICES.....	iv
NOMENCLATURE.....	v
1. INTRODUCTION.....	1
1.1. Aims.....	1
1.2. The Nygård Tunnel.....	2
2. MATERIALS.....	5
2.1. Cement based suspensions.....	5
2.2. Silica sol.....	5
3. METHOD.....	7
3.1. Grouting design.....	7
3.1.2. <i>Pre-investigations</i>	7
3.1.3. <i>Fracture transmissivity distribution and fracture aperture distribution</i>	8
3.1.4. <i>Grouting Agent</i>	8
3.1.5. <i>Penetration distribution</i>	9
3.1.6. <i>Leakage calculation compared with the demands</i>	10
3.2. Grouting Pressure.....	10
3.3. Grouting layout.....	10
3.4. Stop criteria.....	10
3.5. Connectivity radius.....	11
3.6. Dimensionality.....	11
4. RESULTS.....	13
4.1. Grouting agent.....	13
4.1.1. <i>Rheology of the cementitious grout</i>	13
4.1.2. <i>Rheology of the non-cementitious grout (silica sol)</i>	14
4.2. Grouting Design.....	14
4.3. Inflow.....	15
4.4. Transmissivity.....	17
4.5. Volume grouted.....	18
4.6. Connectivity radius.....	19
4.7. Dimensionality.....	20
4.8. Dripping.....	22
5. DISCUSSION.....	23
5.1. Grouting design.....	23
5.2. Inflow and dimensionality.....	23
5.3. Transmissivity and dripping after pre-grouting.....	24
5.4. Volume.....	25
5.5. Connectivity radius.....	25
5.6. Compilation.....	26
6. CONCLUSIONS.....	29
7. REFERENCES.....	31
8. APPENDIX.....	33

TABLE OF APPENDICES

APPENDIX A: Grouting design for the Nygård tunnel

APPENDIX B: Scatter chart, from every grouted fan, which compares the WPTs results obtained from grout-holes before grouting and control-holes after grouting.

APPENDIX C: Column charts, from every grouted fan, which compares the grout-hole volume and the injected grout volume; it also shows the difference in volume.

APPENDIX D: Grouted-holes charts showing the pressure and flow trend over time, accumulated volume trend over injected time and, dimension curves.

APPENDIX E: Fracture mapping of sections 436+723 – 436+637.

APPENDIX F: Drains location in sections 436+723 to 436+637.

NOMENCLATURE

A	[m ²]	area
b	[m]	hydraulic aperture
d	[m]	diameter
g	[m/s ²]	earth acceleration, 9.81 m/s ²
H	[m]	tunnel depth
h	[m]	hydraulic head
l	[m]	penetration length
i	[-]	gradient
K	[m/s]	hydraulic conductivity
k	[-]	distribution coefficient (Pareto analysis)
L	[m]	length
N	[-]	number of fractures
n	[-]	porosity
p	[N/m ²]	pressure
Δp	[N/m ²]	applied pressure
q	[m ³ /s·100 m]	flow per 100 m
Q	[m ³ /s]	flow
Q/dh	[m ² /s]	specific capacity
r_t	[m]	tunnel radius
T	[m ² /s]	transmissivity
t	[s]	time
V	[m ³]	volume
v	[m/s]	velocity
W	[m]	width

Greek letters

γ_w	[kg/s ² m ²]	heaviness of water
ξ	[-]	skin factor
η	[N·s/m ²]	shear rate dependent viscosity
μ	[N·s/m ² , Pas]	viscosity
ρ	[kg/m ³]	density
τ	[N/m ²]	shear stress
τ_o	[N/m ²]	yield strength
π	[-]	pi, 3.1415
σ_1	[N/m ²]	axial stress
σ_3	[N/m ²]	radial stress
ω	[radians/s]	angular velocity

1. INTRODUCTION

Ground water control in underground excavations consists of much more than just pumping water and sealing leaks. All detrimental effects that seepage of water can have on a tunnel structure and the equipment in it can be very expensive. Whether the objective is waterproofing, reducing the inflow, or dealing with high water pressures a planned strategy is required (Jones, 2006).

Tunnels that need a high restriction of water ingress are usually complemented with lining and the use of impermeable membranes in order to stop the leakage. These membranes are placed behind the shotcrete after a corresponding localization of water leakages into the tunnel. The use of this procedure is common nowadays but it is expensive on costs and on time (Funehag, 2007). Further, water dripping from the ceiling should always be minimized, so the pre-grouting design could be focused on this purpose.

Pre-grouting in rock consists on filling faults, joints and bedding planes that usually are completely unknown in size, volume, and configuration. The reason and the extent are influenced by the origin, age and stress history of the rock where the tunnel is built (Warner, 2004). Hence, the importance of preparations and testing that will be used not only in the design but also in the evaluation of the project.

Cement based suspensions have been used widely in grouting purposes during this last decade in major tunnel projects around the world (Stuart, 2003), silica sol has been used recently in some tunnels as a rock grouting material. The Törnskog tunnel in Sweden is one of them where silica sol was used with the objective to permeate and seal small fractures in jointed hard rock. The advantage to use these materials, as a pre-grouting strategy, is that the objective of minimizing the seepage can be achieved and the costs reduced.

86 m of the Nygård tunnel, section 436+723 – 436+637, followed the design, work procedure, and evaluation. This tunnel section was divided in 5 sections “Fans” of 24 m each with 9 m of overlap between fans. In each section 40 grout-holes were drilled, tested, and then grouted, see Figure 9. A secondary 10 grout-holes were drilled and tested; these were used as control holes. All the grout-hole results were used for the evaluation. In general, the design takes into account: which stop criteria should be used, penetration length, gelling time based on the material and rock mass characteristics. An introductory study on dripping and post-excavation grouting was conducted as a separate project by Granberg and Knutsson (2007).

1.1. Aims

The aim of this study is to implement a pre-grouting design that will reduce the water inflow into the tunnel from walls and base, and minimize the dripping from the ceiling to avoid problems when seepage is persistent in underground excavations.

The specific aims are:

- Gather data from pre-investigation tests and data after grouting from control-holes,
- Characterise the rock mass by means of hydrogeological methods,
- Characterise the grouting agents to be used,
- Suggest a pre-grouting procedure and layout,
- Evaluate and discuss the results obtained by means of: inflow, transmissivity, volume, correlation length, and dimensionality.

1.2 The Nygård Tunnel

The Nygård tunnel, which is a railway tunnel, is located in the western part of Sweden. Approximately 3 km long, this tunnel will connect Nygård and Hältorp and is part of the Norway-Vänern line under construction. It consists of one main tunnel and one service tunnel. The main tunnel will be 3030 m long and the service tunnel 2380 m long. The main tunnel will be 10.2 m high and 13.5 m wide, on the other hand the service tunnel will be 6 m high and 5 m wide. The tunnel is located between 40 and 50 m below the ground surface. The rock type in the excavation area is mainly gneiss, see Figure 1a. Some small fractions of amphibolite were also found, see Figure 1b.

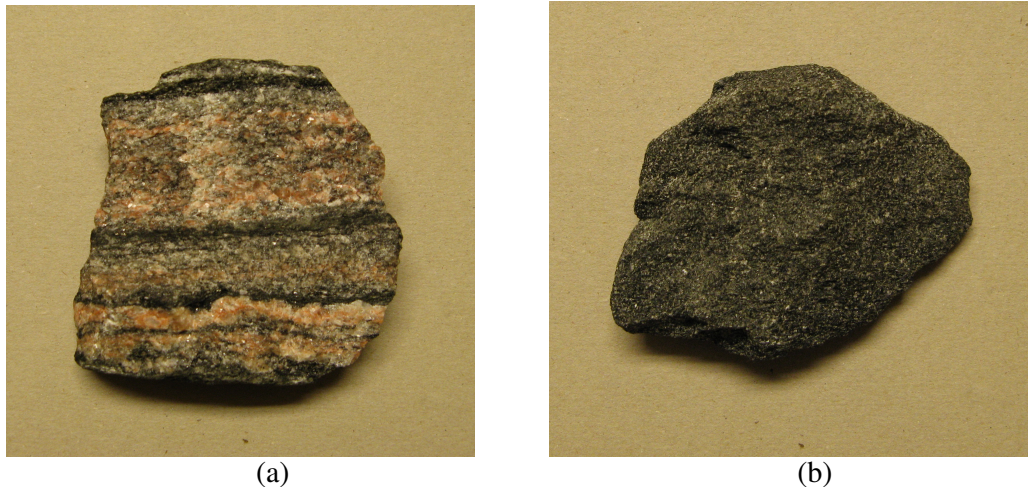


Figure 1. Two main rock types found in the Nygård the tunnel, rock specimens were taken from inside the tunnel. (a) gneiss; (b) amphibolite.

Before the incorporation of the new design, the grouting of the tunnel has been carried out following the layout shown in Figure 2. The tunnel has been completely grouted with a cement-based suspension, sealing in general the major rock fractures. The grout-hole separation was 1,5 m in the ceiling and 2 m in the walls and bottom of the tunnel. The leakage was reduced but dripping remains, which was the reason for this study.

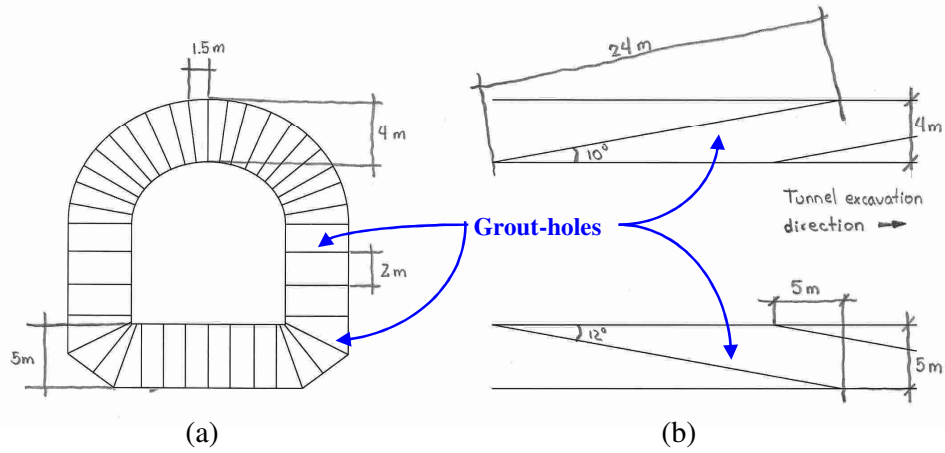


Figure 2. Initial layout of the grouting conducted in the main tunnel; take into account that it will differ when rock conditions are changed: a) Frontal-cut view of the tunnel; b) Side-cut view of the tunnel.

The new design employs the same grouting-layout in all five fans, but the grouting material is changed. The grout-holes are numbered starting at the bottom-left side of the tunnel and continue clockwise. The same figure, Figure 3, shows the separation line assumed to represent the dripping limit. Whereas the upper part produces dripping into the tunnel, the lower part does not. This assumption sets the boundary where to use different grouting materials, see Figure 3.

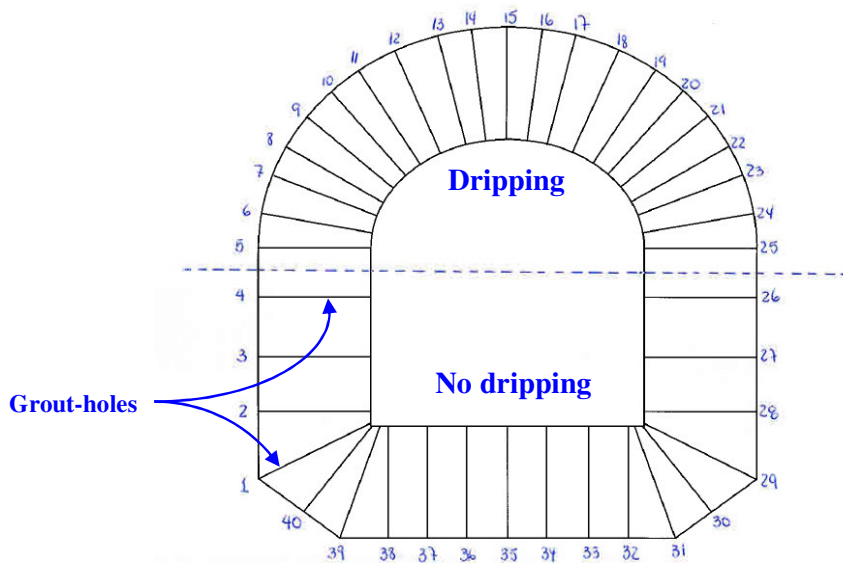


Figure 3. Layout of the grout-holes position for all five fans. The dotted line represents the separation between dripping and no dripping.

2. MATERIALS

2.1. Cement based suspensions

A grout material may be made of Portland cement. In this study one of the grouts used was Injektering 30; it is a micro-cement, sulphate resistant, chromate reduced and has low alkalinity. It was manufactured at Cementa's Degerhamn plant. The most important properties are fineness of grinding and grain size distribution. The upper range of the grain size distribution is responsible for the penetrability of joints and pores, and to pass the channels between them (Kutzner, 1996) and (Eklund, 2003). On the other hand, the fineness of the grinding affects the strength of the grouting after hardening.

Injektering 30 has a particle size distribution where 95% of the material is smaller than 30 μm in particle size. A compact density of 3100 to 3200 kg/m^3 approximately and a bulk density going from 800 to 1500 kg/m^3 (Cementa, 2007).

Injektering 30 (Inj 30) was mixed with regular water and a superplasticizer "SetControl II". SetControl II is an additive, which was used to regulate the setting time and disperse the suspension. It has a fluid form, a density equal to 1476 kg/m^3 and the pH value is approximately six.

Cementitious grouts are characterised as non-Newtonian viscoplastic fluids. The viscosity is not constant, and the fluid will not flow until its yield stress is reached (Axelsson, 2006). In order to express the relationship between the shear rate and the shear stress a Bingham model was used.

2.2. Silica sol

Colloidal silica (silica sol) consists of nanometre-sized particles of amorphous SiO_2 cores with hydroxylated surface. The size can vary from 1 to 500 nm (Björnström, 2005). It is odourless, tasteless, and non-toxic.

The silica sol used in this study has the name "Meyco MP320T" and was manufactured by Eka Chemical AB. It was mixed with a saline solution (NaCl) in order to start a particle aggregation, which at the end hardened as a gel. The mixed silica sol has a fluid form, a density equal to 1200 kg/m^3 and the pH value is approximately 10.

Funehag (2007) characterised silica sol as a Newtonian fluid before gelling. In this model, the viscosity is constant, independent of the shear rate and the fluid will start to flow immediately after a stress is applied.

3. METHOD

3.1. Grouting design

In order to have a more structured design and analysis, the outline presented by Gustafson et al. (2004) was followed. In Figure 4 the steps of the design approach used in this project are illustrated. An example can be found in Funehag and Gustafson (2007) where nine fans were grouted following this approach.

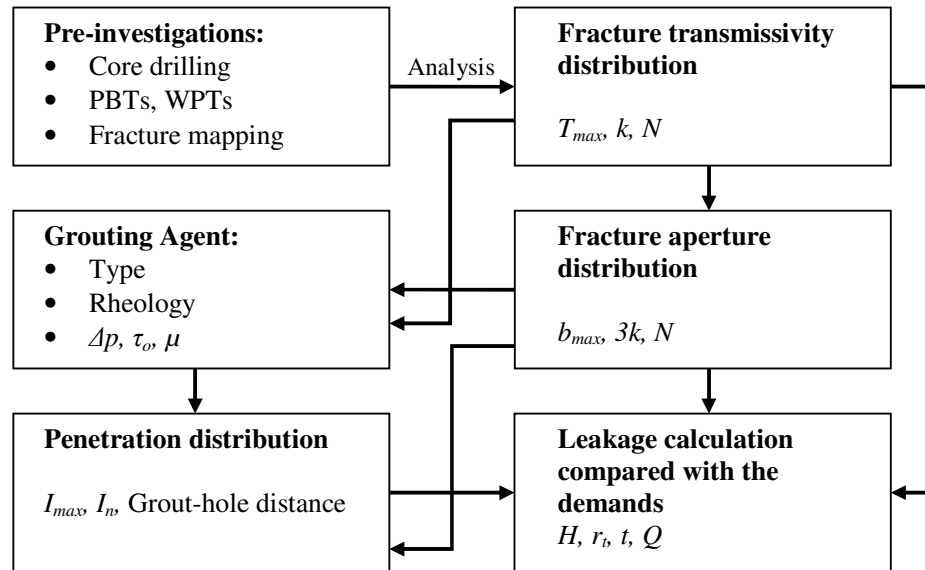


Figure 4. Grouting design process approach (after Gustafson et al., 2004)

3.1.2. Pre-investigations

This study initially involved a data collection. The data gathered included documentation from the project, and results from pressure build-up tests (PBTs). PBTs were conducted in core-drilled boreholes, which by the use of packers were divided into several sections each one 3 m long. During test, water was pressed into the joints and the volume, pressure, and time were registered. Water pressure tests (WPTs) consisted on pressing water in a grout-hole during 2 min at 1.1 MPa of constant over-pressure; they were carried out in each grout-hole before grouting in order to identify connected-holes and tight holes. PBT and WPT procedures are well described by Houlsby (1990) and Kutzner (1996) among others.

Four cored-boreholes (KBH 1 to 4) were made along the tunnel line and a complete core mapping was performed in each core. The specific capacity (Q/dh) was evaluated from the data, which can be approximated to the transmissivity during short time duration tests (Fransson, 2001).

3.1.3. Fracture transmissivity distribution and fracture aperture distribution

Palmqvist (1983) stated that discontinuities in rocks are decisive for grouting results, for this reason these are studied in order to characterize the rock mass for a grouting design purpose. Gustafson and Fransson (2006) found in their study that the transmissivities obtained in the pre-investigation stage fitted a Pareto distribution.

Equation 1 gives the Pareto distribution based on the maximum fracture transmissivity value (T_{max}) to determine the probability that a transmissivity is below a certain transmissivity (T_n). N represents the total number of fractures.

$$P(T_n) = P[T < T_n] = 1 - \frac{(T_{max}/T_n)^k}{N + 1} \quad (1)$$

Rearranging and taking the log of Equation 1, it gives:

$$\log[1 - P(T_n)] = \log\left[\frac{T_{max}^k}{(N + 1)}\right] - k \log(T_n) \quad (2)$$

The Pareto distribution is then recognised as a straight line in a log-log plot. This line has a slope $-k$ (coefficient of the distribution) which was used to evaluate the hydraulic aperture distribution. The cubic law gave the hydraulic aperture of the fracture; see Equation 3.

$$b = \sqrt[3]{T \cdot \frac{12 \cdot \mu_w}{\rho_w \cdot g}} = C \cdot T^{1/3} \quad (3)$$

By ranking the hydraulic aperture, Equation 4 is obtained:

$$b_r = b_{max} / r^{1/3 \cdot k} \quad (4)$$

The last equation uses b_{max} , which was the largest hydraulic aperture that corresponds to the highest transmissivity previously observed. Using PBT results from KBH 1 – 4 a plot with the hydraulic distribution was then obtained, see appendix A.

3.1.4. Grouting Agent

There are two main groups when considering grouting materials, cementitious and non-cementitious. The selection of a material much depends on the aims of the project; in this study, the grouting agents were chosen in order to: reduce the water inflow into the tunnel from the walls and floor, and minimize the dripping from the ceiling

Once the type of grout matched the purposes or degree of sealing needed, its rheology was investigated. Rheology is defined as the science of deformation and flow (Barnes et al., 1998), and it is the rheology of the material which governs its flow property and consequently its penetration. Parameters like yield stress (τ_o) and viscosity (μ) were obtained from the two types of grouting materials selected in the Nygård tunnel, cement and silica sol. The rheology is one among several characteristics more that are important and they can be explored in Axelsson (2006).

Cup tests were used to determine the gelling time of silica sol. Tests were conducted with normal plastic cups with a volume of around 200 ml. A mixed solution of around 100 ml, silica sol and saline solution, was poured into the cup. The time was recorded as soon as both solutions were mixed until the silica sol had gelled. The gelling time was then obtained when the silica sol front did not move or bend any longer after turning the cup 90°, see Figure 5.

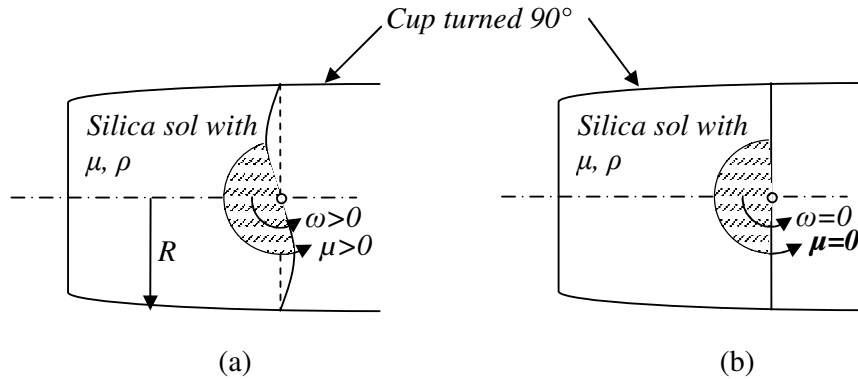


Figure 5. Cup test representation. (a) Silica sol soon to be gelled; (b) Gelled silica sol.

3.1.5. Penetration distribution

The penetration of a Bingham fluid into a fracture is related to the applied pressure Δp , difference of the injection pressure and the groundwater pressure, and the yield strength of the grout (Gustafson and Stille, 2005). Equation 5 gives the expression of the maximum penetration length of cement grout in a fracture with a hydraulic aperture b :

$$I_{\max} = \left(\frac{\Delta p}{2\tau_o}\right) \cdot b \quad (5)$$

The grout penetration of a Newtonian grout is linked to the gel induction time (t_G), the grouting applied pressure (Δp), and its initial viscosity (μ_o). Equation 6 gives the expression of the maximum penetration length of silica sol in a fracture with a hydraulic aperture b in 1D:

$$I_G = b \cdot \sqrt{\frac{\Delta p \cdot t_G}{6 \cdot \mu_o}} \quad (6)$$

Equation 7 can then give the maximum penetration length when using a Newtonian fluid in 2D:

$$I_{\max} = 0.45 \cdot I_G \quad (7)$$

3.1.6. Leakage calculation compared with the demands

An analysis of the data was done and the non-groutable fracture distribution was determined. This data could then be used in Equation 8 to calculate the water inflow to the tunnel before and after grouting (Alberts and Gustafson, 1983). The calculations are associated with the following assumption: The groundwater level is close to the surface, and no substantial lowering of the water table is caused.

$$q_{grouted} \approx \frac{2 \cdot \pi \cdot T_{tot} \cdot (H / L)}{\ln(2 \cdot H / r_t) + (T_{tot} / T_{inj} - 1) \cdot \ln(1 + t / r_t) + \xi} \quad (8)$$

3.2. Grouting Pressure

For a long penetration of grouting into the rock mass through the fractures, it was advantageous to use high pressures, but is difficult to control the spread of it. On the contrary, low pressures give shorter penetrations but more controlled ones. A reasonable estimation is given by Gustafson and Stille (1996): Use a pressure that is twice as high as the groundwater pressure (approximately 0.5 MPa), but below the minimum rock stress (approximately 3.5 MPa) which is assumed to be equal to the vertical stress due to the overburden. In this study, when using high pressures, it was important to take into consideration the thickness of the rock cover and the strength of the rock in order to avoid problems like jacking.

3.3. Grouting layout

The grouting layout and type of grout depend on the purpose of the project. Due to an initial layout or geometry was already in use, the following parameters were taken as input data:

- Number of grout-holes: 40 grout-holes
- Grout-hole length: 24 m
- Grout-hole inclination: 10° upper part (ceiling) and 12° lower part (walls and floor)
- Distance between grout-holes: 1.5 m upper part (ceiling) and 2 m lower part (walls and floor)
- Distance between grouting sections “fans”: 20 m
- Overlap between fans: 5 m

Using all the above, parameters like pumping pressure, pumping time, overlap between grout-holes, and mixing ratios among others were calculated in order to fulfil the demands and specification of the project, see Chapter 1.

3.4. Stop criteria

Commonly the expression “stop pressure” is used as a parameter to end the injection of grout in a grout-hole. In principle there is no stop pressure (Gustafson and Stille, 2005); if the pumping pressure is increased, the grout will be further spread. Instead, the stop criteria used in this project was the “grouting time” predetermined in the grouting design in order to accomplish the purpose of grouting. Gustafson and Stille (2005) give an example on how to use a predetermined grouting time in order to calculate a needed penetration length when grouting with cement, and Funehag (2007) gives an example when grouting with silica sol.

3.5. Connectivity radius

The rate of change in specific capacity (Q/dh) along a specific orientation was obtained with the use of the semi-variogram. Larsson and Zetterlund (2004) used a variogram analysis to predict the radius of influence of control-holes. Following the same method, a variogram was established for all the grout-holes and control-holes in the Nygård project and a spherical model was fitted. Figure 6 shows the coordinates of each grout-hole in Fan 1. The software used was Surfer version 8.01. The model used logarithmic values of the transmissivities and the hole coordinates as input data.

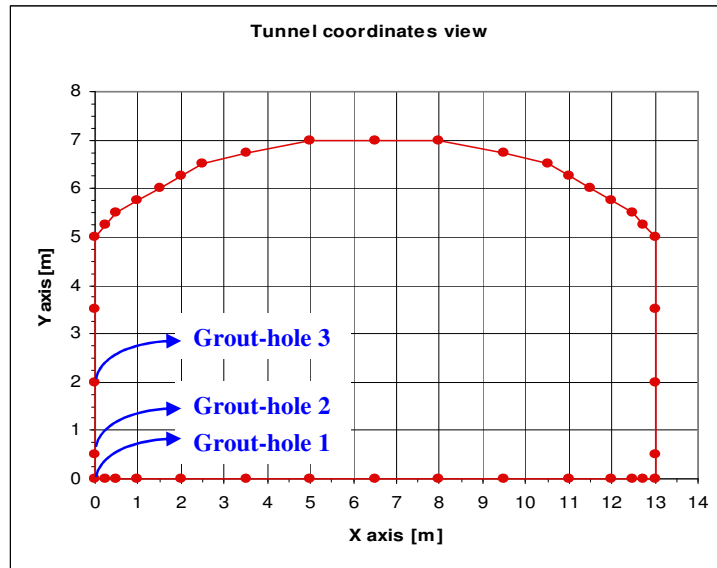


Figure 6. Grout-hole coordinates used in Fan 1 for a variogram analysis. The dots represent grout-holes; they are numbered clockwise.

3.6. Dimensionality

The fracture system during grouting was investigated by a dimensionality analysis. Gustafson and Stille (2005) developed an equation that can be used to diagnose the flow regime when volume, pressure and time (VPT) recordings during grouting are taken. Equation 9 gives the relation between injected time, flow, and volume:

$$\frac{d \log V}{d \log t} = \frac{Q \cdot t}{V} \quad (9)$$

As it was shown by Gustafson and Stille (2005), the logarithmic slopes can be calculated as a function of a relative time t_d and plotted in a log-normal plot. The following table shows the assumed slope values, flow regime, and its denotation. These curves can be used for silica sol and cement grouts.

Table 1. Slope value and flow regime denotation.

Slope (approximate value)	Flow regime	Denotes
0.45	1D	Channelled fracture system
0.8	2D	Planar fractures
1	3D	Network of interconnected planar fractures and/or channels

4. RESULTS

Five tunnel sections, each 24 metres long, were grouted with the designed grouting layout, which is well explained in Appendix A. WPTs were carried out before grouting in each grout-hole and after grouting in each control-hole. Due to the measurement limit of the equipment, all results obtained from WPTs that were equal to 0 l/min, before and after grouting, were assumed to be 0.1 l/min. A theoretical groutable bore-hole volume of 74 l was assumed based on a bore-hole diameter of 0.064 m and length of 23 m.

4.1. Grouting agent

Cement based suspensions can penetrate and seal fractures that are bigger than approximately 0.1 mm; silica sol on the other hand can penetrate and seal those fractures smaller than 0.1 mm which can cause the problem of dripping in tunnels. Based on the hydraulic aperture distribution, in the Nygård tunnel 99 % of the fractures had a hydraulic aperture smaller than 0.1 mm, see Appendix A. Therefore, there was a need to come up with a design that had the combined characteristics of cement and silica sol.

4.1.1. Rheology of the cementitious grout

The shear stress development is shown in Figure 7. The w/c-ratios are defined as 0.8, 1.0 or 1.5 parts of water per 1 part of cement measured by volume. The tests were performed at 20 °C and 10 min after mixing. The initial yield strengths obtained are identified in the figure below; they were used for grouting design purposes. A common shear rate 50 [1/s] was used for the evaluation.

- w/c 0.8:1 an initial yield strength of 2.5 Pa
- w/c 1:1 an initial yield strength of 1 Pa
- w/c 1.5:1 an initial yield strength of 0.5 Pa

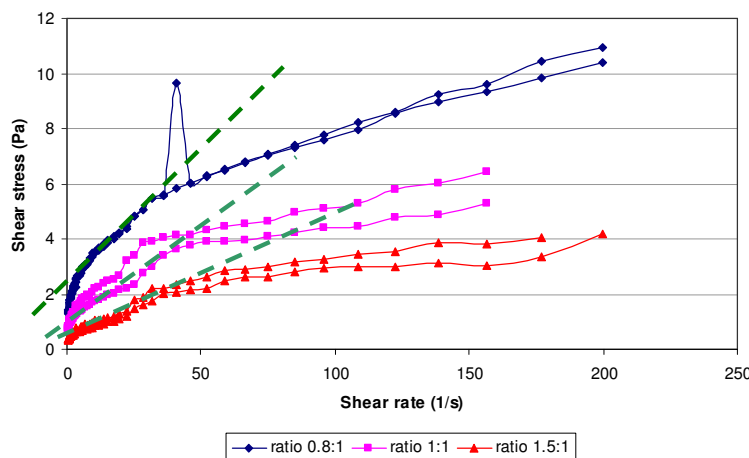


Figure 7. Normalised shear stress development over shear rate; three mixed cement based suspensions at different ratios where measured. Trend lines intersecting the shear stress gives the initial yield stress of the suspension.

4.1.2. Rheology of the non-cementitious grout (silica sol)

Viscosity is defined as the fluid's resistance to flow due to inner friction and is generally temperature dependent. The viscosity development for three mixed solutions is shown in Figure 8. The ratio is defined as 4, 5 or 6 parts of silica sol per 1 part of saline solution measured by weight. The tests were conducted at 15° C. The initial viscosity and gel induction time values obtained from such tests were used for grouting design purposes.

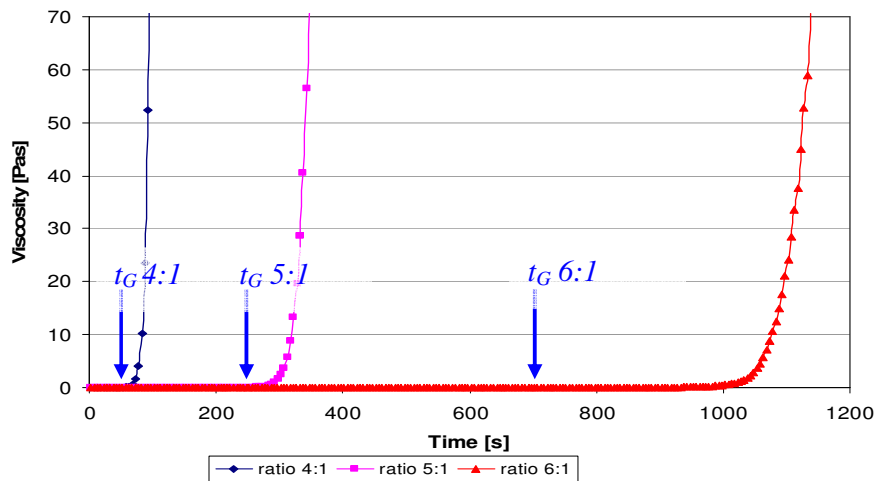


Figure 8. Normalised viscosity development over time; three mixed solutions at different ratios where measured; the tests started one minute after mixing.

Cup tests, described in Chapter 3.1.4, were used to determine the gelling time. The gel induction time (t_G) of the solution is another parameter used in the design and can be determined by the same test. The gelling times and gel induction times obtained for the different mixes were:

- Ratio 4:1 a gelling time of 180 s, and a t_G around 60 s
- Ratio 5:1 a gelling time of 720 s, and a t_G around 240 s
- Ratio 6:1 a gelling time of 2100 s, and a t_G around 700 s

4.2. Grouting Design

Appendix A presents the complete grouting design process for the Nygård tunnel, which followed the design steps described in Chapter 3.1. Below follows, a short summary of the grouting layout and parameters suggested to be used during grouting. Figure 9 shows the designed grouting layout. The dotted line in Figure 9a represents the separation of grout used; the upper part (ceiling) of the tunnel was grouted with silica sol, and the lower part (walls and floor) was grouted with cement.

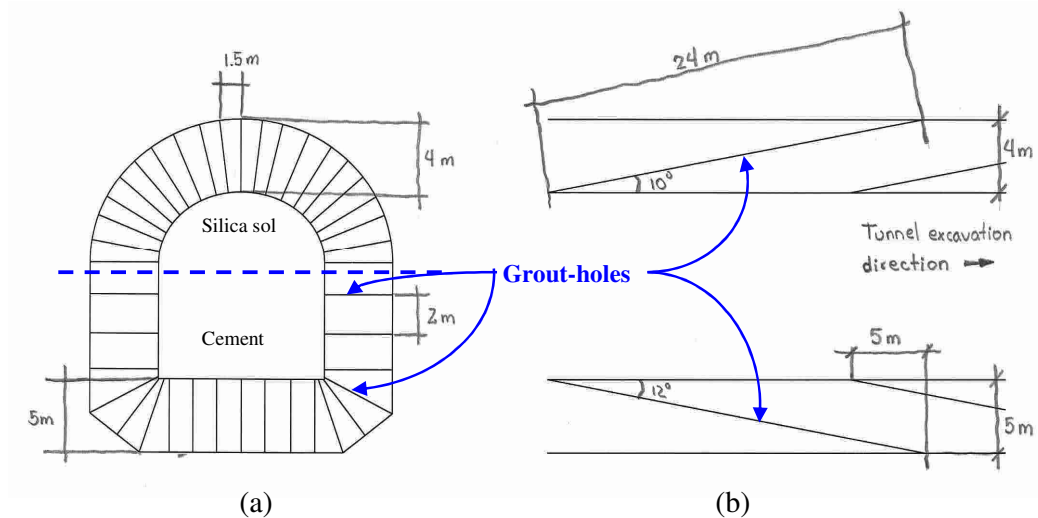


Figure 9. Designed grouting layout: (a) frontal-cut view of the layout, the dotted line represents the separation of the grout type used; (b) side-cut view of the tunnel.

Table 2 shows the protocol suggested to be followed during grouting. Note that the gelling time in the protocol is 40 min (silica sol to salt ratio 4:1), which was obtained in situ following the same mixing procedure as in the laboratory, 5 min higher than in the laboratory. The temperature in situ was around 10 °C, which is 5 °C less than in the laboratory.

Table 2. Summary of the grouting protocol for each one of the grouted fans. This protocol was used in each grout-hole. For the control-holes the same procedure was used, but the location was decided in situ.

Silica sol	Cement
<ul style="list-style-type: none"> • b: 14μm • Gelling time: 40 min • 20 boreholes • 1,5 m spacing • Pumping time: 21 min each borehole at designed pressure • Δp: 2.5 MPa • p_w: 0.5 MPa 	<ul style="list-style-type: none"> • b: 0,1 mm • $\tau_o > 1.5$ Pa • 20 boreholes • 2,0 m spacing • Pumping time: 25 min each borehole at designed pressure • Δp: 2.5 MPa • p_w: 0.5 MPa

4.3. Inflow

An example of the results obtained from WPTs conducted in grout-holes and control-holes in Fan 3 are given in Figure 10. The values are given as cumulative distribution and a log-normal plot is fitted to the same grout-holes value. This fitted curves show a median value of 0.4 l/min before pre-grouting. After pre-grouting a log-normal plot was not fitted to the control-holes value due to the majority of the inflow-values were lower than the measurement limit and the log-normal fit was influenced in great extent by these values. In appendix B, all five fans are presented with the same format.

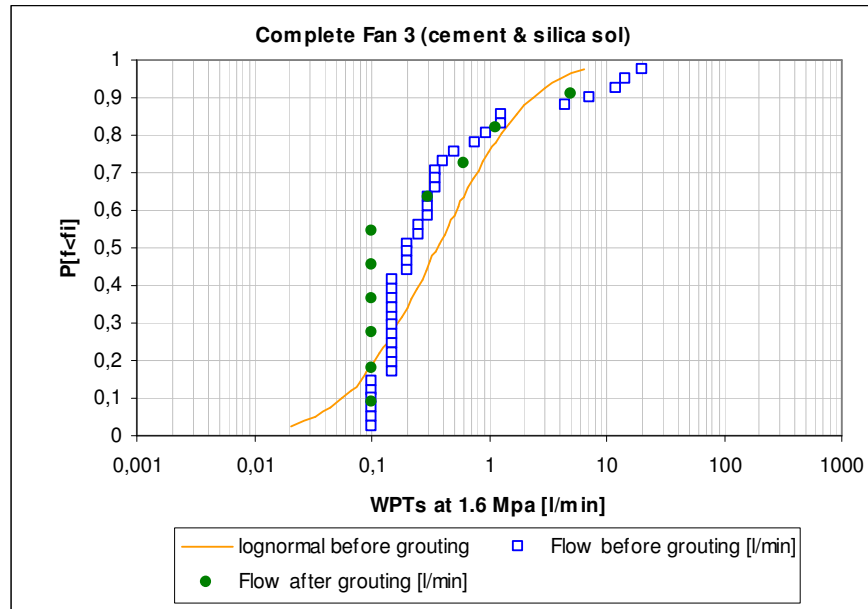


Figure 10. Comparison of WPTs results obtained from grout-holes before grouting and control-holes after grouting with 1.6 MPa in total pressure (0.5 MPa in water pressure).

Figure 11 shows WPTs results divided by grout used in Fan 3. Figure 11a shows the results of the cement part and Figure 11b shows the results from the silica sol part. Before pre-grouting, the median inflow-value of the fitted-plot for the cement part is 0.6 l/min and for the silica sol part is 0.2 l/min. In appendix B all five fans are presented.

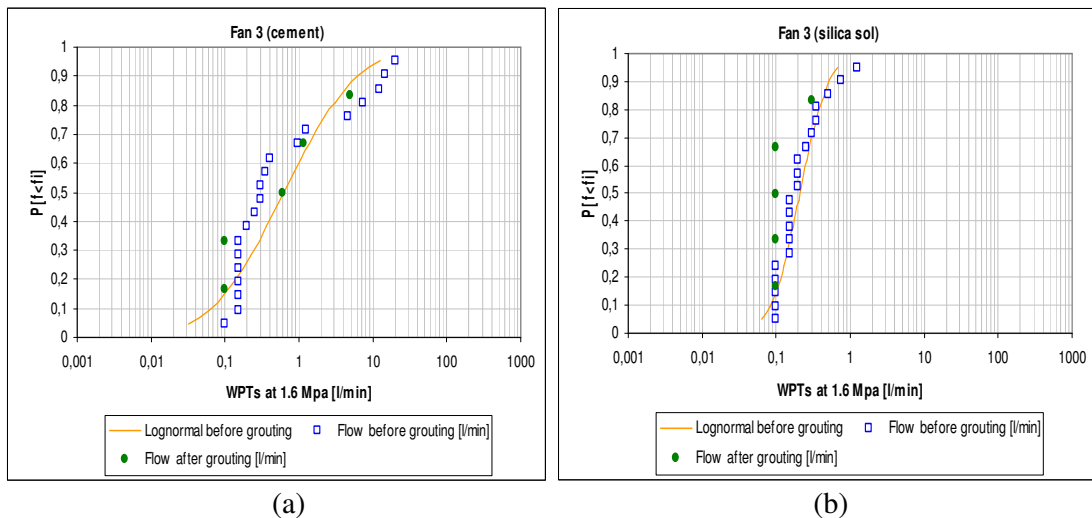


Figure 11. Comparison of WPTs results obtained from grout-holes and control-holes with 1.6 MPa in total pressure (0.5 MPa in water pressure). (a) cement part; (b) silica sol part.

In Table 3 a summary of the interpreted median and average values from the log-normal plots are shown. These values are calculated from WPTs conducted before and after pre-grouting in all five fans. The inflow-values after pre-grouting are assumed to be 0.1 l/min when more than 50 % of the values were lower than the measurement limit. If more than 50 % of all values are higher than 0.1 l/min then a maximum inflow is assumed, i.e. the inflow before grouting. This criterion is based on a pessimistic or risk-averse decision. The type of grout used is also given and the ratios are calculated as the median and average value obtained before grouting divided by the median and average value obtained after grouting from the fitted log-normal distribution plots.

Table 3. Summary of results obtained from WPTs conducted on grout-holes and control-holes. The median and average values from all five fans are presented. The ratio is calculated as the median or average value before grouting divided by the median or average value after grouting.

Fan	Grout used	Average [l/min]		Median [l/min]		Ratio [-]	
		before grouting	after grouting	before grouting	after grouting	Average	Median
1	Both	0.6	0.6	0.4	0.4	1	1
1	Cement	0.4	0.4	0.3	0.3	1	1
1	Silica sol	0.9	0.9	0.6	0.6	1	1
2	Both	2.4	0.1	1	0.1	24	10
2	Cement	1.9	0.1	1	0.1	19	10
2	Silica sol	2.6	0.1	1.1	0.1	26	11
3	Both	0.8	0.1	0.4	0.1	8	4
3	Cement	1.8	1.8	0.6	0.6	1	1
3	Silica sol	0.3	0.1	0.2	0.1	3	2
4	Both	0.5	0.5	0.2	0.2	1	1
4	Cement	0.4	0.4	0.2	0.2	1	1
4	Silica sol	0.4	0.4	0.2	0.2	1	1
5	Both	2.3	0.1	0.6	0.1	23	6
5	Cement	0.7	0.1	0.3	0.1	7	3
5	Silica sol	3.8	0.1	1.4	0.1	38	14

4.4. Transmissivity

In Chapter 3.1.2 was explained that the specific capacity (Q/dh) can be approximated to the transmissivity during short time duration tests. Assuming that the water table is stable above the tunnel, it gives a natural water pressure of 0.5 MPa. The WPTs were conducted with a total pressure of 1.6 MPa giving an applied over-pressure of 1.1 MPa.

Using all these parameters, the local transmissivity can be calculated. If we divide this transmissivity by the length of each fan then the hydraulic conductivity can be evaluated. Table 4 shows the calculated transmissivity and hydraulic conductivity for each fan before and after grouting using the median inflow values shown in Table 3.

Table 4. Transmissivity and hydraulic conductivity values for each fan before and after grouting using the median inflow values.

Fan	Grout used	Median [l/min]		Transmissivity [m^2/s]		Hydraulic conductivity [m/s]	
		before grouting	after grouting	before grouting	after grouting	before grouting	after grouting
1	Both	0.4	0.4	$6.5 \cdot 10^{-08}$	$6.5 \cdot 10^{-08}$	$2.7 \cdot 10^{-09}$	$3.0 \cdot 10^{-09}$
1	Cement	0.3	0.3	$4.9 \cdot 10^{-08}$	$4.9 \cdot 10^{-08}$	$2.0 \cdot 10^{-09}$	$2.2 \cdot 10^{-09}$
1	Silica sol	0.6	0.6	$9.8 \cdot 10^{-08}$	$9.8 \cdot 10^{-08}$	$4.1 \cdot 10^{-09}$	$4.5 \cdot 10^{-09}$
2	Both	1	0.1	$1.6 \cdot 10^{-07}$	$1.6 \cdot 10^{-08}$	$6.8 \cdot 10^{-09}$	$7.4 \cdot 10^{-10}$
2	Cement	1	0.1	$1.6 \cdot 10^{-07}$	$1.6 \cdot 10^{-08}$	$6.8 \cdot 10^{-09}$	$7.4 \cdot 10^{-10}$
2	Silica sol	1.1	0.1	$1.8 \cdot 10^{-07}$	$1.6 \cdot 10^{-08}$	$7.5 \cdot 10^{-09}$	$7.4 \cdot 10^{-10}$
3	Both	0.4	0.1	$6.5 \cdot 10^{-08}$	$1.6 \cdot 10^{-08}$	$2.7 \cdot 10^{-09}$	$7.4 \cdot 10^{-10}$
3	Cement	0.6	0.6	$9.8 \cdot 10^{-08}$	$9.8 \cdot 10^{-08}$	$4.1 \cdot 10^{-09}$	$4.5 \cdot 10^{-09}$
3	Silica sol	0.2	0.1	$3.3 \cdot 10^{-08}$	$1.6 \cdot 10^{-08}$	$1.4 \cdot 10^{-09}$	$7.4 \cdot 10^{-10}$
4	Both	0.2	0.2	$3.3 \cdot 10^{-08}$	$3.3 \cdot 10^{-08}$	$1.4 \cdot 10^{-09}$	$1.5 \cdot 10^{-09}$
4	Cement	0.2	0.2	$3.3 \cdot 10^{-08}$	$3.3 \cdot 10^{-08}$	$1.4 \cdot 10^{-09}$	$1.5 \cdot 10^{-09}$
4	Silica sol	0.2	0.2	$3.3 \cdot 10^{-08}$	$3.3 \cdot 10^{-08}$	$1.4 \cdot 10^{-09}$	$1.5 \cdot 10^{-09}$
5	Both	0.6	0.1	$9.8 \cdot 10^{-08}$	$1.6 \cdot 10^{-08}$	$4.1 \cdot 10^{-09}$	$7.4 \cdot 10^{-10}$
5	Cement	0.3	0.1	$4.9 \cdot 10^{-08}$	$1.6 \cdot 10^{-08}$	$2.0 \cdot 10^{-09}$	$7.4 \cdot 10^{-10}$
5	Silica sol	1.4	0.1	$2.3 \cdot 10^{-08}$	$1.6 \cdot 10^{-08}$	$9.5 \cdot 10^{-09}$	$7.4 \cdot 10^{-10}$
All	Sum. both:	2.6	0.9	$4.2 \cdot 10^{-07}$	$1.5 \cdot 10^{-07}$	$1.8 \cdot 10^{-08}$	$6.7 \cdot 10^{-09}$
	Av. both:	0.5	0.2	$8.4 \cdot 10^{-08}$	$2.9 \cdot 10^{-08}$	$3.5 \cdot 10^{-09}$	$1.3 \cdot 10^{-09}$

4.5. Volume grouted

In appendix C, each column chart shows a comparison between the theoretical bore-hole volume (74 l) and the volume of grout injected in each grout-hole; they also show their volume-difference. The results illustrate which grout-holes took and did not take grout during the injection process. Table 5 presents some features registered during grouting (e.g. grout-hole number, location, grout used, and fan number) in grout-holes where the volume difference is higher than 0. Results show that in Fan 3 no grout-hole took more grout than the theoretical volume. The volume injected in each grout-hole was different and it goes up to 860 l, i.e. grout-hole 4 in Fan 5, see appendix C.

Table 5. Grouted-holes description

Fan	Grout-holes that took grout	Location	Grout used
1	1, 3, 28, 29, 30, 31, 32, 34, 35, 36, 37, 39, 40	Walls and floor	Cement
1	8, 11, 14, 16, 18, 19	Ceiling	Silica sol
2	2, 3, 4, 24, 25, 28, 30, 31, 32, 33, 35, 37, 38, 40	Walls and floor	Cement
2	5, 6, 7, 8, 9, 11, 12, 13, 14, 15, 16, 17, 18, 19, 20, 22	Ceiling	Silica sol
3	2, 3, 24, 25, 27, 28, 30, 31, 32, 34, 35, 36, 37, 38, 39, 40	Walls and floor	Cement
3		Ceiling	Silica sol
4	1, 2, 3, 24, 25, 27, 30, 31, 32, 33, 34, 37, 38, 39, 40	Walls and floor	Cement
4	4, 6, 9, 10, 11, 12, 13, 14, 15, 16, 17, 20, 21, 23	Ceiling	Silica sol
5	3, 4, 37	Walls and floor	Cement
5	5, 6, 7, 8, 9, 11, 12, 13, 14, 15, 16, 17, 18, 20, 21, 23	Ceiling	Silica sol

4.6. Connectivity radius

Figure 12 shows the resultant variogram for a data set that includes coordinates and transmissivity (specific capacity) values from grout-holes in all five fans studied. It also shows a length or grout-hole range equal to 4 m and a nugget effect of 0.8. During the modelling logarithmic values of the transmissivities were used.

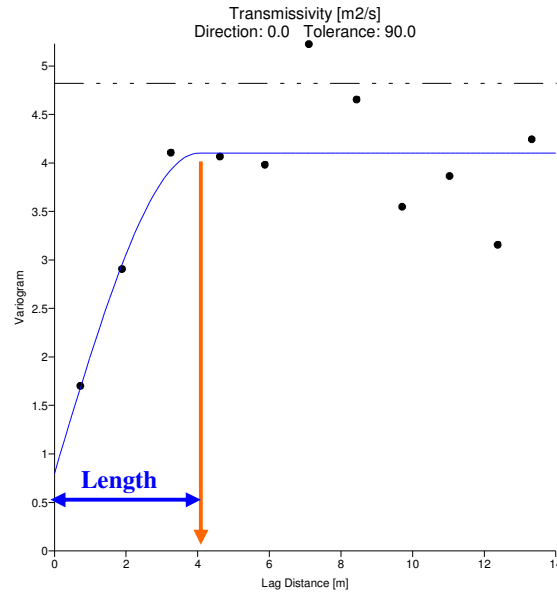


Figure 12. Variogram model of the transmissivity values before grouting. Values are taken from all grout-holes in all five Fans.

Figure 13 shows the modelled variogram of all control-holes from all five fans. This variogram gives a length or control-hole range equal to 0.3 m and a nugget effect of 2.4. Logarithmic values of the transmissivities were used during modelling.

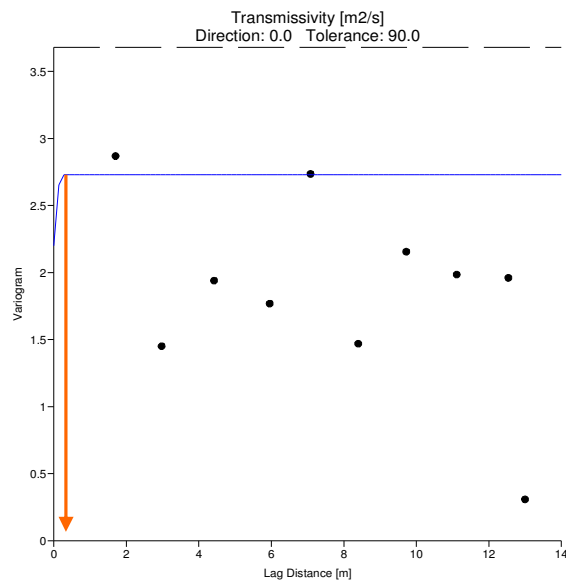


Figure 13. Variogram model of the transmissivity values after grouting. Values are taken from all control-holes in all five fans.

4.7. Dimensionality

In the Nygård tunnel the same grouting layout was used in all fans, see Figure 14. The grouted-holes were numbered starting at the bottom-left side of the tunnel and continued clockwise. The same figure, Figure 14, shows the separation line where the different agents were employed; the upper part (ceiling) was grouted with silica sol, the lower part (walls and floor) was grouted with cement. The suggested injection of grout was to go side by side, i.e. in the silica sol part was to start in grout-hole number 5, continued with 25, then 6, 24, 7, 23, etc. This routine was not always followed though.

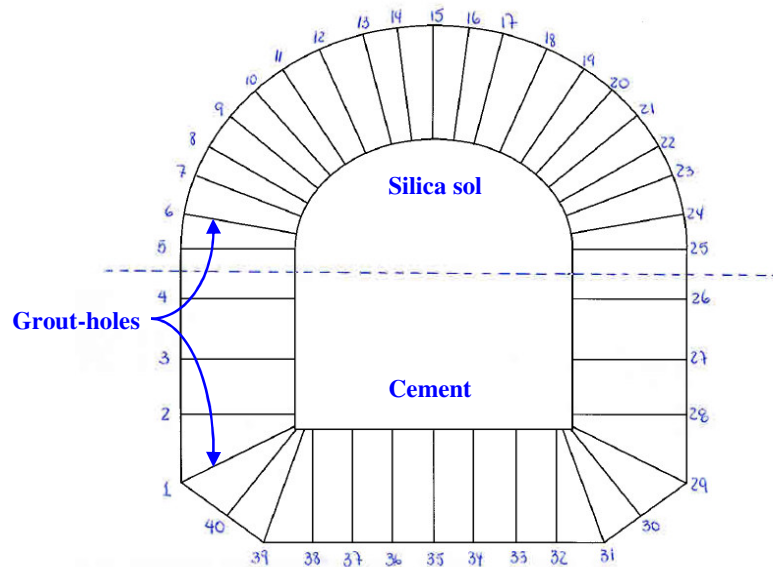


Figure 14. Layout of the grout-holes position for all five Fans. The dotted line represents the separation of different agents used; upper part with silica sol, lower part with cement.

An example of the results obtained from the pressure, volume and time recordings during grouting are given in Figure 15 and Figure 16. Figure 15 shows the flow and pressure trend over time for the grouted-hole 32 in Fan 1. Figure 16 presents the calculated accumulated volume over injected time.

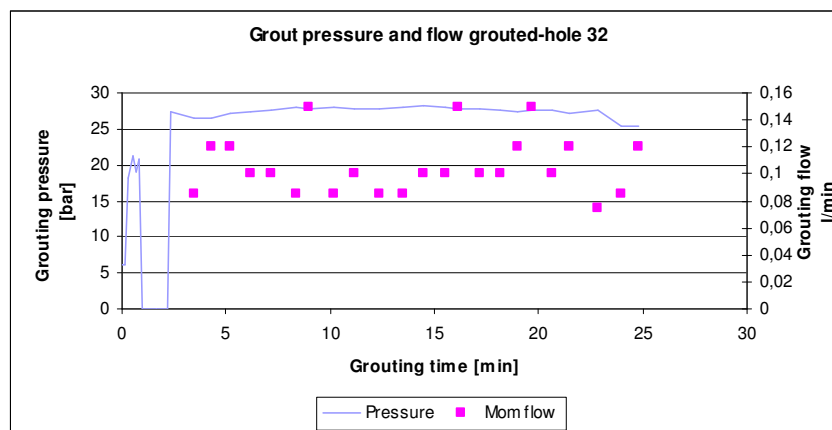


Figure 15. Grout pressure and flow trend as function of grouting time for grout-hole 32 in Fan 1. Note that the first minutes are used to fill the empty grout-hole.

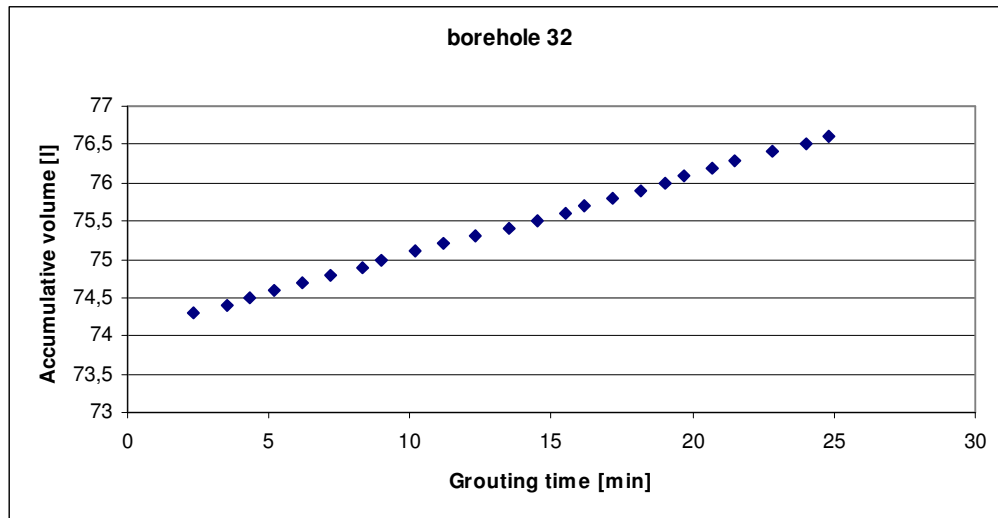


Figure 16. Accumulated volume trend as function of time for grout-hole 32 in Fan 1. The first three minutes were used for filling the grout-hole (74 l).

The dimension curve, which represents the injected volume as function of grouted time, is illustrated in Figure 17. Note that Figure 17 uses values once the grout-hole has been filled. The combination of values shows that: the resultant values of $Q \cdot t/V$, i.e. equation 9, in the grout-hole 3 is approximately equal to 1, which is equal to a 3D-flow system, see Table 1. It can be seen that the grouted-hole was filled during the first 4 min. In Appendix D, results from Fan 1 and Fan 5 are presented in the same format. A detailed process of diagnostic curves and their implication is described in Gustafson and Stille (2005).

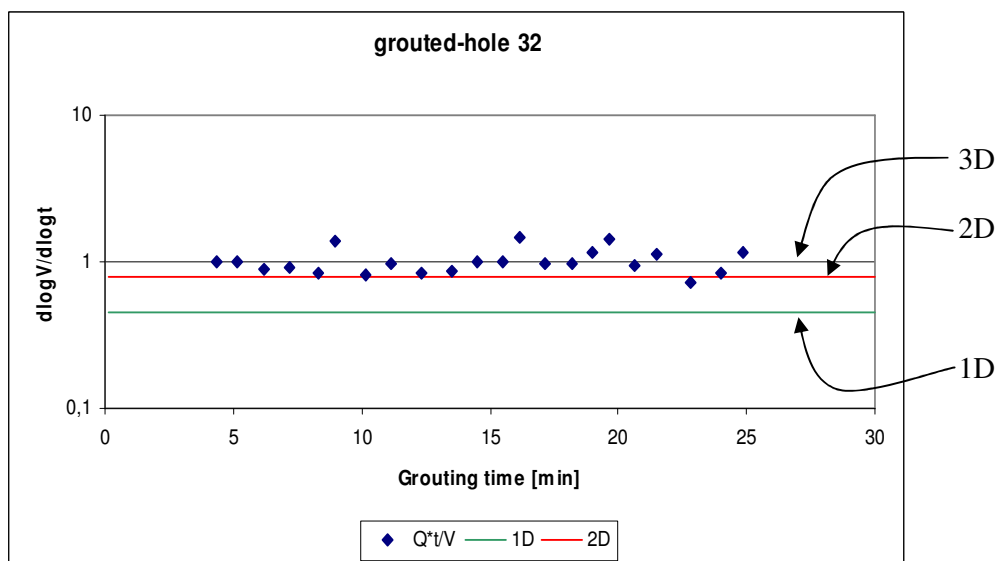


Figure 17. Diagnostic curves for determination of flow dimensions. Grout volume as function of grout time in grout-hole 32 in Fan 1. Note that $Q \cdot t/V$ is in log scale.

Technical difficulties emerged during the data storage and only two fans succeeded on recovering data for a dimensionality analysis. The results come from Fan 1 and Fan 5, and they are shown in Figure 18; a complete set of results can be found in Appendix D.

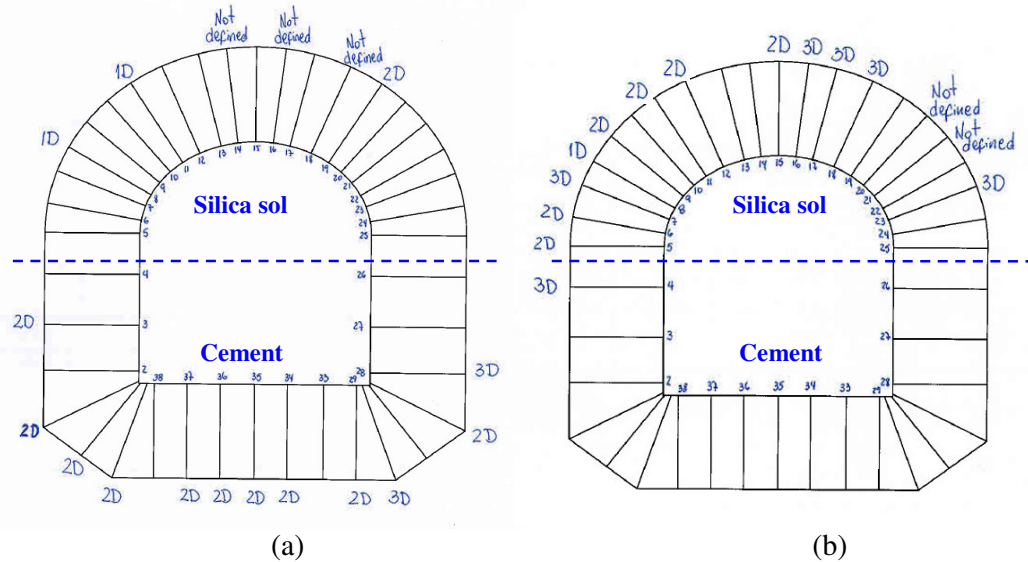


Figure 18. Dimensionality results layout, the number states the type of regime 1D-, 2D- or 3D-flow. Grout-holes with injected volume less than the theoretical (74 l) have no dimension representation. (a) Fan 1; (b) Fan 5.

4.8. Dripping

Granberg and Knutsson (2007) made a complete study of the dripping characterisation in the Nygård tunnel. One part of the characterisation took place in the section that followed the proposed design. Figure 19 shows the number of dripping places located in the study area and the flow obtained.

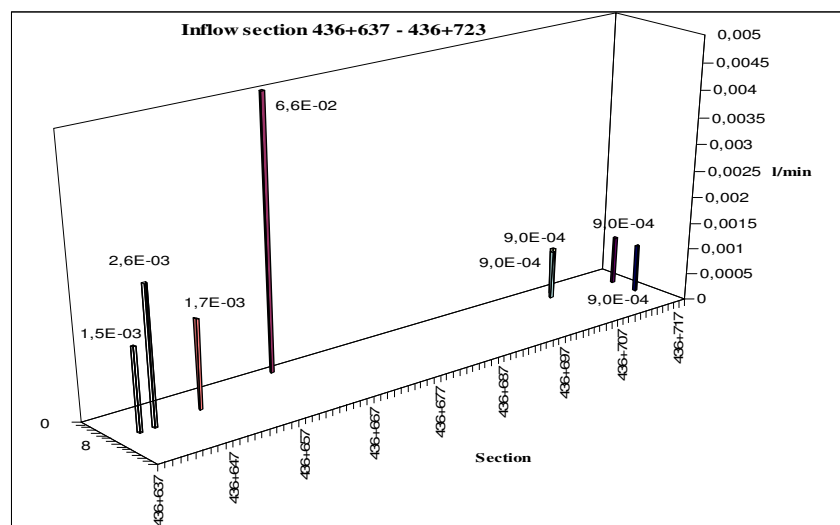


Figure 19. Drip characterisation in the designed grouted section, (after Granberg and Knutsson, 2007).

5. DISCUSSION

5.1. Grouting design

Results showed that a structured design and specific measurements during and after grouting gave useful information to be analysed; and what is more important the layout was followed successfully in field. An example of the designed grouting layout in field can be seen below. Figure 20 shows the grout-holes location in Fan 1 which are marked with numbers; it also shows the grouting rig used in this project i.e. the yellow truck standing just in front of the tunnel face.



Figure 20. Grouting layout in field, Fan 1. The numbers represent the location of the grout-holes.

5.2. Inflow and dimensionality

Results from Table 3 show different ratio values which represent the reduction scale of the inflow after pre-grouting, i.e. a ratio 1 means no reduction of inflow while a higher value represents a higher reduction of the inflow. Using this idea it can be stated that fans 2, 3, and 5 achieved good sealing efficiency while fans 1 and 4 show no decrease in the inflow after pre-grouting. Fan 5, after grouting, shows inflows lower than the measurement limit. These results alone seem not to describe the real sealing efficiency of the grouting, and they need to be discussed further; specially be coupled with more parameters in order to give a valid justification.

Further, these results can be seen in both, the silica sol and cement parts. One way to explain it is if we accept that there is no such thing as a completely waterproof tunnel, and whatever the target is it is uncertain that it can be achieved. Instead, another explanation can be given if the dimensionality of the flow system is introduced in the analysis. Figure 21 show the dimensionality results obtained plus the control-holes location in Fans 1 and 5. The flow systems calculated are noted as 1D, 2D or 3D next to the grouted-hole evaluated. Grouted-holes that did not take more than the theoretical volume have no representation as can be seen in the figure below. A not defined designation means the flow system is not distinct, e.g. Appendix D hole 14.

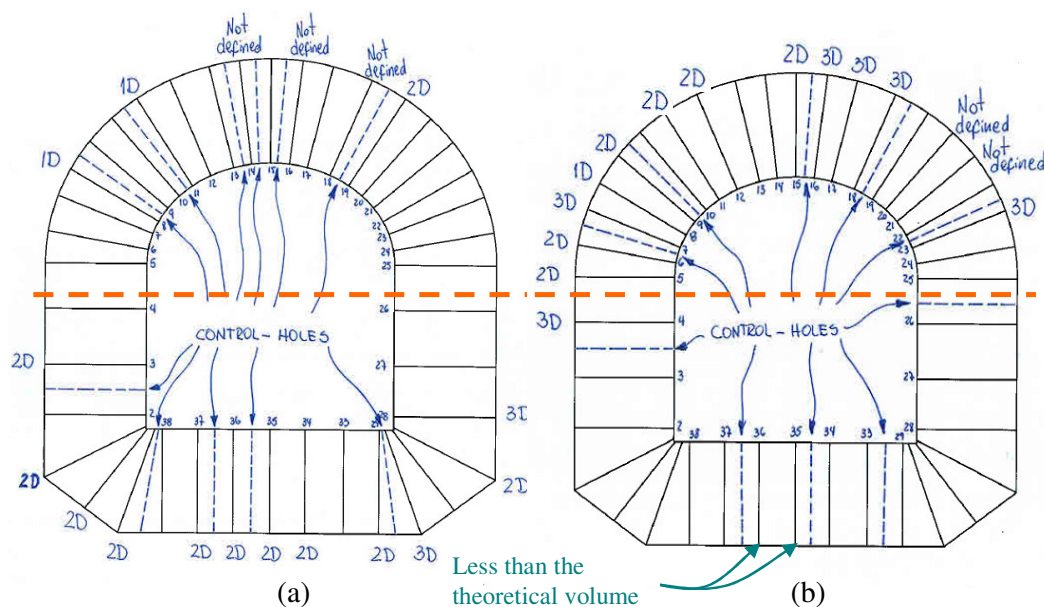


Figure 21. Dimensionality results layout and control-holes location. The dotted line represents the separation of the different agents used. (a) Fan 1; (b) Fan 5.

Fan 1 shows that half of the control-holes are located next to grout-holes that have 1D flow system or not defined whereas Fan 5 shows that all control-holes are located next to grout-holes that have 2D- or 3D-flow system, see Figure 21. For 2D- and 3D-flow systems, the possibility of intersecting fractures is extremely high, unless their orientation is unfavourable. On the contrary, for 1D-flow systems the possibility to intersect all the pervious channels is very limited. This could be a better explanation why control-holes gave equal water leakage after than before grouting in Fan 1 where 1D-flow systems were found.

Considering this evidence, it could not be advisable to drill a second round of grout-holes with the same method in the vicinity where such a system is found, i.e. 1D-flow; the chances to hit the channels are limited. Therefore measurements and data retrieval during and after pre-grouting are important in order to design a suitable post-grouting protocol and layout if needed.

5.3. Transmissivity and dripping after pre-grouting

For the 86 m grouted-section the total transmissivity obtained before grouting was about $4.2 \cdot 10^{-7} \text{ m}^2/\text{s}$, which is 3 times higher than the transmissivity obtained after grouting, i.e. $1.5 \cdot 10^{-7} \text{ m}^2/\text{s}$. Even though WPTs carried out on grout-holes are rough estimates of the rock mass transmissivity, the values obtained can be compared and give an assessment of the achieved sealing-effect. The transmissivity after grouting presented in Table 4 corresponds to a hydraulic conductivity of approximately $6.7 \cdot 10^{-9} \text{ m/s}$. A variogram analysis makes this value close to reality when considering the designed grouting-zone; the reasons are explained in chapter 5.5.

The dripping characterisation in the pre-grouted section was not compared with the respective section in the service tunnel due to they did not present the same geological characteristics (Granberg and Knutsson, 2007). Examining the data it can be seen that

very few dripping points were spotted and the highest inflow found was 0.06 l/min in an 1 m² area, see Figure 19. What can be done is a comparison of the inflow from the grout-holes before pre-grouting and the inflow from the dripping characterisation realized after pre-grouting (0.07 l/min). The median inflow before pre-grouting in Fan 4 where the maximum dripping inflow is localised is 0.4 l/min, see Table 4. The comparison shows that the inflow was reduced around 7 times. Following the same procedure, the rest of the values show a reduction of 100 or 400 times of the inflow after pre-grouting.

5.4. Volume

It is clear from Table 5 that each grouted fan did not take the same injected volume, e.g. Fan 3 had no volume injected in the ceiling. Further, each grouted-hole took a different amount of grout-volume within each fan. Comparing the dimensionality results and the injected volumes, it can be stated that the grout volume is very much dependent of the flow system, and the hydraulic aperture. This will be discussed further in Chapter 5.6.

The grouted-hole shown in Figure 22 gives an indication of a connected-hole, where the first 10 min illustrates a 1D-flow penetration, followed by a bore-hole filling during 5 min and then a fracture-flow penetration for 10 min. The total injected volume in this hole was 178 l, which is logic if two holes of 74 l each have to be filled, leaving 30 l of grouting material in the discontinuities. The hole 10 which was grouted afterward took 1 l of grout which means that in fact it was grouted by the grout-hole 11; corroborating that these two bore-holes were connected. Connected-holes seem to appear more in the ceiling of the tunnel where silica sol was used, e.g. hole 11 Fan 1, grout-holes 15, 17 and 23 in Fan 5. This may be the result of the better penetration of the silica sol that fills a whole fracture plane, whereas cement penetrates channels.

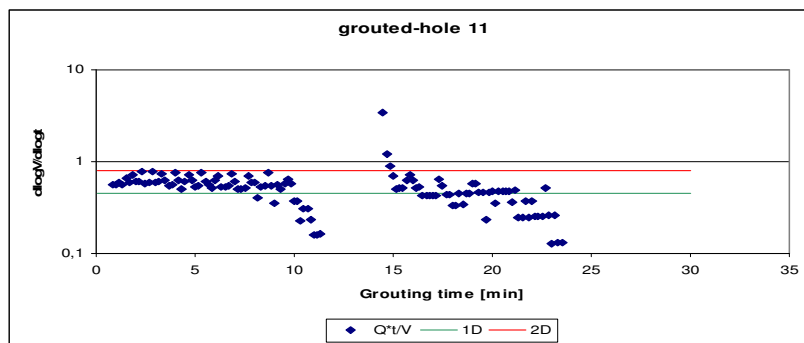


Figure 22. Diagnostic curves, illustration of the injected volume as function of grouted time; Fan 1 grouted-hole 11.

5.5. Connectivity radius

Results of variogram-modelling gave a grout-hole specific capacity range of 4 m, which is a measure of how quickly the transmissivity changes on the average. This implies that the grout-hole separation given in the design, 2 m, is in the predictable range; and all measurement results found are similar within this range. The nugget effect, 0.8, in this model gives the random variation in which the data appears to have no spatial correlation, therefore knowing your data is essential to address any decision.

When control-holes are modelled, the range was 0.3 m with a large nugget effect i.e. 2.4. Even though the change in characteristics around the hole will be quick, control-holes are drilled to perceive if the penetration went according to the design; if not a larger grout-hole overlap should be used. Again, knowing the data is essential, which means that a dimensionality check should be conducted and if 1D-flow systems are found results could be local and not representative of the rock mass.

5.6. Compilation

It should be pointed that in order to make a grouting evaluation all parameters have to be taken into account. Figure 23 shows a comparison between calculated and measured grouted volumes with respect of the specific capacity obtained from WPTs. In addition, the flow system regime is also illustrated. From such a graph, it can be seen that most of the transmissivity values are in a range of $2 \cdot 10^{-8}$ to $1 \cdot 10^{-6}$ m²/s which gives a range of 30 to 100 μ m in hydraulic aperture for Fan 1. Figure 24 shows transmissivity values in a range of $1 \cdot 10^{-8}$ to $1 \cdot 10^{-5}$ m²/s which gives a range of 30 to 110 μ m in hydraulic aperture for Fan 5. An example is shown below: a grouted-hole took 2 l of grout which corresponds to a specific capacity of $6 \cdot 10^{-8}$ m²/s and a theoretical volume of 4 l from a fracture (assumed) with 40 μ m in hydraulic aperture.

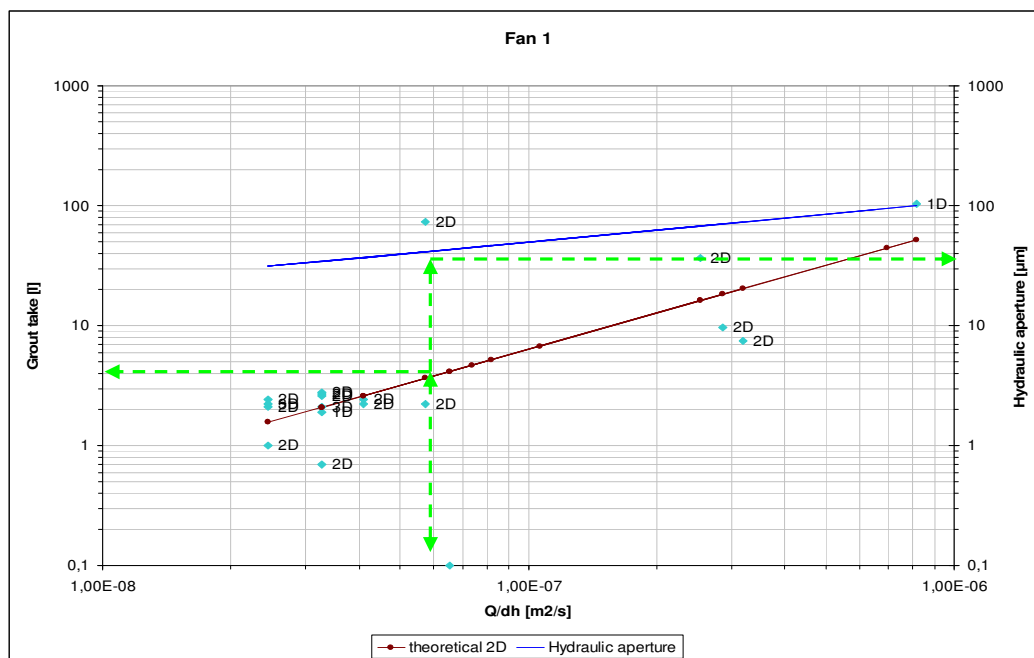


Figure 23. Fan 1 crossplot of specific capacity during WPTs and grouted volume obtained during grouting the flow system is also illustrated. Both measured and calculated grouted volume are presented. Their hydraulic aperture is also plotted.

Fractures with a hydraulic aperture range illustrated in Figure 24 can be grouted by silica sol (Chapter 2.2). From Appendix C most of the grouted-holes with injected volume are located in the ceiling of the tunnel. A possible reason is that not grouted-holes have had small apertures (within a range of 30 to 100 μ m) and cement was not able to penetrate them. Another reason could be that 1D-flow systems are nearby. Large volumes are not considered in the analysis due to they could be the result of bore-hole connections or batch-volume run out, e.g. hole 11 Fan 1.

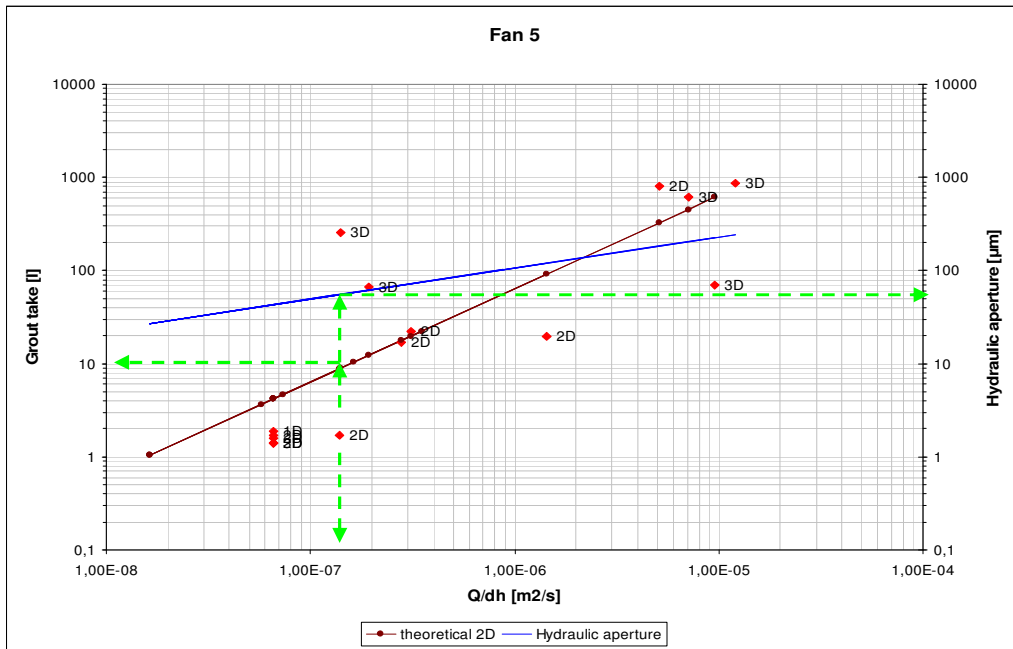


Figure 24. Fan 5 crossplot of specific capacity during WPTs and grouted volume obtained during grouting, the flow system is also illustrated. Both measured and calculated grouted volumes are presented. Their hydraulic aperture is also plotted.

Both Figure 23 and Figure 24 show a small relative spread when small volumes are considered; in some cases the grouted volume is higher than the theoretical volume expected. The reason for this spread in values, when small volumes are considered, could be explained by grout-hole interference. This means that while the first grouted-hole shows real values the second grout-hole has less penetration volume due to the pre-defined overlapping and the real grouted volume will differ from the theoretical, see Figure 25. In addition, a planar fracture will be expected to be injected with less than the theoretical volume due to contact zones inside it that reduce its effective volume.

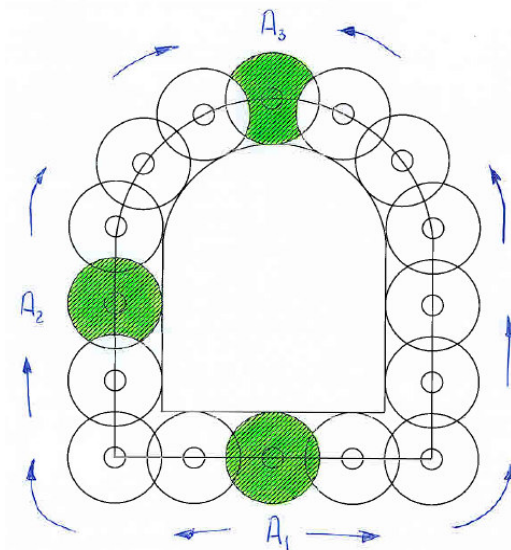


Figure 25. Theoretical grouted-hole volume distribution. $A_1 > A_2 > A_3$.

Appendix E also shows that no fracture zones were observed but fracture sets are crossing each other making evident the existence of connected grouted-holes. This is the case of large volume intake in some grouted-holes. Figure 26 shows the large amount of volume injected in the hole 11 (approximately 180 l), and the small amount of volume injected in hole 10 (approximately 1 l) due to connection between holes. This corroborates that there is always borehole interference when evaluating the grouted volume intake. When no connection between boreholes is established, a larger intake of grout could be caused probably by the rough aperture that gives a higher volume intake than the corresponding to the hydraulic aperture.

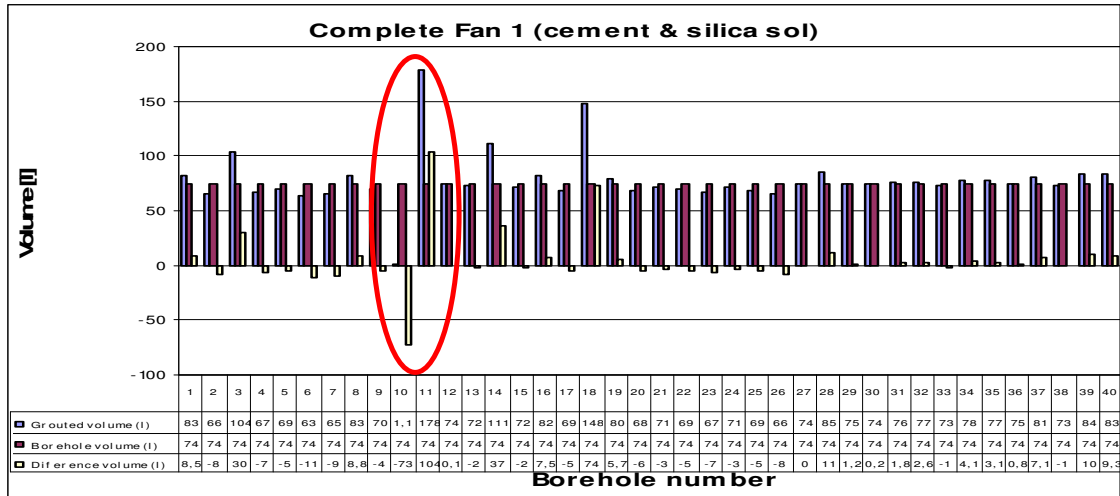


Figure 26. Column chart, from Fan 1, which compares the grout-hole volume and the volume of grout injected in each grout-hole; it also shows the difference.

Figure 27 shows the location and extent of the drains placed in the whole grouted section. The area covers approximately 10% of 1290 m² which implies that the dripping sources are few if compared with other sections of the tunnel. It can be seen that some areas did not required any drain at all. Appendix F shows the drain map for the complete grouted section and the different grouted fans location.

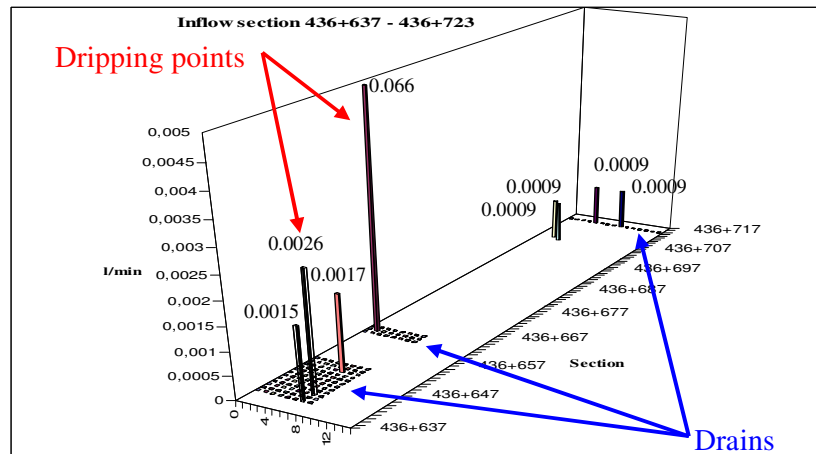


Figure 27. Drains location and extension in the whole grouted area. Dripping points are also shown plus their calculated inflow.

6. CONCLUSIONS

The aim of this project was to implement a pre-grouting design that will reduce the water inflow into the tunnel from walls and bottom and minimize the water dripping from the ceiling of the tunnel. A structured grouting design and measurements were followed in order to characterise the rock mass, design the grouting procedure, design the grouting layout, and evaluate the results obtained; making data retrieval and continuous evaluation very important. In general, the inflow was reduced and dripping was minimized. It was also seen that a pre-grouting design could be followed in the field even if two different agents were used. Considering all these steps the following conclusions can be made:

1. Whether the design approach is to reduce the water inflow, minimize dripping or waterproofing, preparation is essential. Control-holes are proven to be important for the evaluation.
2. The total transmissivity obtained in the section grouted with this design is $1.4 \cdot 10^{-8} \text{ m}^2/\text{s}$ which is 10 times lower than the transmissivity before grouting.
3. Results showed eight spotted dripping places in 86 m of tunnel, which present a reduction of the inflow of 10, 100 or 1000 times lower. This means that in this section of the tunnel, dripping was minimised but the tunnel is not totally waterproof.
4. WPTs on grout-holes showed values with a correlation length of 4 m, which means that the grout-hole separation given in the design, 2 m, was in the predictable range.
5. The volume taken by a grout-hole and intersecting fractures is very much dependent of the flow system and the penetration interference among grouted-holes.
6. Connected-holes can be detected in field and corroborated by data analysis.
7. A generalization of the flow system can not be done, but it can be determined from pressure, volume and time recordings; depending of the grouting purposes, decisions have to be updated continuously.
8. After this study. It is obvious that all these parameter are important before deciding if a second round of grouting is needed or profitable.

7. REFERENCES

- Alberts, C. and Gustafson, G. 1983. Undermarksbyggande i svagt berg- 4 Vattenproblem och tätningsåtgärder. BeFo nr 106. Stockholm, Sweden. In Swedish.
- Axelsson, M. 2006. Strength criteria on grouting agents for hard rock: laboratory studies performed on gelling liquid and cementitious grout. Licentiate Thesis. Department of Civil and Environmental Engineering, Chalmers University of Technology, Göteborg.
- Barnes, H. A., et al. 1998. An Introduction to Rheology. Elsevier Science B. V., Amsterdam, The Netherlands.
- Björnström, J. 2005. Influence of nano-silica and organic admixtures on cement hydration: a mechanistic investigation. Doctoral Thesis. Department of Chemistry, Göteborg University, Göteborg.
- Cementa 2007, October 18, 2007. *Injektering 30*. Retrieved October 18, 2007, 2007, from http://www.heidelbergcement.com/NR/rdonlyres/07AD9AB4-7821-44E5-9007-141BEBD804E6/0/Inj30_Eng.pdf.
- Eklund, D. 2003. Penetrability for cementitious grouts. Licentiate Thesis. Division of Soil and Rock Mechanics, Royal Institute of Technology, Stockholm.
- Fransson, Å. 2001. Characterisation of fractured rock for grouting using hydrogeological methods. Doctoral Thesis. Department of Geology, Chalmers University of Technology, Göteborg.
- Funehag, J. 2007. Grouting of fractured rock with silica sol: grouting design based on penetration length. Doctoral Thesis. Department of Civil and Environmental Engineering, Chalmers University of Technology, Göteborg.
- Granberg, N. and Knutsson, S. 2007. Kvalitetssäkring av efterinjektering: En fältstudie i Nygårdstunneln. Master Thesis. Department of Civil and Environmental Engineering, Chalmers University of Technology, Göteborg.
- Gustafson, G. and Fransson, Å. 2006. The use of the Pareto distribution for fracture transmissivity assessment. *Hydrogeology Journal*, Vol. 14, No. 1-2, pp. 15-20.
- Gustafson, G., et al. 2004. Ett nytt Angreppssätt för Bergbeskrivning och Analysprocess för Injektering. *Väg och vattengygaren* nr 4. Stockholm, Sweden. In Swedish.
- Gustafson, G. and Funehag, J. 2007. Design of grouting with silica sol in hard rock - New design criteria tested in the field, Part II. *23 (2008)*, 1, 9-17.
- Gustafson, G. and Stille, H. 1996. Prediction of groutability from grout properties and hydrogeological data. *Tunnelling and Underground Space Technology*, Vol. 11, No. 3, pp. 325-332.
- Gustafson, G. and Stille, H. 2005. Stop Criteria for Cement Grouting. *Felsbau Rock and Soil Engineering*, Vol. 23, No. 3, pp. 325-332.
- Houlsby, A. C. 1990. *Construction and Design of Cement Grouting: A Guide to Grouting in Rock Foundation*. New York, USA.
- Jones, M. 2006. Deterring drips and deluge. *Tunnels & Tunnelling International*, Vol. 38, No. 6, pp. 46-48.
- Kutzner, C. 1996. *Grouting of rock and soils*. A.A. Balkema, Rotterdam, The Netherlands.
- Larsson, T. and Zetterlund, M. 2004. Evaluation of water pressure tests in control boreholes as a method of appraising the grouting result: a case study of

- Nordlänken, Öxnered - Trollhättan. Institutionen för geologi och geoteknik, Chalmers Tekniska Högskola, Göteborg.
- Palmqvist, K. (1983). Tätning av Bergtunnlar: Injekteringsutförande och Resultat. Stockholm, Stiftelsen Bergteknisk Forskning.
- Stuart, L. 2003. The development of practice in permeation and compensation grouting a historical review (1802 - 2002) part 1 permeation grouting. New Orleans, LA, USA, American Society of Civil Engineers.
- Warner, J. 2004. Practical Handbook of Grouting. John Wiley & Sons, New Jersey.

8. APPENDIX

APPENDIX A: Grouting design for Nygård tunnel

Koncept 2006-10-16

Banverket

Nygårdstunneln- Injektering med cement och silica-sol för dropptätning

Injekteringsdesign med Silica-sol

Gunnar Gustafson, GEO, Chalmers Tekniska Högskola
Christian Butron, GEO, Chalmers Tekniska Högskola

Inledning

För närvarande byggs Nygårdstunneln som en del av Norge-/Vänerbanan som skall förbättra järnvägsförbindelserna från Göteborg norrut mot Oslo och Karlstad. I denna PM redovisas ett underlag för att utföra bergtätningen i provsträcka i tunneln med syftet att tätta tunneltaket mot dropp. Injekteringen tänks ske med en kombination av silica-sol och cement. Materialet utgör ett underlag för att bestämma om ett jämförande försök med denna teknik skall utföras i ett 100 m långt avsnitt av tunneln.

Underlagsmaterial

Följande utredningsmaterial har ställts till förfogande och utgjort underlag för utvärderingen av de hydrogeologiska egenskaperna i området:

- Bergsäker Konsult AB, GEOLOGISK OCH BERGTEKNISK BESKRIVNING, Bergtunnel Km 434+560 – 437+590. Förundersökning CD.
- Tyréns AB, Tunnelritningar, CD.
- Bergsäker Konsult AB, Kärnkartering och hydrauliska tester, Förundersökning CD.

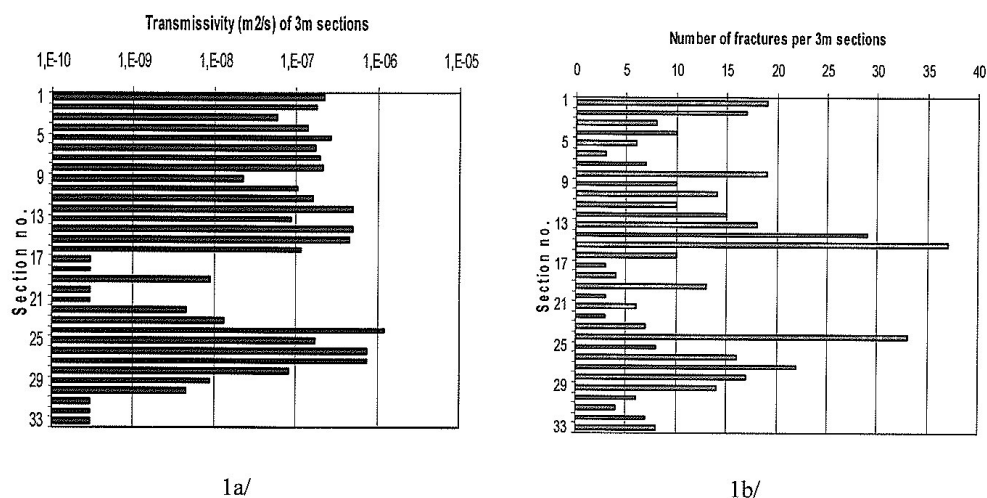
Utvärdering av bergets sprickighet och genomsläpplighet

Under förundersökningarna borrades 4 kärnborrhål, KB 1 – 4. Alla utfördes lutande och syftet med borrhålen var att undersöka förmodade partier med dåligt berg. För borrhålen finns kärnkarteringar där öppna sprickor noterats och hydrauliska tester har genomförts. Speciellt finns manschettmätningar gjorda i tremetersintervall för samtliga borrhål. I samtliga hål finns ett parti nära markytan med mycket hög genomsläpplighet, som inte bedömts som representativt för berget på tunnelnivån. För att få ett rimligt representativt prov på bergets hydrauliska egenskaper har därför de testade avsnitten under det genomsläppliga ytberget lagts samman. Genom detta har ett dataunderlag bestående av 33 hydraultestade och sprickkarterade sektioner erhållits. Någon korrektion för borrhålsriktningar och har inte varit möjligt att göra utan analysen bygger på ett antagande om ett isotopt spricksystem. Detta är givetvis diskutabelt, men analysen torde ändå vara en rimlig ansats.

Borrhålsdata

Vattenförlustmätningar har utförts i 33 st. 3 m-sektioner. Mätningarna utvärderades med Moyes formel¹ och öppna sprickor har karterats och lagts in i databasen på ett sådant sätt att de kan knytas till manschettmätningarna.

I Figur 1 redovisas uppmätta intervalltransmissiviteter och antal sprickor för varje intervall.



Figur 1 Transmissiviteter och sprickantal för vattenförlustmätta intervall.

Som framgår av figuren finns en viss korrelation mellan sprickantal och transmissivitet. Detta är inte unikt för dessa borrhål eller för det berg vi har i området. För att kunna använda data måste de därför överföras till en spricktransmissivitetsfördelning. En redovisning av bakgrunden till detta redovisas i Bilaga 1: Bergbeskrivning och analysprocess för injektering – Ett nytt angreppssätt. Vi kan dessutom konstatera att sprickfrekvensen i medeltal är drygt 4 öppna sprickor per meter för hela datamaterialet.

Spricktransmissiviteter

I Bilaga 1 redovisas en metod att utvärdera en statistisk fördelning för spricktransmissiviteter. Den bygger på följande resonemang. Sannolikheten, p_i , för att alla sprickor i ett testat intervall, i , ska ha en transmissivitet mindre än T_n kan om de är statistiskt oberoende av varandra beräknas som:

$$p_i = p(T < T_n)^{n_i} \quad (1)$$

Här är n_i antalet sprickor i intervallet. T_n är spricka nr. n i ett storlekssorterat sample av N st. totalt. Antalet intervall, av I totalt, där detta gäller kan då beräknas som:

$$I_r = \sum_{i=1}^I p_i = \sum_{i=1}^I p(T < T_n)^{n_i} \quad (2)$$

Om vi antar att I_r motsvarar antalet intervall som har transmissiviteten T_r , transmissiviten med rang r kommer vi således att få:

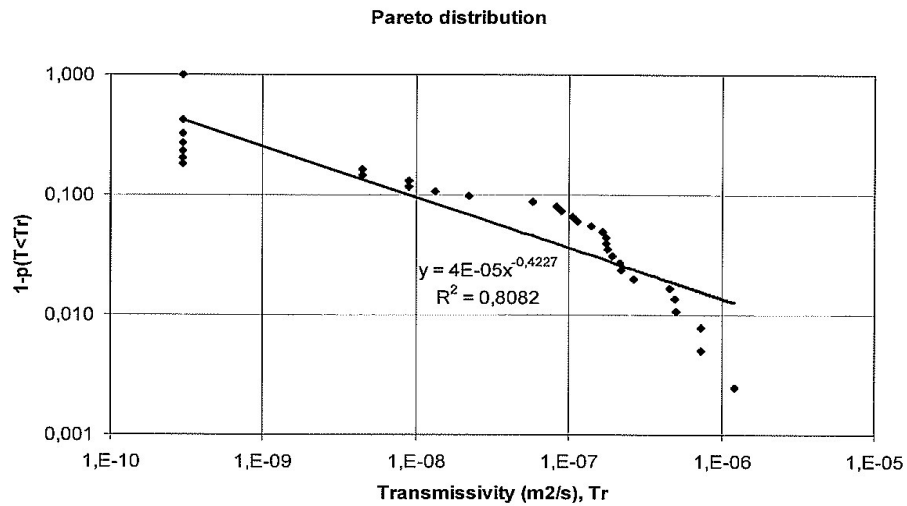
$$I_r \approx \sum_{i=1}^I p(T < T_r)^{n_i} \quad (3)$$

Vilket i princip ger lika många ekvationer som vi har mätvärden från vattenförlustmätningarna. Genom att lösa dessa t. ex. med Newton-Rhaphson iteration kan vi ge punktvärden för fördelningsfunktionen: $p(T < T_r)$. För att kunna göra en injekteringsdesign behöver vi anpassa en fördelningsfunktion till de empiriska data som analysen ger. Analyser av ett antal mätningar från olika platser har visat att man kan anta att spricktransmissiviteterna är paretofördelade. Fördelningsfunktionen för denna är:

$$P(T_n) = 1 - \frac{(T_{max}/T_n)^k}{N+1} \quad (4)$$

Om båda leden i ekvationen minskas med 1 och logaritmeras erhålles:

$$\log[1 - P(T_n)] = \log\left[\frac{T_{max}^k}{(N+1)}\right] - k \log(T_n) \quad (5)$$



Figur 2 Paretofördelning av utvärderade spricktransmissiviteter

Detta är en rät linje i ett dubbellogaritmiskt diagram, se Figur 2. I denna ekvation är k fördelningens formparameter och T_{max} transmissiviteten hos fördelningens största spricka. Här har båda fördelningsfunktionerna lagts in. Som framgår följer mätdata, utom de högsta värdena, väl räta linjer vars ekvationer redovisas i diagrammet. Vi finner vidare att de två fördelningsfunktionerna ligger mycket nära varandra. I fortsättningen används p_r för analysen. Att de högsta värdena inte följer fördelningen har visat sig även i andra fall, men det saknar betydelse för dimensioneringen av injekteringen eftersom dessa konduktiva sprickor är lättinjekterade. Problemet är att kunna bestämma den resttransmissivitet som kvarstår efter injekteringen av dessa. Från den utvärderade fördelningsfunktionen erhålles $k = 0,4227$ och $T_{max} = 6,04 \cdot 10^{-5} \text{ m}^2/\text{s}$.

Från fördelningsfunktionen, se Bilaga 1, kan transmissiviteten för en spricka med rangen r Beräknas som:

$$T_r = T_{\max} / r^{1/k} \quad (6)$$

Med hjälp av (7) skulle därmed hela borrhålets transmissivitet beräknas som:

$$T_{\text{tot}} = T_{\max} \cdot \left[\frac{1}{1^{1/k}} + \frac{1}{2^{1/k}} + \frac{1}{3^{1/k}} + \dots + \frac{1}{N^{1/k}} \right] = T_{\max} \cdot S(k, N) \quad (7)$$

Våra data ger $T_{\text{tot, fördelning}} = 8,5 \cdot 10^{-5} \text{ m}^2/\text{s}$ vilket är större än summan av vattenförlustmätningarna $T_{\text{uppmätt}} = 6,4 \cdot 10^{-6} \text{ m}^2/\text{s}$. Detta orsakas av den observerade avvikelser från fördelningen för de höga värdena. I de fortsatta beräkningarna har vi kompenserat för detta, dvs. summan av spricktransmissiviteterna är alltid lika med den uppmätta summan. Serien i Ekvation (7) ger möjlighet att beräkna resttransmissiviteten det vill säga summan av alla transmissiviteter med rang lägre än r som:

$$T_{\text{rest}} = T_{\max} \cdot [S(k, N) - S(k, r)] \quad (8)$$

Sprickviddsfördelning

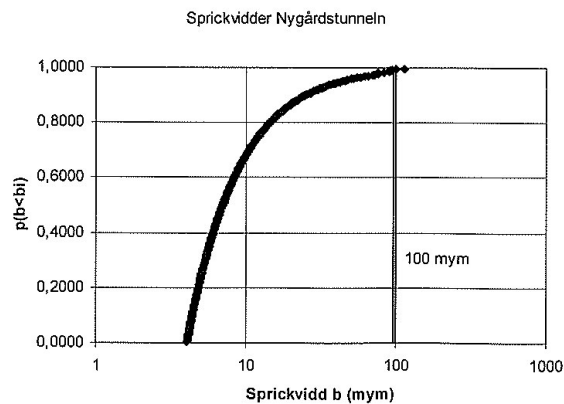
Den hydrauliska vidden, b , hos en spricka är kopplad till transmissiviteten genom den kubiska lagen:

$$b = \sqrt[3]{T \cdot \frac{12\mu_w}{\rho_w g}} = C \cdot T^{1/3} \quad (9)$$

Här är ρ_w och μ_w vattnets densitet och viskositet. Den hydrauliska vidden har visat sig också ge ett rimligt värde för den injekterbara vidden. Som Ekvation (9) anger finns det ett direkt samband mellan spricktransmissivitet och sprickvidd. Om Ekvation (7) och (9) kombineras kan vi beräkna vidden hos en spricka med rangen r som:

$$b_r = b_{\max} / r^{1/3k} \quad (10)$$

Där b_{\max} beräknas med Ekvation (10). Sprickviddsfördelningen redovisas i Figur 3. I figuren har också gränsen för vad man konventionellt anser injekterbart med cement, $b_{\min} = 0,1 \text{ mm}$, lagts in. I figuren har de uppmätta transmissiviteterna använts för de största sprickorna.



Figur 3 Beräknad sprickviddsfördelning i borrhålen.

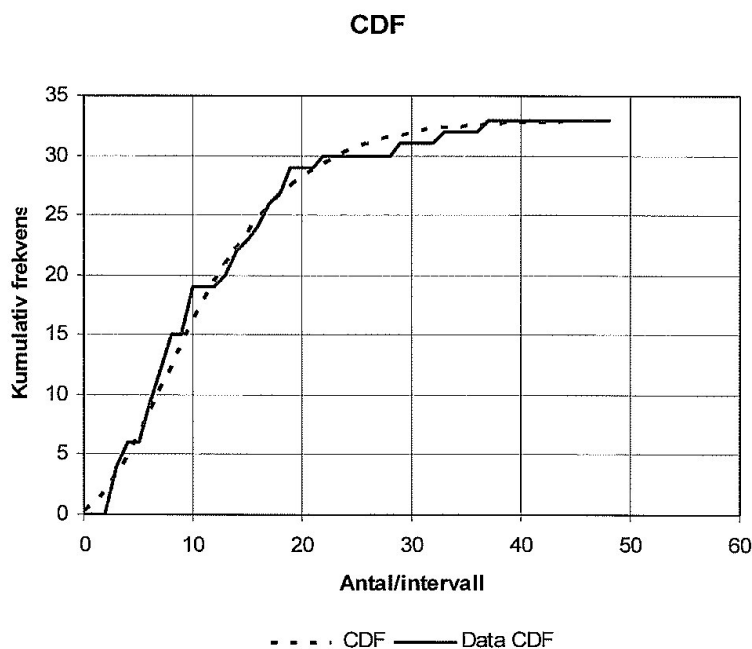
Som framgår av figuren är 99 % av sprickorna mindre än 0,1 mm och därmed inte injekterbara med cement. De sprickor som är större än 0,1 mm står emellertid för 58 % av genomsläppligheten för vatten, så genom att tätta de största sprickorna reducerar man snabbt bergets permeabilitet. Emellertid finns det ett stort antal sprickor strax under 0,1 mm som leder vatten i tillräcklig mängd för att ge droppproblem.

Sprickfrekvens

En viktig information för injekteringsdesign är sprickfrekvensen. Analys av flera kärnborrhål har givit att denna är approximativt har en Negativ Binomiakfördelning (NB)². NB-fördelningen ger sannolikheten för att ett visst antal sprickor påträffas i ett mätintervall (manschettintervall). Fördelningen har två parametrar:

- t , som är proportionell mot medelantalet sprickor i mätintervallet och därför kan användas till att skala upp kartering i en viss skala (manschettavstånd) till en annan (injekteringskärm).
- p , som är kopplad till hur sprickorna tenderar att forma grupper i borrhålet (kluster).

En analys av den sammansatta datamängden som utvärderats för spricktransmissiviteterna ger: $t = 2,85$ och $p = 0,188$. En jämförelse mellan uppmätta sprickfrekvenser och den anpassade fördelningen ges i Figur 4.

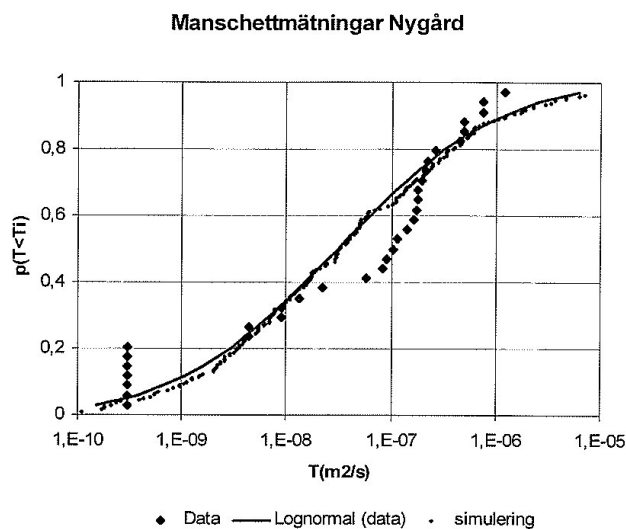


Figur 4. Jämförelse mellan den anpassade sprickfrekvensfördelningen (CDF) och data från kärnborrhålen (Data CDF).

Kontrollsimulering av transmissivitetesfördelningen

För att kontrollera rimligheten av de utvärderade spricktransmissivitets- och sprickfrekvensfördelningarna kan man göra en Monte-Carlosimulering av

manschettmätningarna. Sedan kan man göra en direkt jämförelse mellan utgångsdata och simuleringsresultatet för att se om man får tillbaka det man gick ut ifrån. Figur 5 visar transmissiviteten hos 200 simulerade manschettintervall jämfört med uppmätta data och en lognormalfördelning direkt baserad på uppmätta data.



Figur 5. Jämförelse mellan uppmätta transmissiviteter och 200 simulerade intervalltransmissiviteter. Parametrar: $t = 2,85$, $p = 0,188$, $k = 0,4227$, $T_{max} = 6,04E-5$ och $N = 406$.

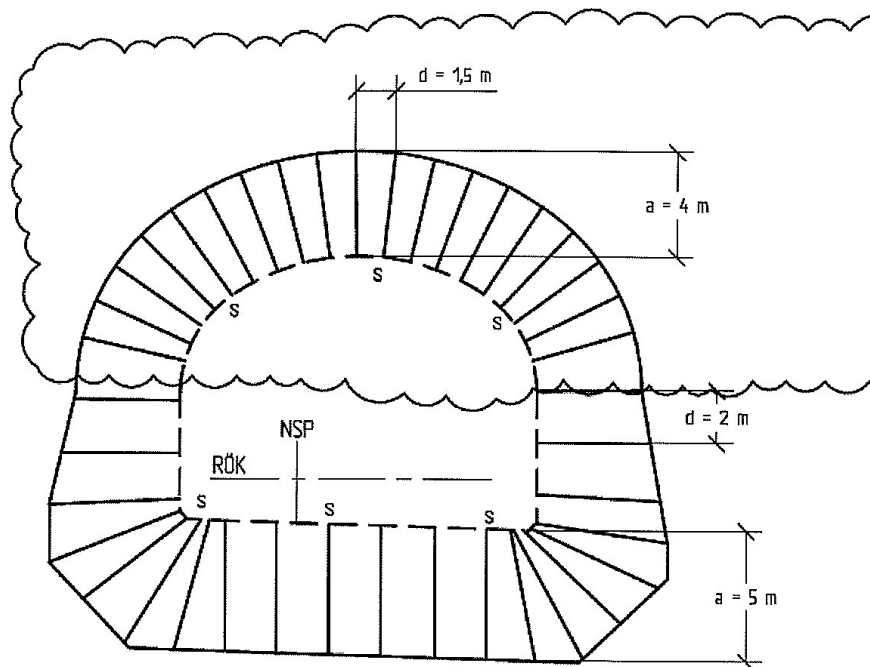
Som framgår är överensstämmelsen god mellan mätdata och simulering.

Översiktlig inläckningsberäkning

För att analysera vilken injektering som krävs för att uppfylla inläckagekraven till tunneln har en approximativ beräkning av läckaget till ett spårtnunneln utgående från den injekteringsdesign som redovisas på Ritning 1-532 373/4060 A, Tätningsklasser mm. Den utförda beräkningen ger större läckage än i verkligheten men anger storleksordningar på de krav som ställs. Detta kan sedan kontrolleras med en noggrannare beräkning för en mer realistisk geometri. Analysen följer Gustafson et al³: Ett nytt angreppssätt för bergbeskrivning och analysprocess för injektering. V-byggaren nr 4, 2004.

Tunnelgeometri och tätningssklass

Tunnel och borrhingsgeometri redovisas i Figur 6.



Figur 6. Borrhingsgeometri för injektering i huvudtunneln (Tyréns).

Översiktlig inläckageberäkning

Tunnelarean är ca 100 m^2 vilket ger en effektiv tunnelradie av ca $r_t \approx 6 \text{ m}$. I Figur 4 redovisas en tätad zon med en tjocklek av $t = 4 - 5 \text{ m}$. Djupet till tunnelcentrum från markytan (\approx ursprunglig grundvattennivå) är ca $40 - 60 \text{ m}$. För att beräkna storleksordningen på läckaget är dock kravet på noggrannhet i denna uppgift inte så stor. Vi antar därför ett karakteristiskt värde $H \approx 50 \text{ m}$.

Inläckaget till en tunnel för en sträcka som motsvarar ett undersökt borrhål kan beräknas som:

$$q_{inj} = \frac{2\pi T_{tot} H / L}{\ln(2H/r_t) + (T_{tot}/T_{inj} - 1) \cdot \ln(1+t/r_t) + \xi} \quad (11)$$

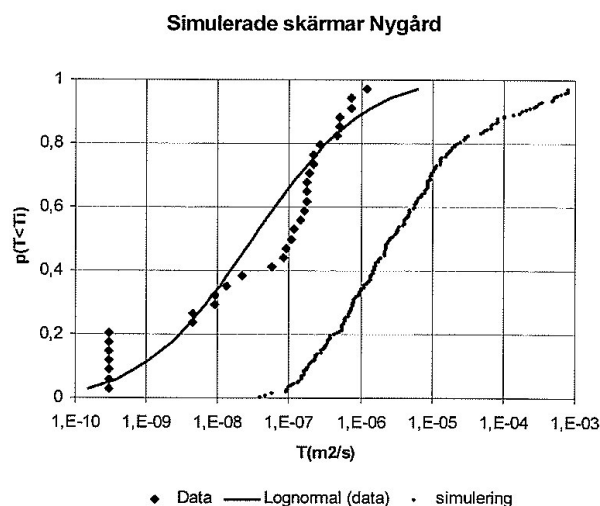
Här är T_{tot} borrhålets transmissivitet före och T_{inj} transmissiviteten hos motsvarande berg efter injektering. ξ är en för tunnlar naturlig igensättningsfaktor, skinfaktor, som erfarenhetsmässigt visat sig ligga i intervallet $3 - 10$. Borrhålslängden är $L = 99 \text{ m}$. Med data från de använda kärnborrhålen erhålles de inläckage som redovisas i Tabell 1.

Tabell 1 Resultat av översiktlig inläckageberäkning

Minsta sprickvidd tätad, b_{min} (μm)	Inläckage, q_{ber} (l/min·100 m)	T_{inj} (m^2/s)	Anmärkning
112	9,2	6,2E-06	Otätad tunnel
100	9,0	4,3E-06	Cementinjektering
50	7,0	8,1E-07	Max cement/silica sol
14	2,3	7,6E-08	Silica sol

Erfarenheterna är att Ekvation (11) överskattar inläckaget och att cementinjekteringen fungerar något bättre än vad sprickfördelningen i Figur 3 antyder. Gränsen för silica-solinjektering har något godtyckligt satts till 14 μm . Vi vet dock att en dimensionering mot detta målvärde har gett en väsentlig droppreducering i Törnskogstunneln.

En sprickvidd av ca 100 μm ger en spricktransmissivitet ca $T_s \approx 5 \cdot 10^{-7} \text{ m}^2/\text{s}$. För att cementinjektering skall vara meningsfull bör alltså den skärm som injekteras minst ha en transmissivitet av den storleksordningen. Detta kan kontrolleras genom att utnyttja uppskalningsmöjligheten i sprickfrekvensfördelningen. Figur 7 visar transmissiviteten för 200 simulerade skärmar av 18 m längd med i övrigt samma parametrar som i Figur 5.



Figur 7. Transmissiviteten för 200 simulerade injekteringsskärmar om 18 m. Som jämförelse visas också resultaten av manschettmätningarna.

Som framgår av figuren har över 80 % av de simulerade skärmarna en transmissivitet av över $T_s \approx 5 \cdot 10^{-7} \text{ m}^2/\text{s}$. Det innebär att cementinjekteringen är både meningsfull och nödvändig.

Dimensionering av injekteringen

Den ansats som föreslås är en injektering av botten och väggar med cement och en injektering av taket med silica-sol. Om cementinjekteringen genomförs systematiskt från botten och upp till anfangen parallellt på båda sidor kan den fungera som grovtätning för takhålen om inträngningen är så stor att man får ett överlapp i de största sprickorna, dvs. en inträngning av halva spännvidden, ca. 7 m, i 100 µm sprickan.

I taket måste ett rimligt överlapp skapas mellan injekteringshål, ca 1,5 m. I verkligheten går inte bruket raka vägen mellan borrhålen utan slingrar sig fram i kanaler i sprickplanen. Det gör att den teoretiska inträngningen bör vara klart större än halva hålavståndet.

Cementinjektering (denna måste kontrolleras mot verklig reologi för bruket)

En kontroll av inträngningen för cementinjektering görs som referens. I denna förutsätts ett stabilt bruk med plasticerare baserat på IC 30. Följande injekteringsparametrar antas:

Brukets flytgräns $\tau_0 = 1,4$ Pa
 Binghamviskositet $\mu_g = 0,02$ Pas
 Injekteringsövertryck $\Delta p = 2,5$ MPa

Den kritiska inträngningen gäller för den minsta injekterbara sprickan, $b_{min} = 0,1$ mm. Teoretisk maximal inträngning i denna är:

$$I_{max} = \left(\frac{\Delta p}{2\tau_0}\right) \cdot b_{min} = 89 \text{ m}$$

Den karakteristiska injekteringstiden för detta är:

$$t_0 = \frac{6\Delta p \cdot \mu_g}{\tau_0^2} = 2551 \text{ min}$$

Då en inträngning av 7 m fordras ger detta en relativ inträngning i en 100 mm spricka av $I_D = 89/7 = 0,0784$. Om inträngningsfunktionerna i Gustafson & Stille⁴ (2005) ger detta en dimensionlös injekteringstid av $t_D = 0,001$ och en injekteringstid av $t_{inj} = t_D \cdot t_0 = 25$ min.

Injektering med silica-sol

Den följande beräkningen utgår från den silica-sol vi har mest erfarenhet av, Meyco MP320. Givetvis kan andra soler användas, men det fordrar att man noggrant bestämmer deras reologi och stelningsegenskaper. Geltiden bör väljas så lång att solen kan spridas tillräckligt långt för att täta mellan injekteringshål. I detta föreslår vi en blandning, som ger en upplevd geltid (bestämd med bägarmetoden) till ca 41 min. Detta innebär ett accelerator-gelförhållande för 10 % NaCl av ca 1:6.

De styrande parametrarna för silica-sol är dels viskositeten och gelningstiden. Stelning och inträngning behandlas i Bilaga 2, Härledning av inträngningsfunktion för Silica sol (Newtonvätska) i en spricka.

Medlets startviskositet $\mu_0 = 0,0055$ Pas
 Gelninduktionstid $t_G \approx 1056$ s = 14 minuter
 Injekteringsstryck $\Delta p = 2,5$ Mpa
 Borrhålsradie $r_w = 0,028$ m (56 mm borrhål)
 Kritisk spricköppning $b_{cr} = 14$ µm

För inträngningsberäkningen definieras:

$$\text{Referensinträngningen } I_G = b \sqrt{\frac{\Delta p \cdot t_G}{6 \cdot \mu_0}} = 3,5 \text{ m}$$

Max-min inträngningen för en stelrande silica-sol i ett tvådimensionellt sprickplan kan sedan approximativt beräknas som:

$$I = 0,45 I_G = 1,6 \text{ m}$$

För ett fullgott injekteringsresultat bör man injektera till minst halva geltiden, eller mer än 21 minuter. Denna dimensionering ger ett teoretiskt överlapp som är större än halva borrhålsavståndet. Detta bör ge den säkerhetsmarginal, som våra försök visat att man bör ha. Detta kan minskas antingen genom att sänka injekteringstrycket något, som här är valt att vara samma som för cementinjekteringen, eller att korta geltiden. Då målet är att minska droppläckaget tror vi att det kan vara förnuftigt att överdimensionera något och minska injekteringstrycket om erfarenheterna visar att man överträffar målen eller om injekteringsmängderna skulle bli orimligt stora. Att korta geltiden gör injekteringsprocessen mer känslig för störningar och bör vidtas först när organisationen är väl intrimmad.

Praktiskt genomförande

Före injekteringen av varje skärm utförs vattenförlustmätningar på alla hål. Vid dessa används ett övertryck över vattentrycket av högst 2 bar. Mätningarna bör ske, dels för att det är ett försök som genomförs och goda data behövs för att det skall kunna utvärderas väl, dels bör man göra dessa förmätningar i båda tunnelrören för att man direkt skall kunna jämföra berget i båda på ett bra sätt. Efter injektering utförs minst fyra kontrollhål placerade mellan de borrhål i taket som gett högst vattenförlust eller där hålsamband konstaterats vid vattenförlustmätningen (split spacing). I väggarna utförs två kontrollhål på samma sätt. Kontrollhålen skall vara en (1) m kortare än injekteringshålen. Alla kontrollhål vattenförlustmäts. Därefter injekteras/pluggas kontrollhålen med cement eller silica sol.

Mätning av inläckaget till tunnelavsnittet bör ske på samma sätt som i övriga delar av tunneln. *(Hur detta sker i dag måste klarläggas)*

Sammanfattning av injekteringsförloppet

1. Borrning av skärm enligt Ritning 1-532 373/4060 A.
2. Vattenförlustmätning i alla borrhål ($\Delta p = 2$ bar under 5 min per hål)
3. Injektering med cement (*Recept detaljbestäms efter mätning av bruksegenskaper*) systematiskt från centrum sula upp till anfang. Designtryck, $\Delta p = 2,5$ MPa över vilande vattentryck som hålles under hela injekteringsförloppet. Injektering under 25 minuter i varje hål. Om tidigare givna mängdkriterier överskrids avbryts injekteringen i hålet. (*Dessa måste klarläggas*)
4. Injektering med silica sol: Meyco MP320 eller motsvarande, geltid: $t_{gel} \approx 41$ min. Injekteringsövertryck $\Delta p = 2,5$ MPa. Injektering under minst 21 min i varje hål.
5. Borrning av kontrollhål, ≥ 6 st, i split spacing mellan mest vattenförande hål enligt ovan
6. Vattenförlustmätning i kontrollhålen ($\Delta p = 2$ bar under 5 min per hål)
7. Injektering av kontrollhålen med cement eller silica sol enligt tidigare.
8. Salvborrning, sprängning, utlastning etc. vid godkänt resultat.

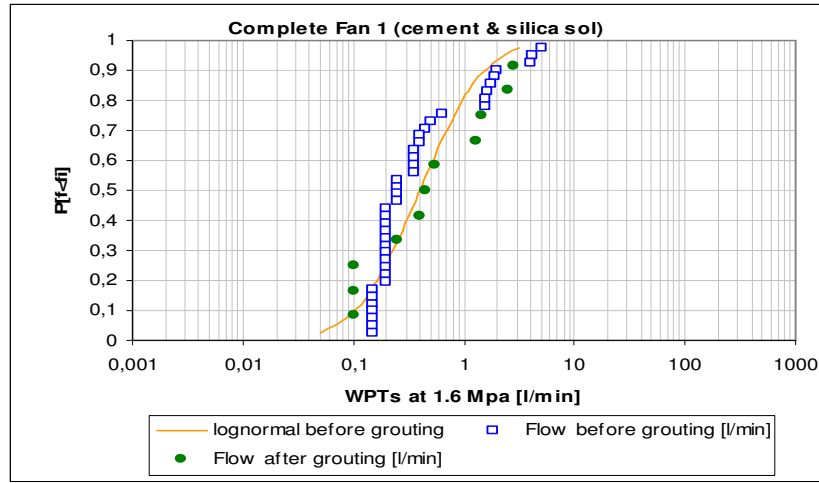
¹ Moye D G 1967: Diamond drilling for Foundation Exploration. Civil Engineering Transactions, April 1967, pp. 95 – 100.

² Kozubowski T, Meerschaert M, Gustafson G, in prep: A new stochastic model for fracture transmissivity assessment. Insänd till Hydrogeology Journal (2006).

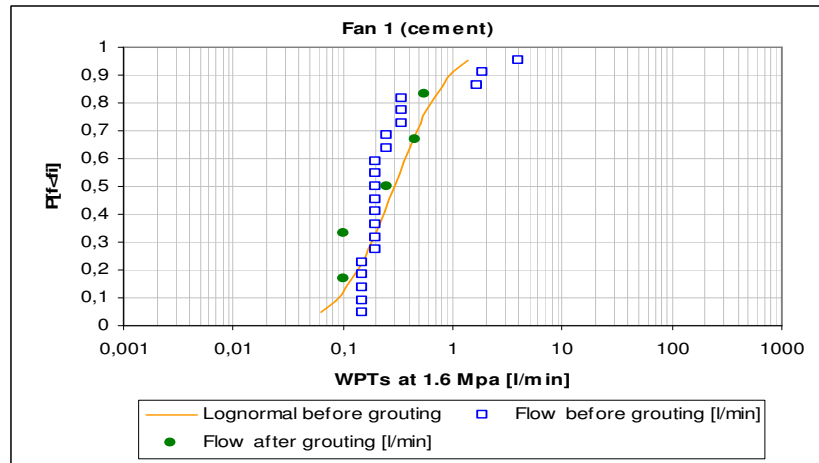
³ Gustafsson G, Fransson Å, Funehag J, Axelsson M 2004: Ett nytt angreppssätt för bergbeskrivning och analysprocess för injektering, V-byggaren 4:2004.

⁴ Gustafson G, Stille H 2005: Stop criteria for cement grouting. Felsbau 23 (2005) NR. 3.

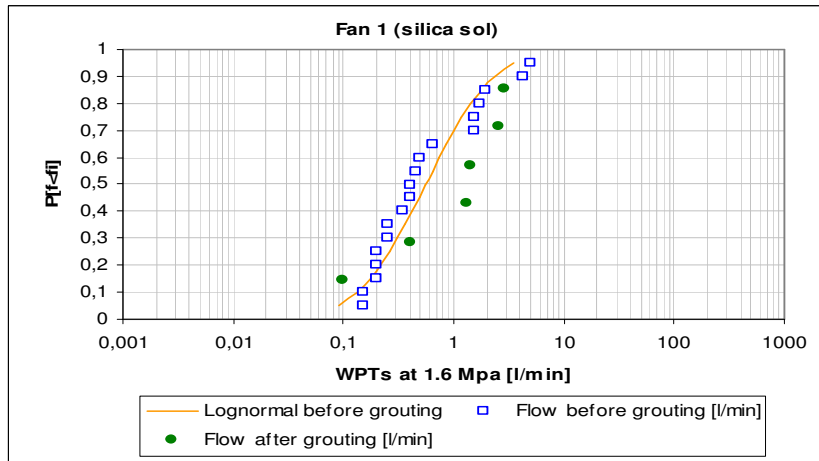
APPENDIX B: Scatter chart, from every grouted fan, which compares the WPTs results obtained from grout-holes before grouting and control-holes after grouting.



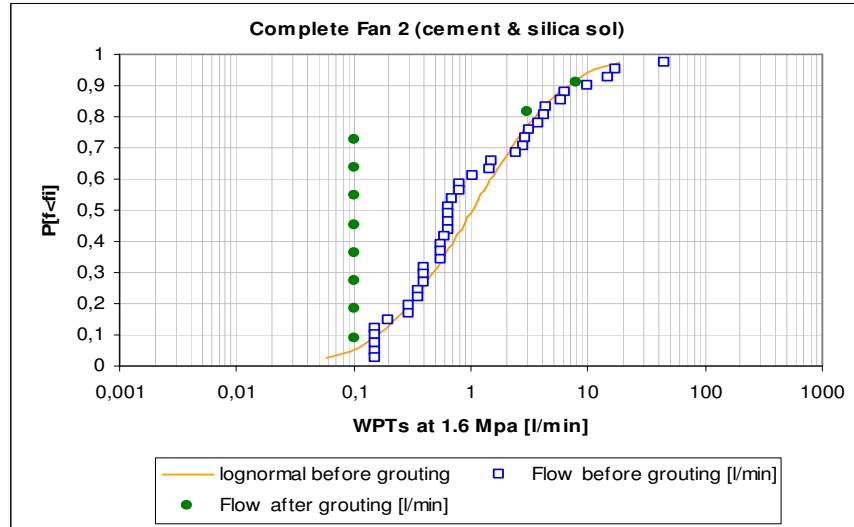
Fan1, 1.6 MPa of total pressure and 0.5 MPa of water pressure.



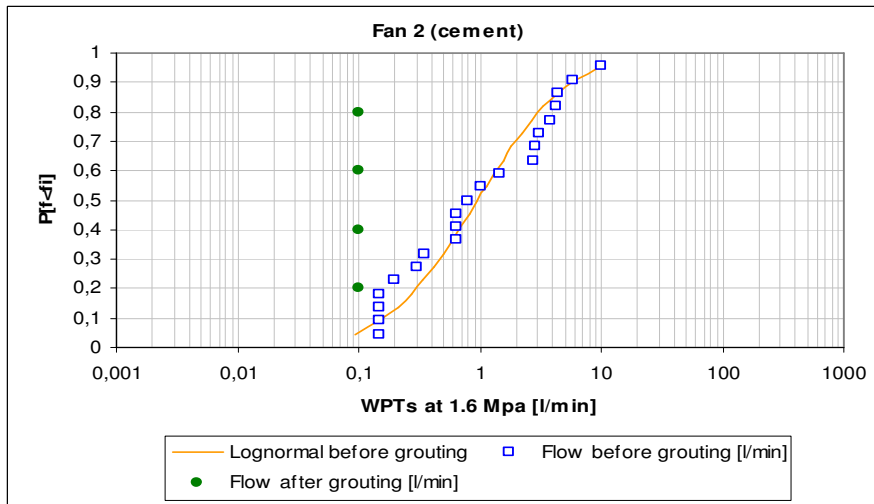
Fan 1, 5 control-holes were drilled for the cement part



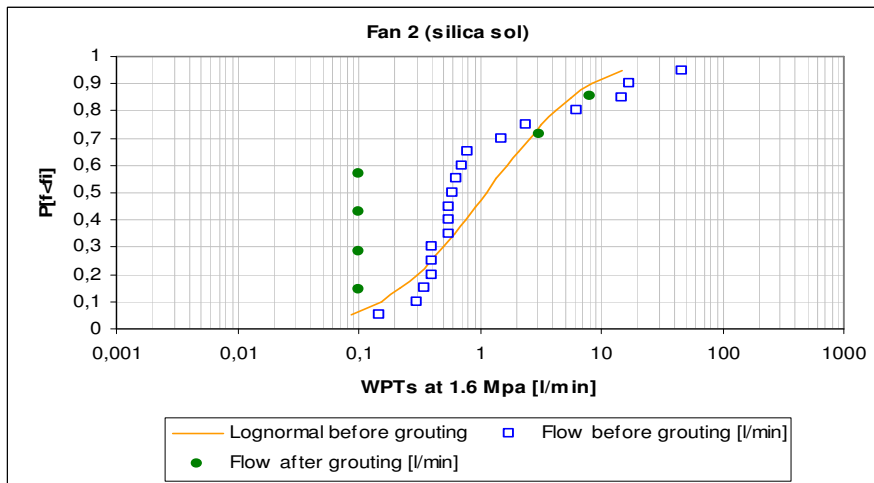
Fan 1, 6 control-holes were drilled for the silica sol part.



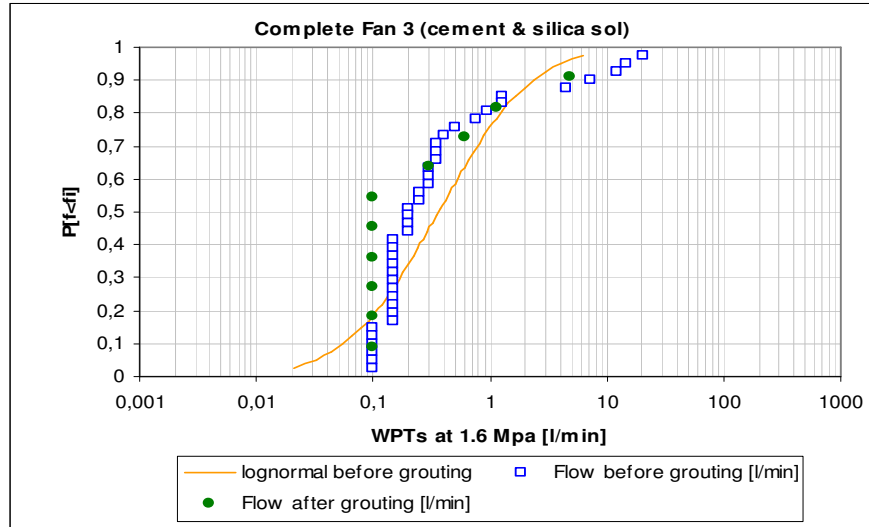
Fan 2, 1.6 MPa of total pressure and 0.5 MPa of water pressure



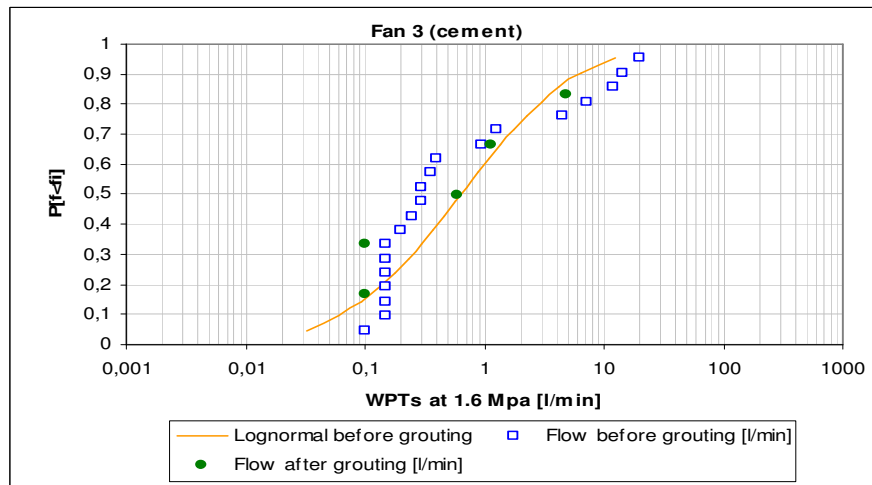
Fan 2, 4 control-holes were drilled for the cement part



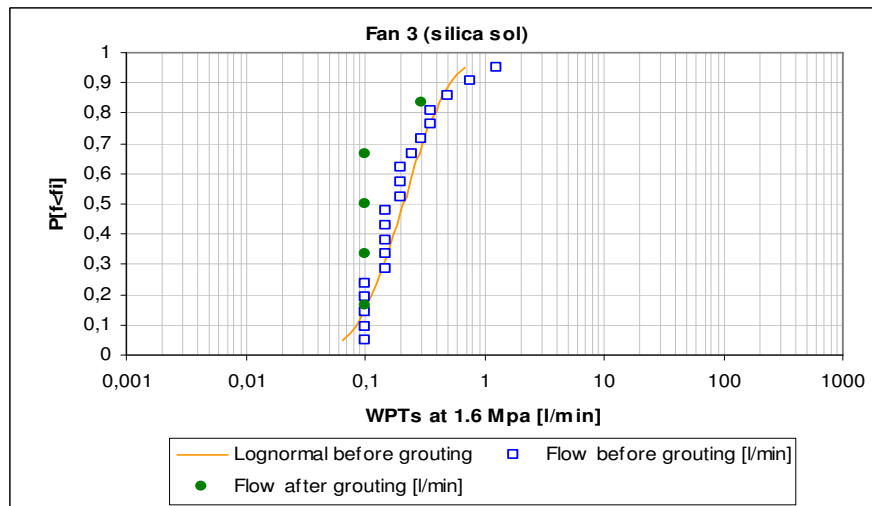
Fan 2, 6 control-holes were drilled for the silica sol part.



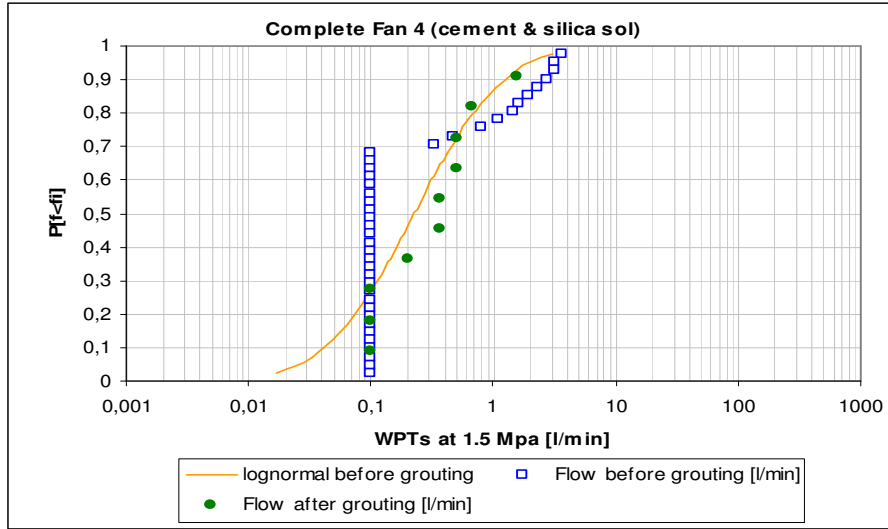
Fan 3, 1.6 MPa of total pressure and 0.5 MPa of water pressure



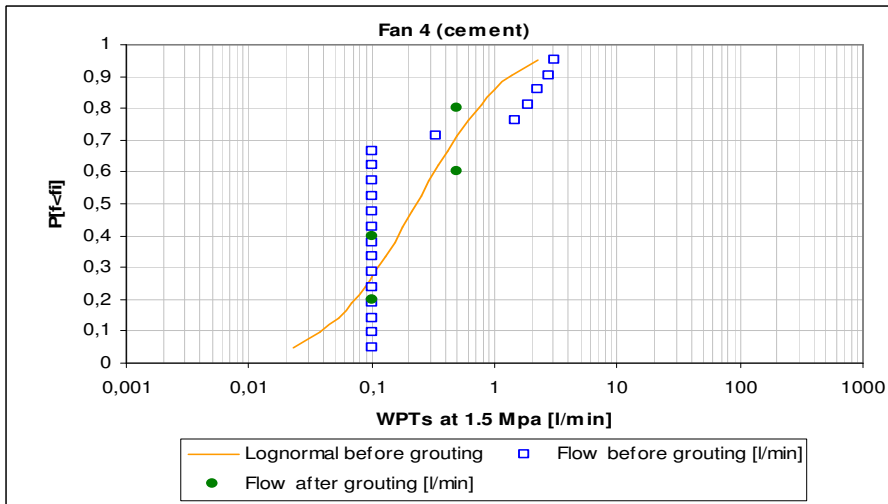
Fan 3, 5 control-holes were drilled for the cement part



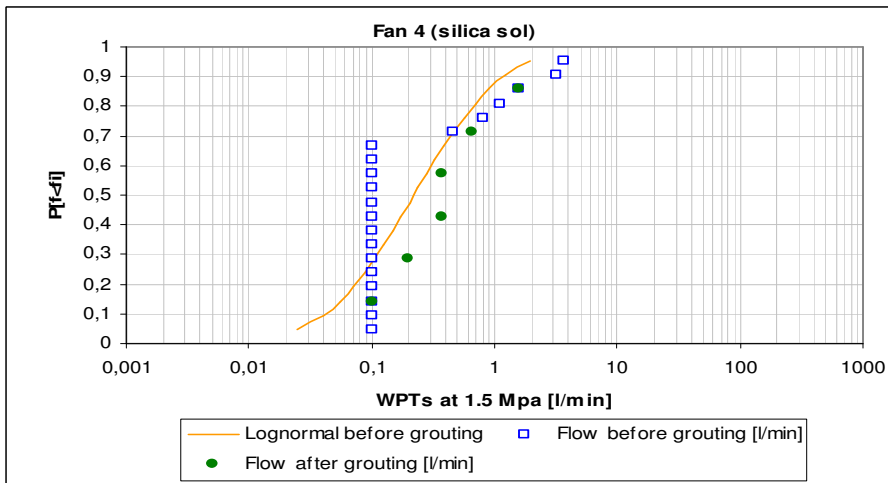
Fan 3, 5 control-holes were drilled for the silica sol part.



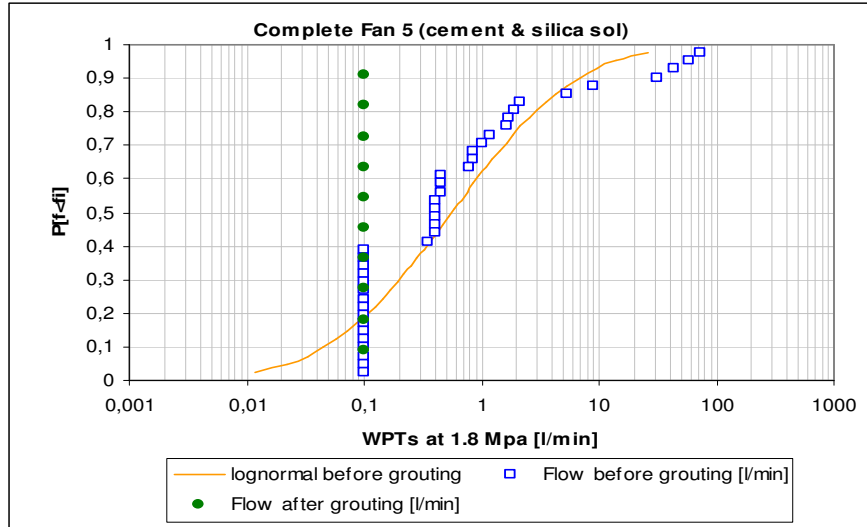
Fan 4, 1.5 MPa of total pressure and 0.5 MPa of water pressure



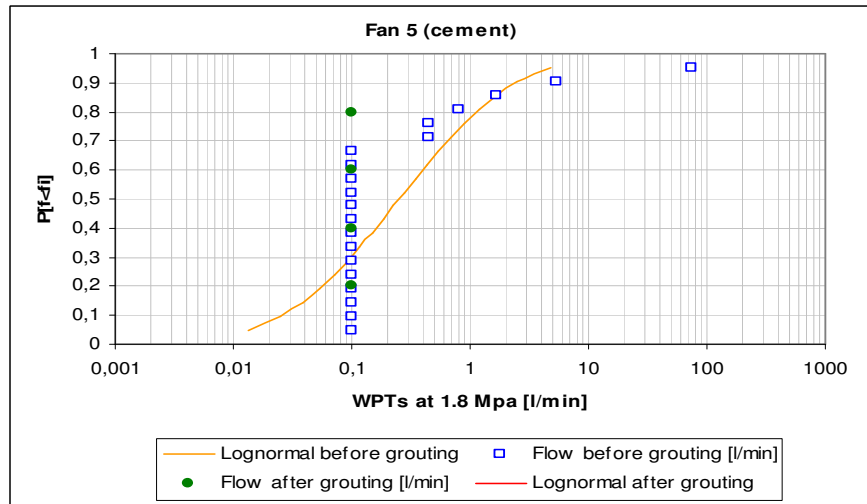
Fan 4, 5 control-holes were drilled for the cement part



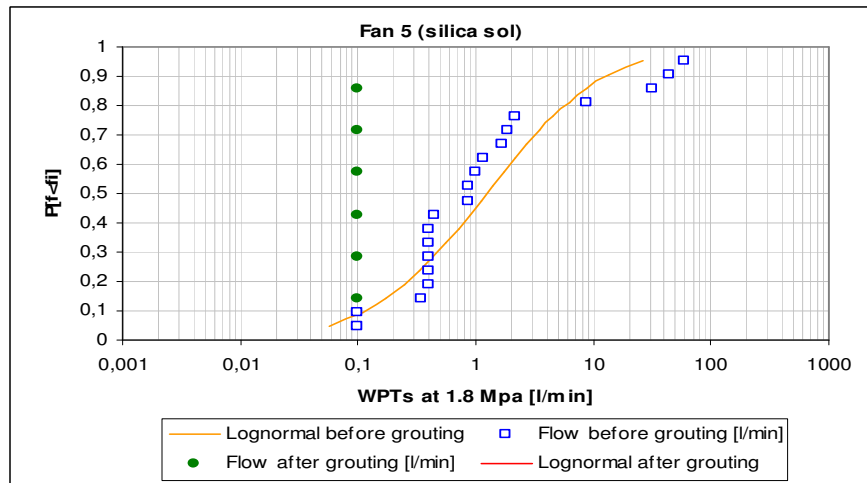
Fan 4, 6 control-holes were drilled for the silica sol part.



Fan 5, 1.8 MPa of total pressure and 0.5 MPa of water pressure

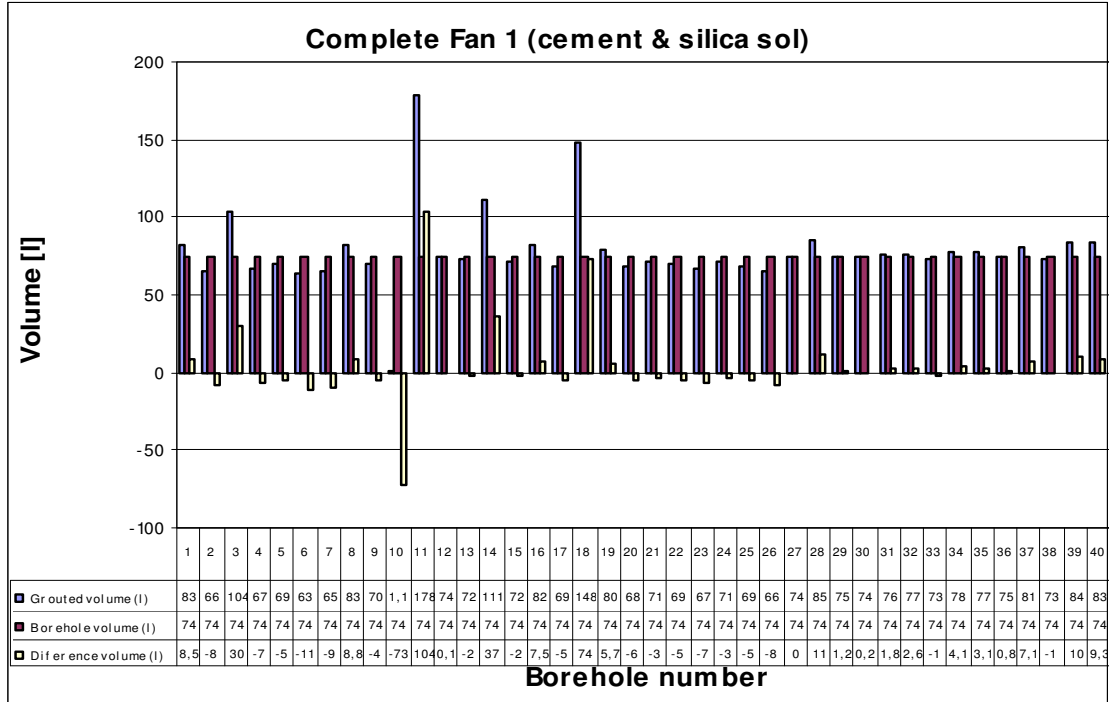


Fan 5, 5 control-holes were drilled for the cement part;

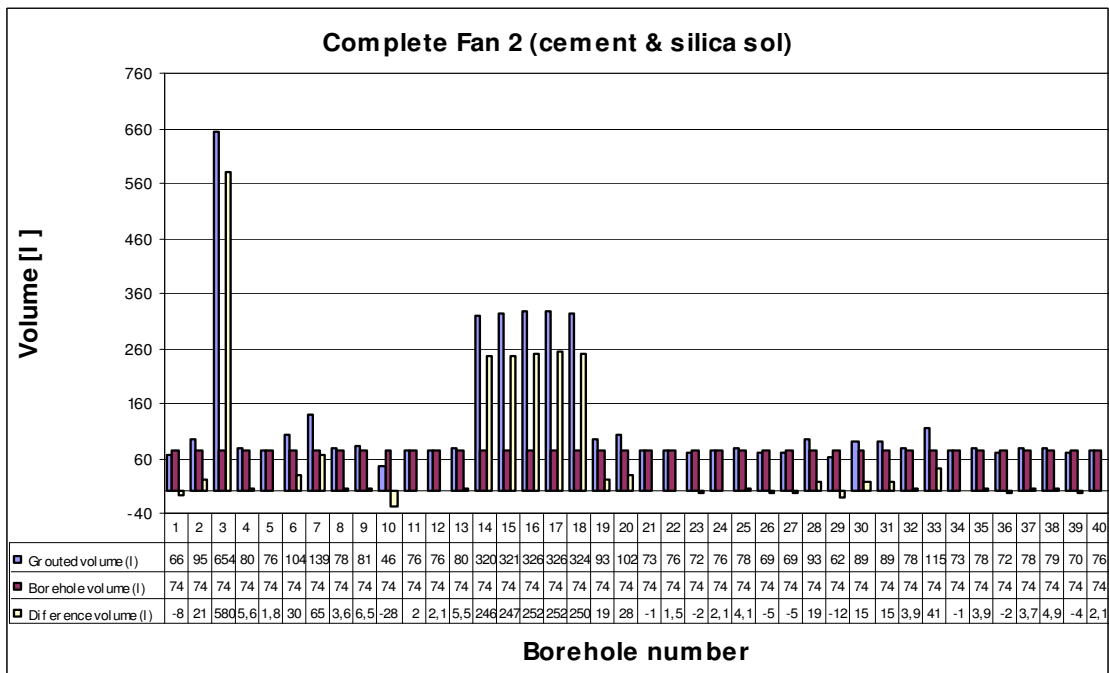


Fan 5, 5 control-holes were drilled for the silica sol part.

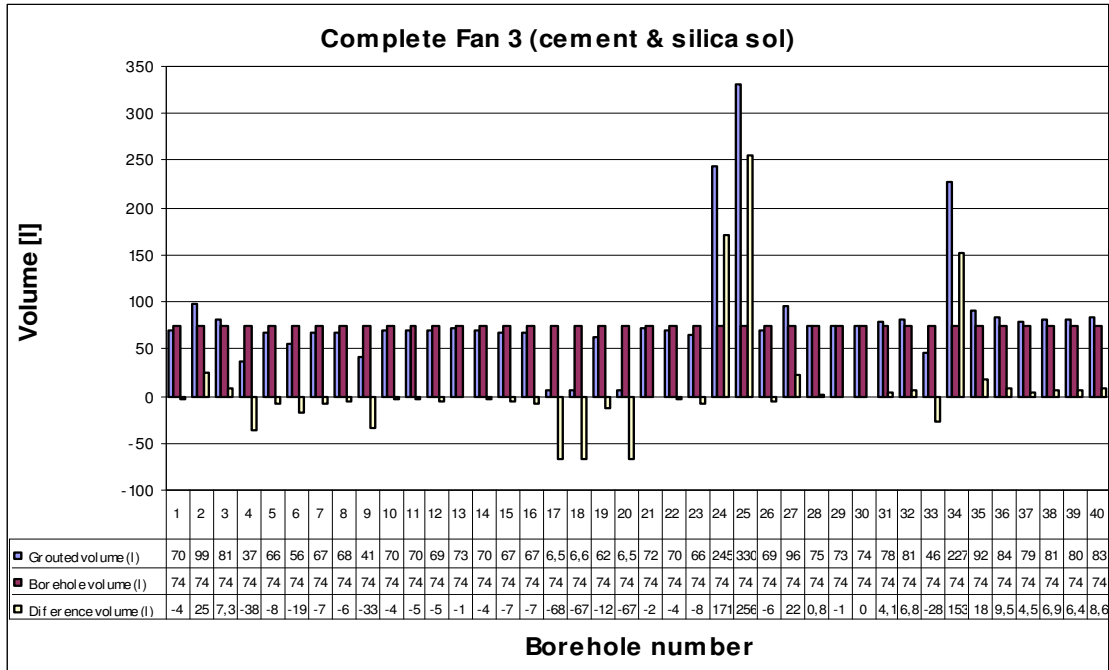
APPENDIX C: Column chart, from every grouted fan, which compares the grout-hole volume and the volume of grout injected in each grout-hole; it also shows the difference.



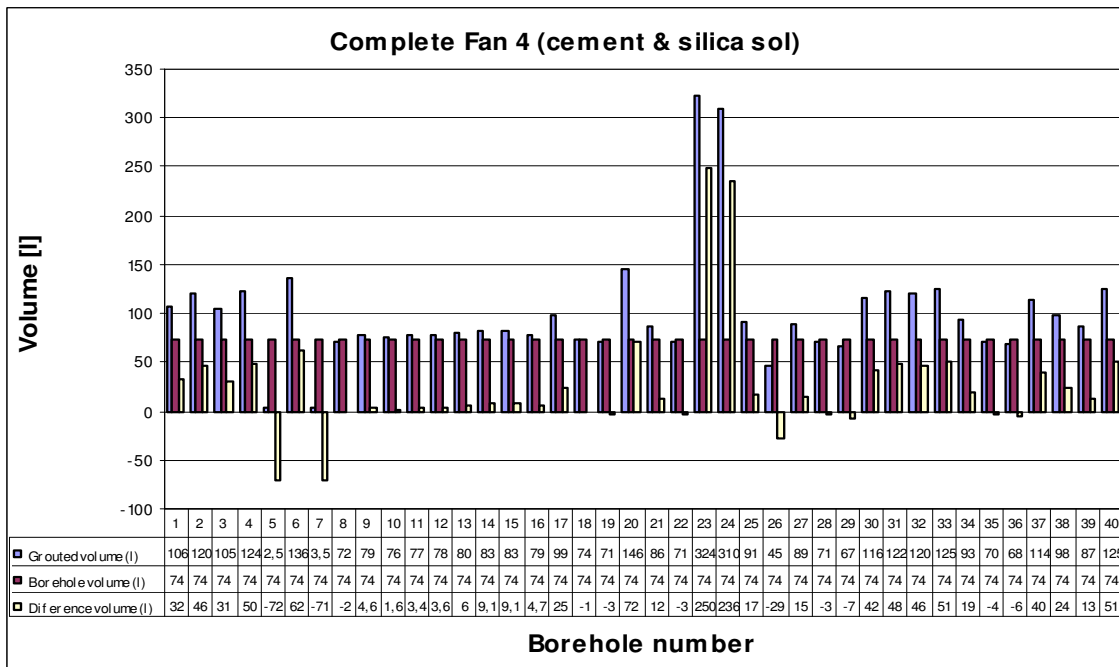
Fan 1



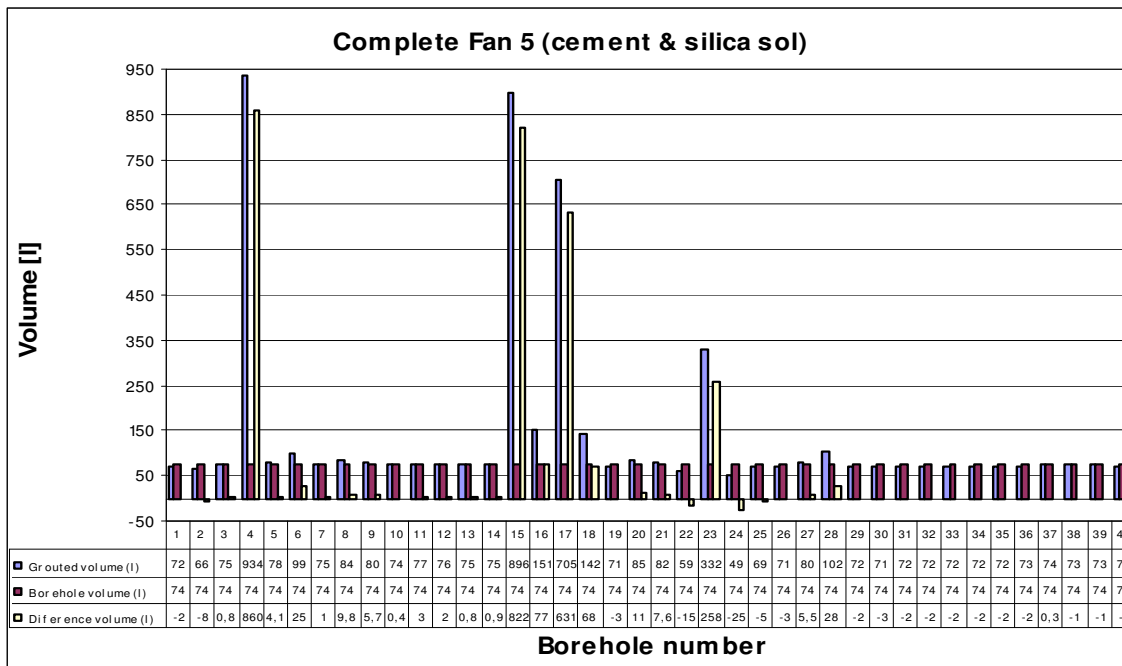
Fan 2



Fan 3

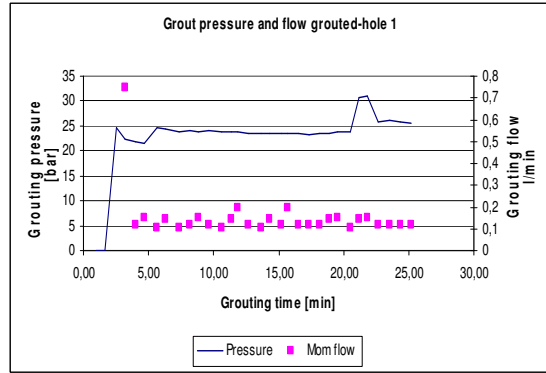
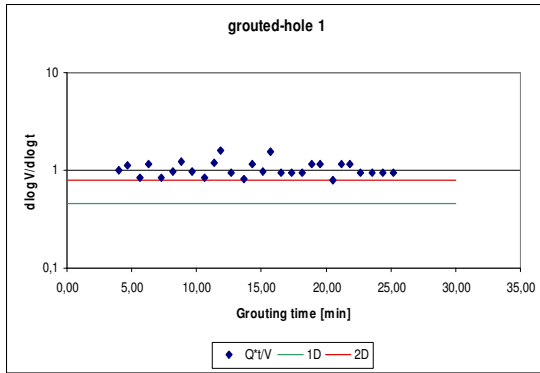


Fan 4

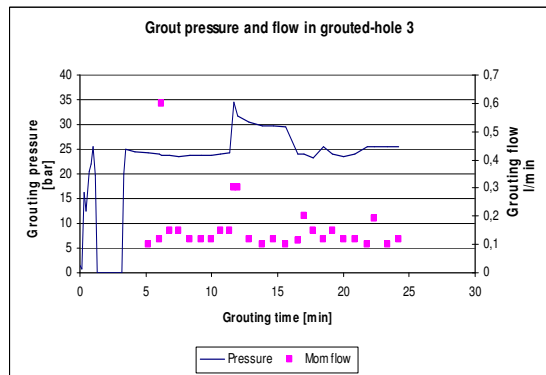
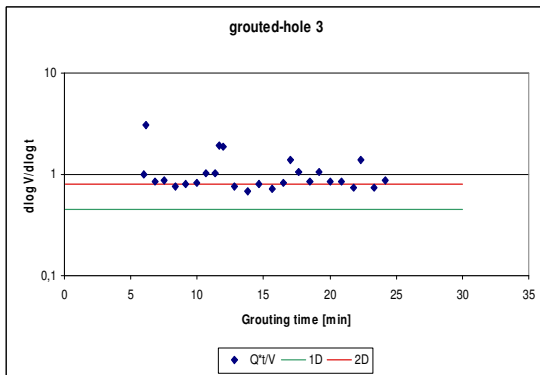


Fan 5

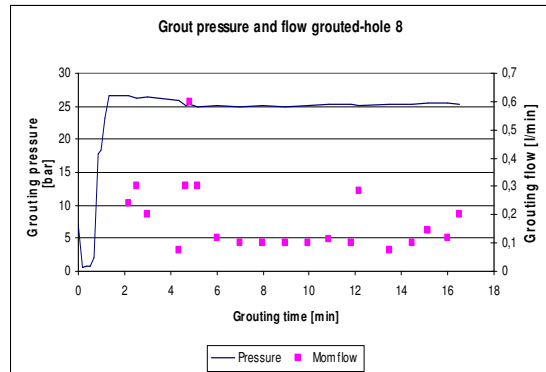
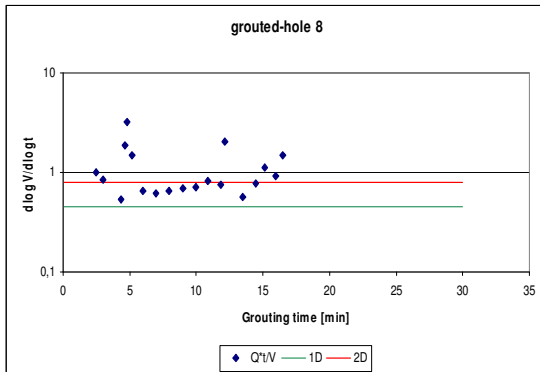
APPENDIX D: Grouted-holes charts showing the pressure and flow trend over time, accumulated volume trend over injected time and, diagnostic curves.



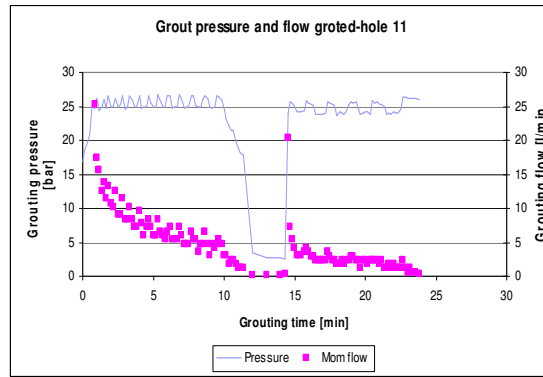
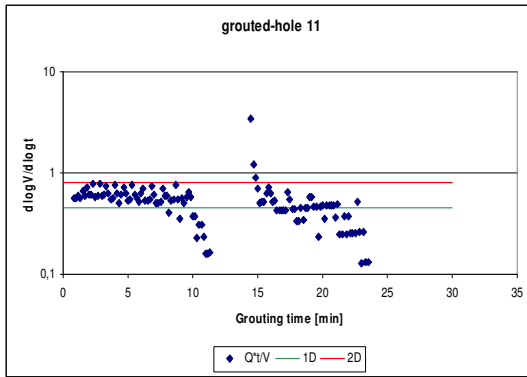
Fan 1, grouted-hole 1



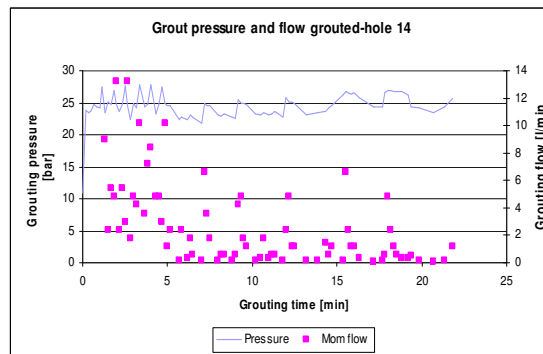
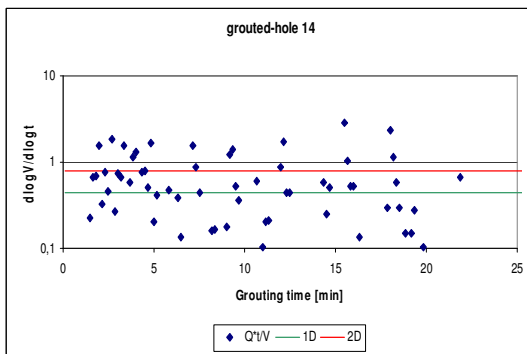
Fan 1, grouted-hole 3



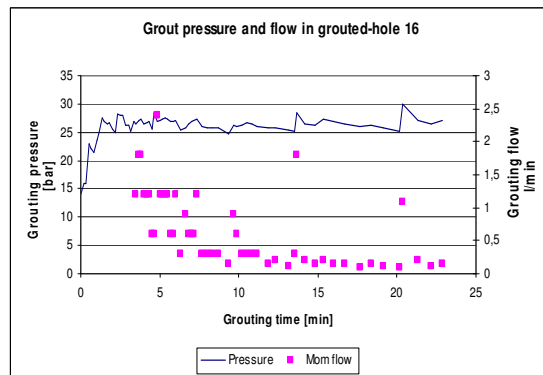
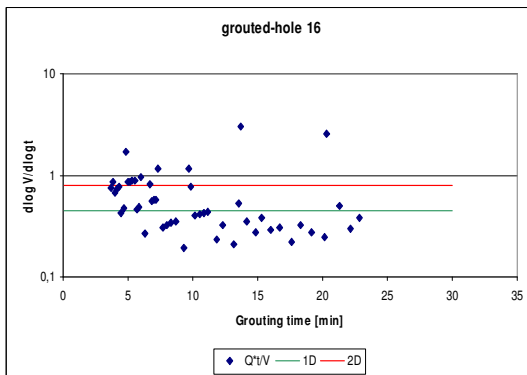
Fan 1, grouted-hole 8



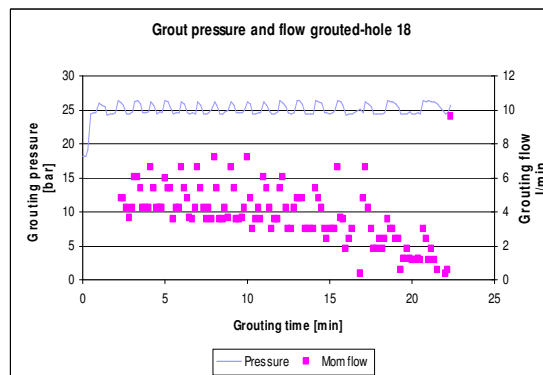
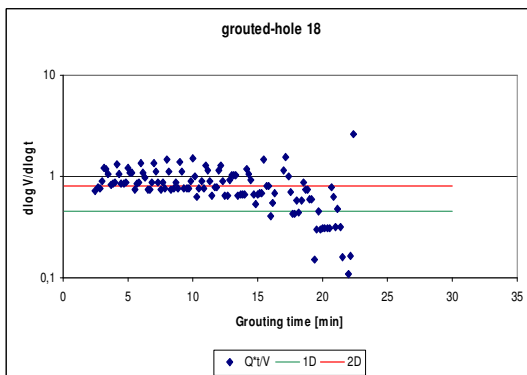
Fan 1, grouted-hole 11



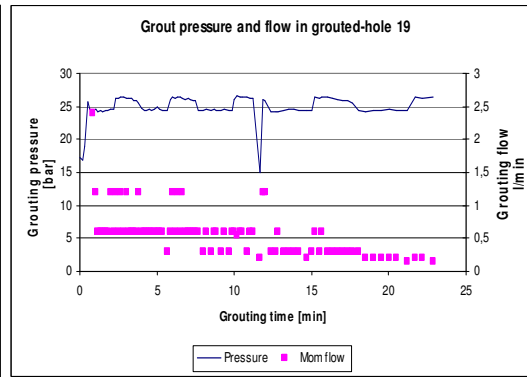
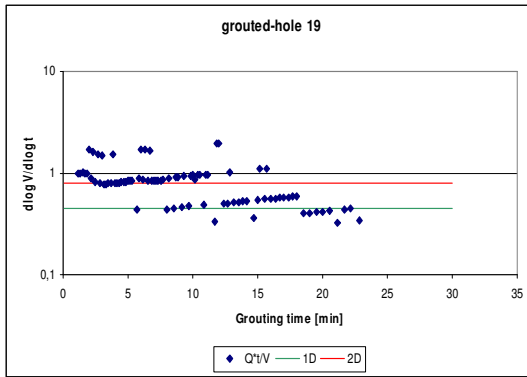
Fan 1, grouted-hole 14



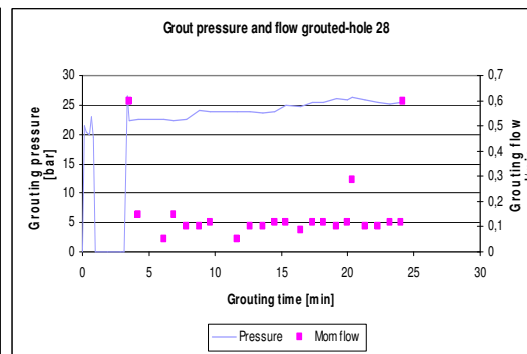
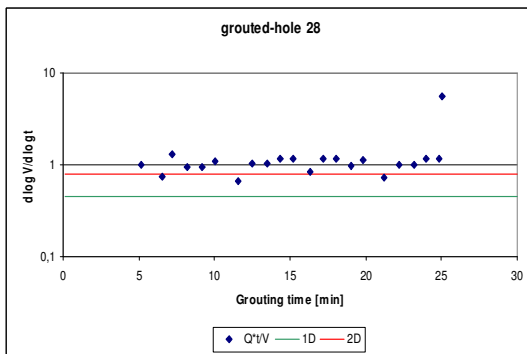
Fan 1, grouted-hole 16



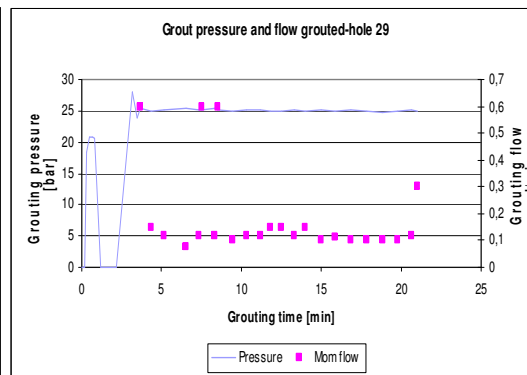
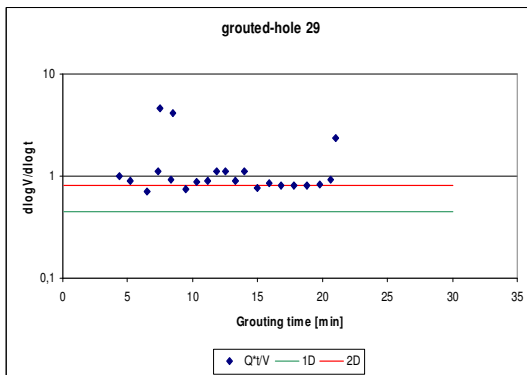
Fan 1, grouted-hole 18



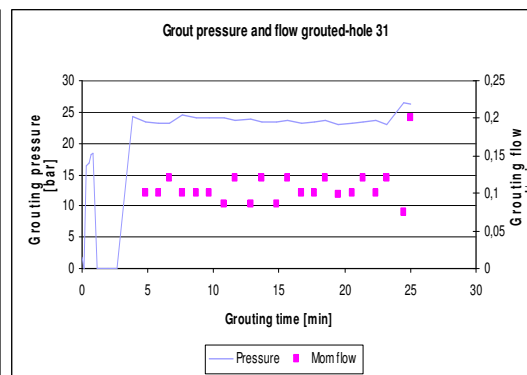
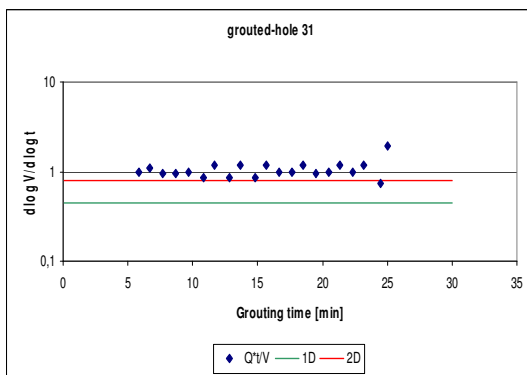
Fan 1, grouted-hole 19



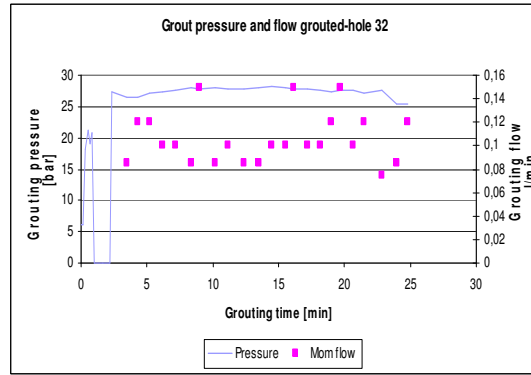
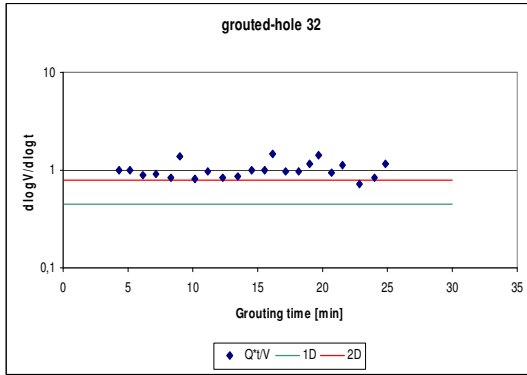
Fan 1, grouted-hole 28



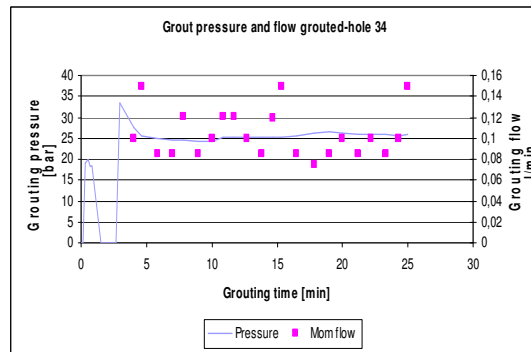
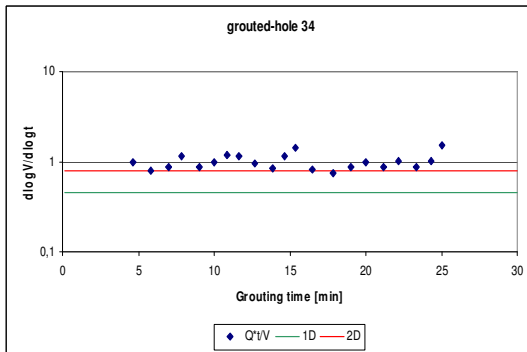
Fan 1, grouted-hole 29



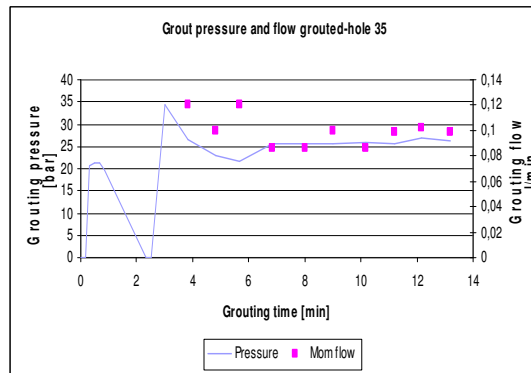
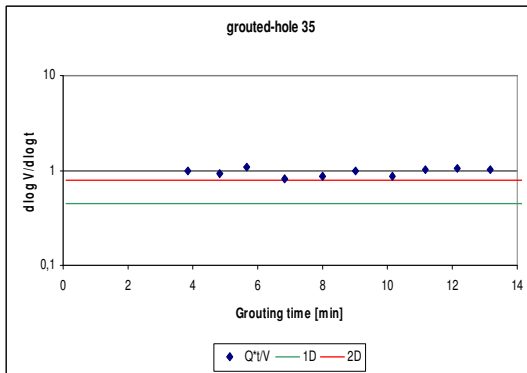
Fan 1, grouted-hole 31



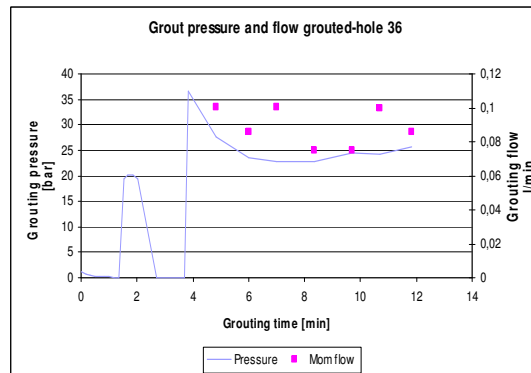
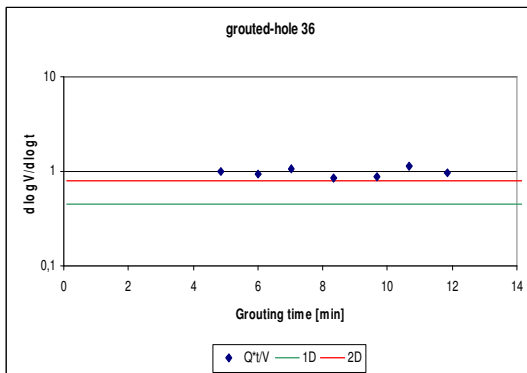
Fan 1, grouted-hole 32



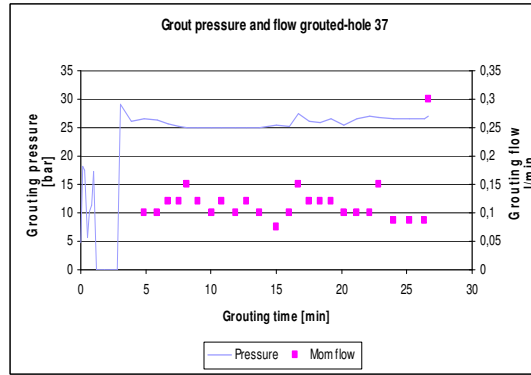
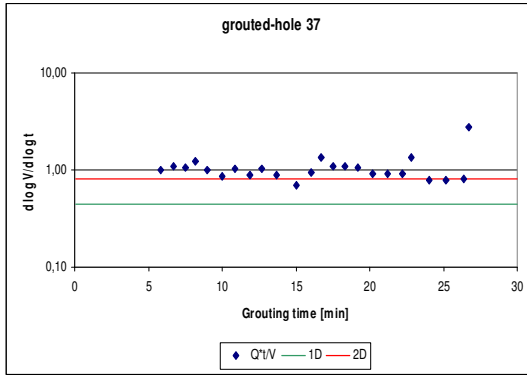
Fan 1, grouted-hole 34



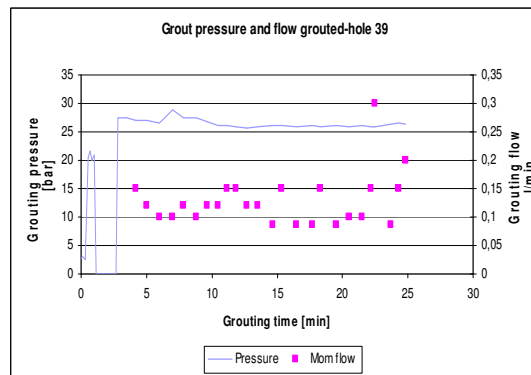
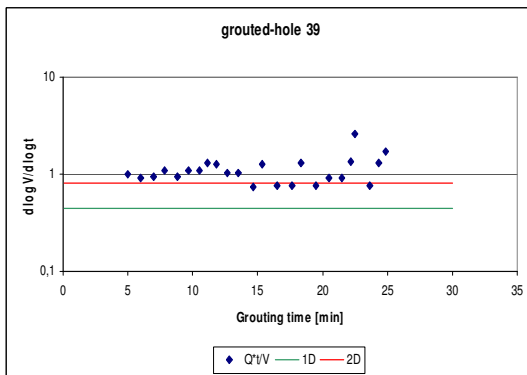
Fan 1, grouted-hole 35



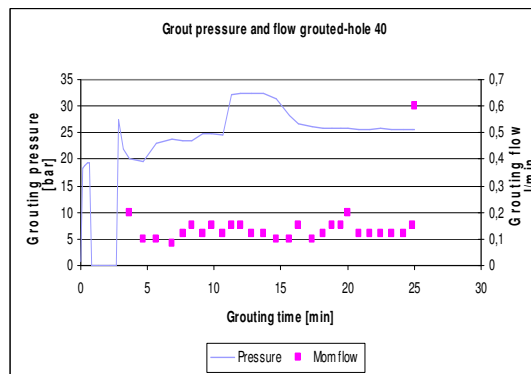
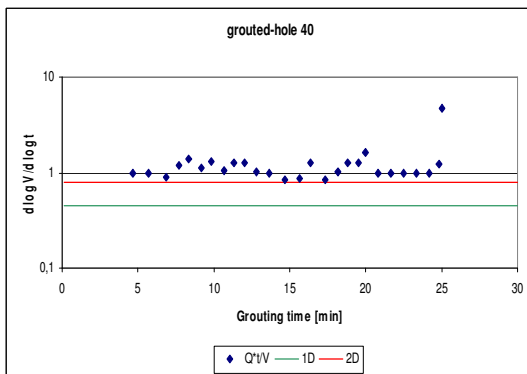
Fan 1, grouted-hole 36



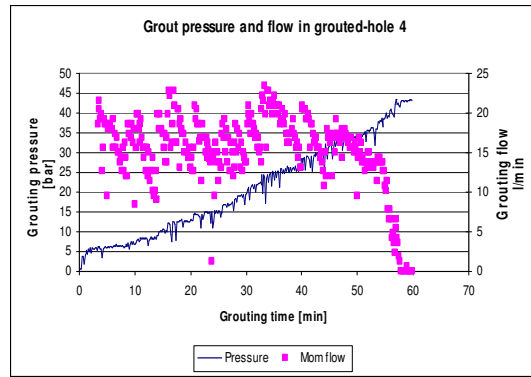
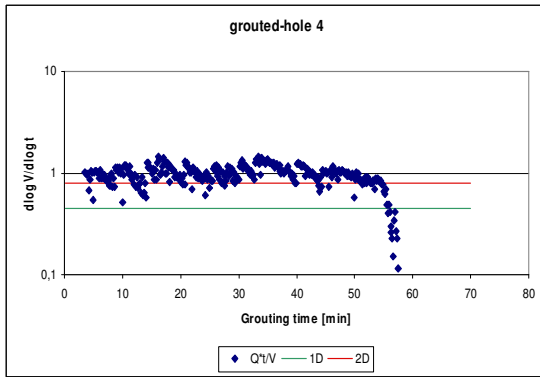
Fan 1, grouted-hole 37



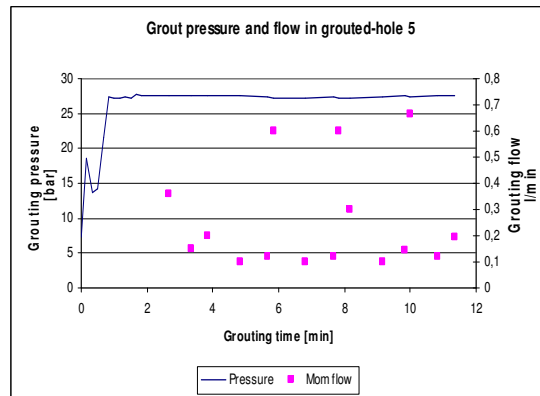
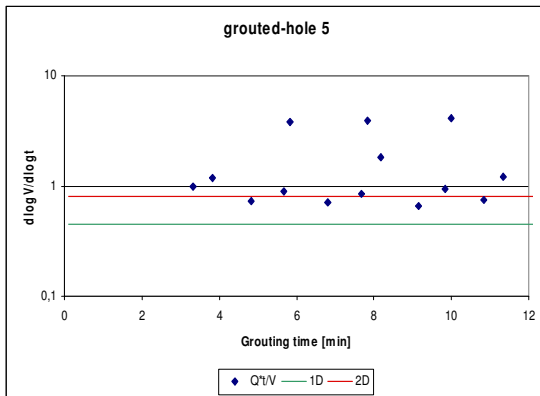
Fan 1, grouted-hole 39



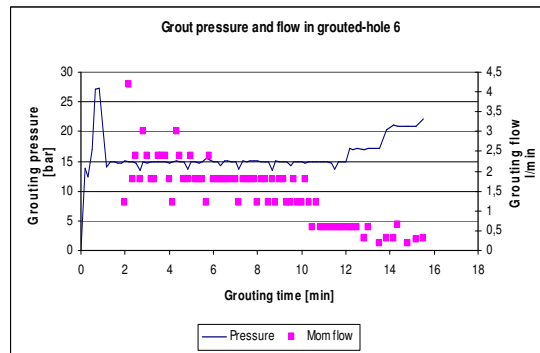
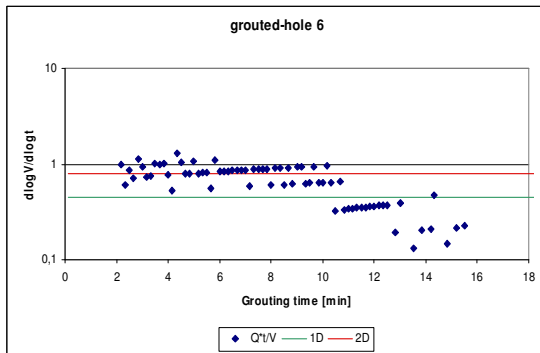
Fan 1, grouted-hole 40



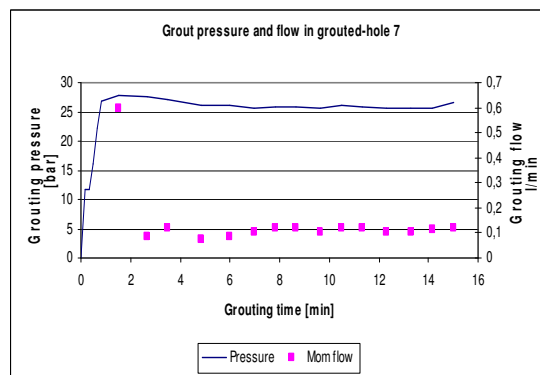
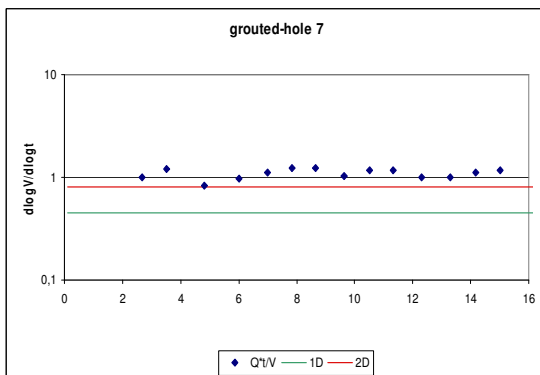
Fan 5, grouted-hole 4



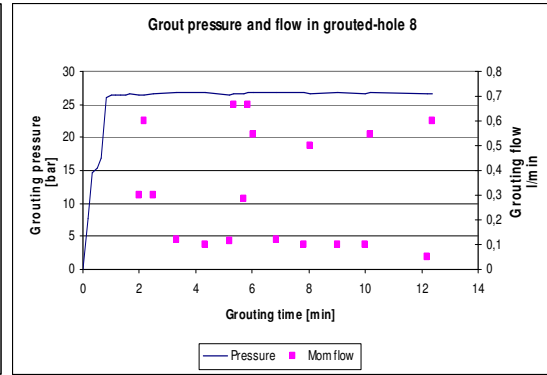
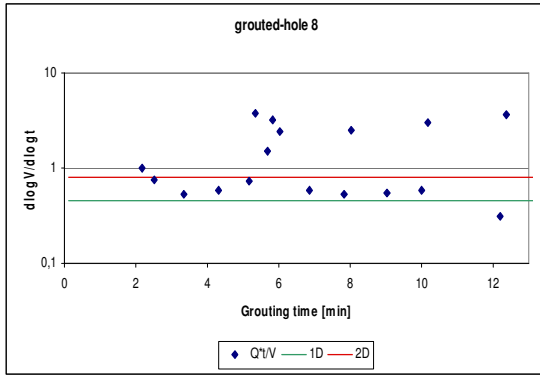
Fan 5, grouted-hole 5



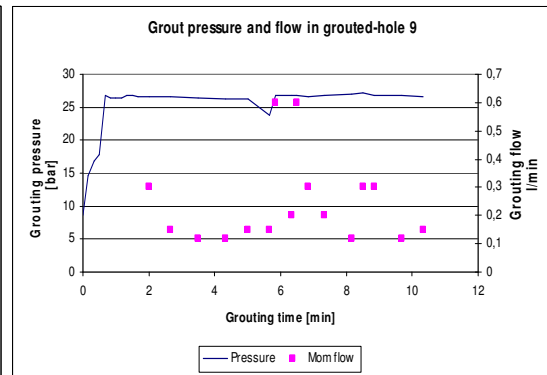
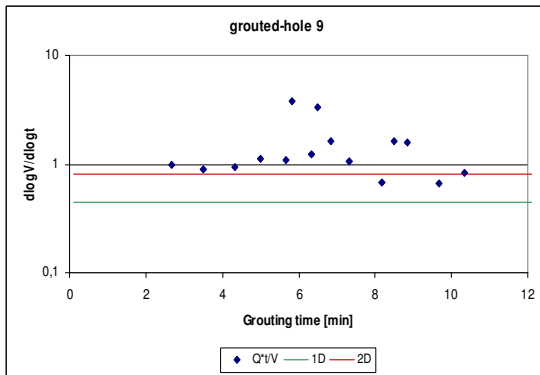
Fan 5, grouted-hole 6



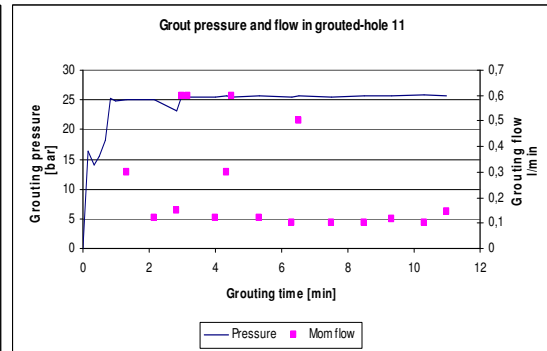
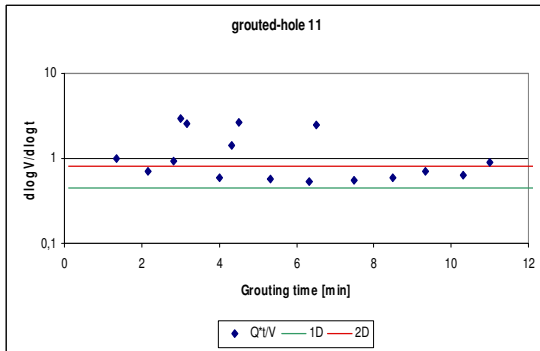
Fan 5, grouted-hole 7



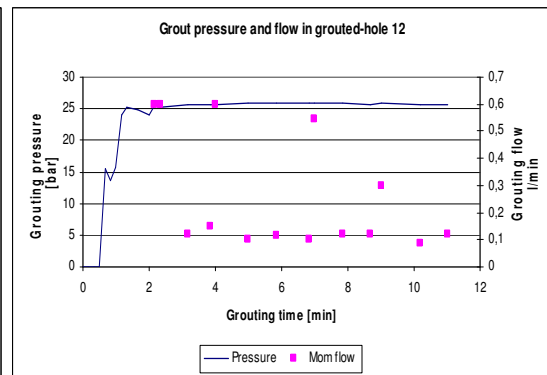
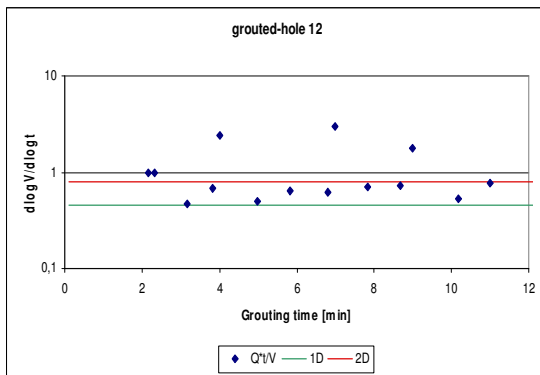
Fan 5, grouted-hole 8



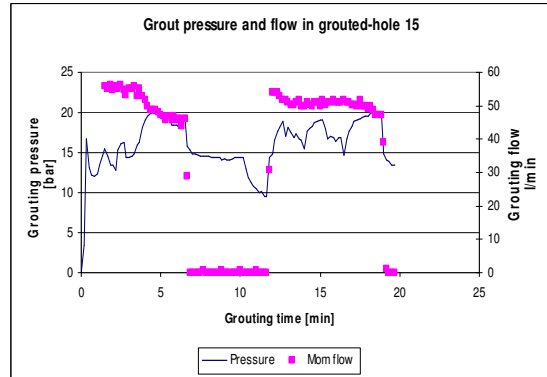
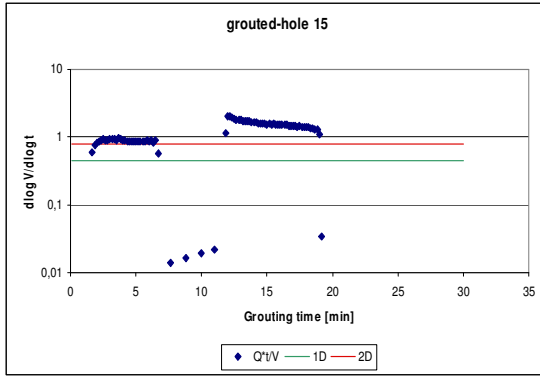
Fan 5, grouted-hole 9



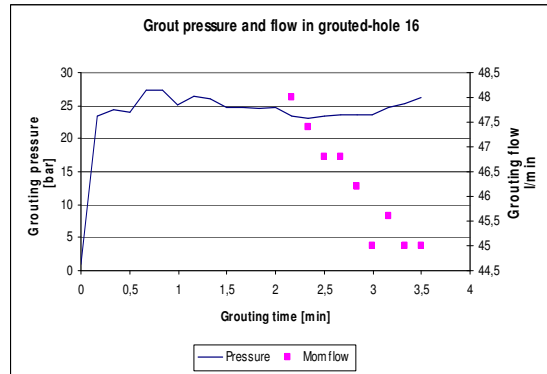
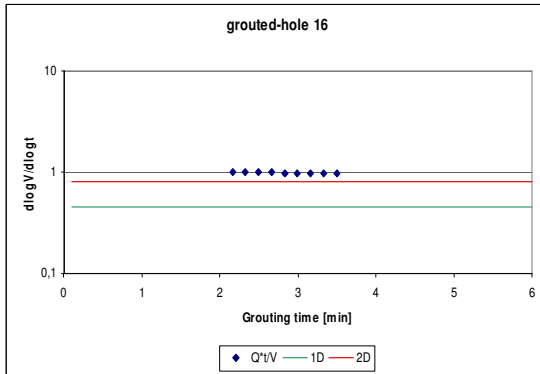
Fan 5, grouted-hole 11



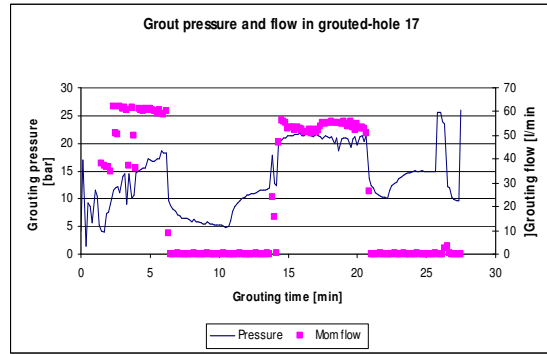
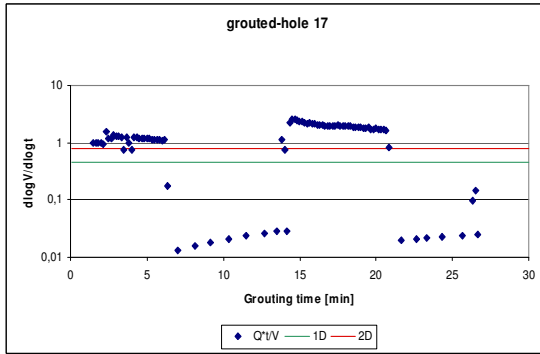
Fan 5, grouted-hole 12



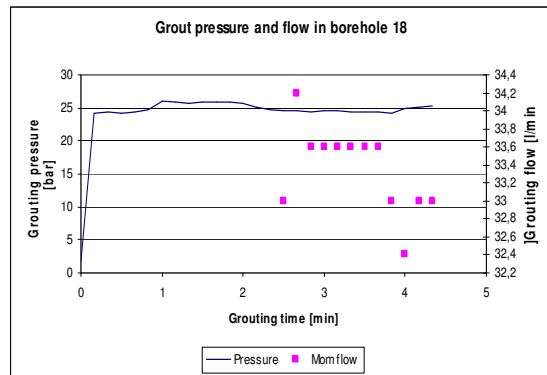
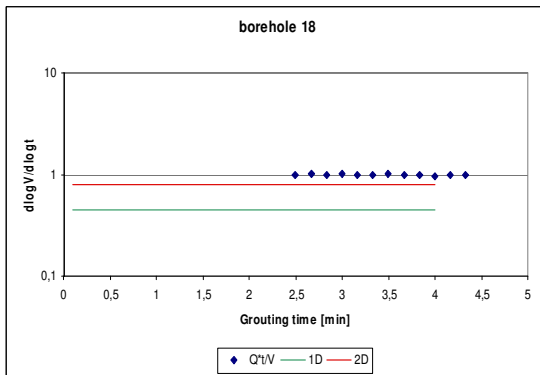
Fan 2, grouted-hole 15



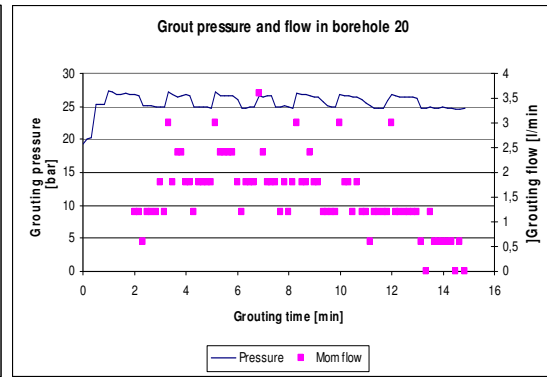
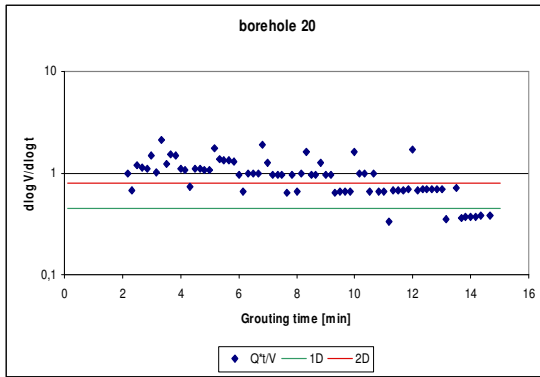
Fan 2, grouted-hole 16



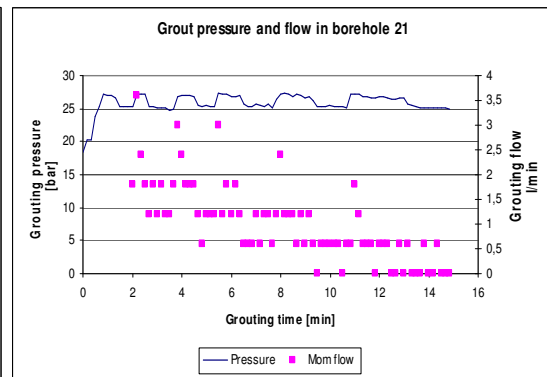
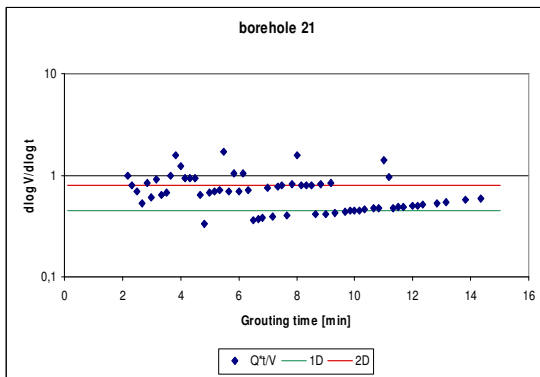
Fan 2, grouted-hole 17



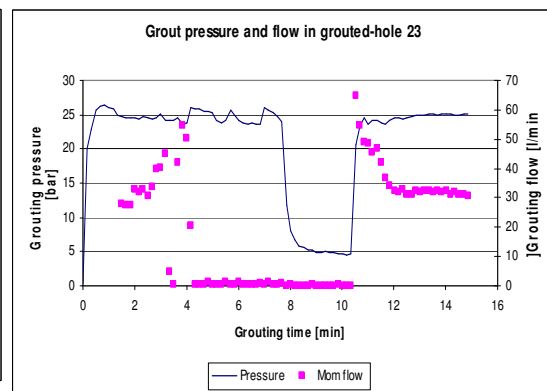
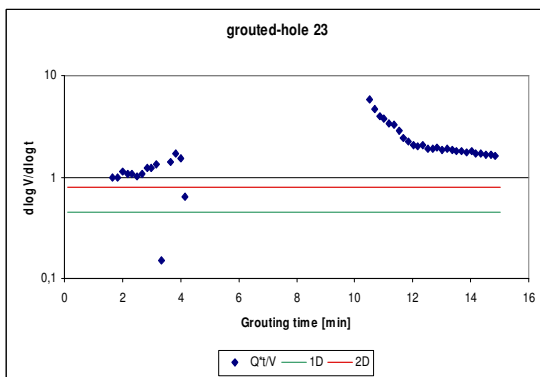
Fan 2, grouted-hole 18



Fan 2, grouted-hole 20



Fan 2, grouted-hole 21

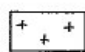
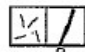



Fan 2, grouted-hole 23

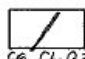
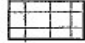


APPENDIX E: Fracture mapping of sections 436+723 to 436+637; this map has been drawn in situ by a geologist. The squares represent the respective area grouted/blasted fans. The overlap between fans is not specified. This first page is a key note to read the following pages.

BETECKNINGAR TILL GEOLOGISK KARTERING TORBACKEN - HEDE

BERGARTER (Huvudbergart markeras ej med raster)

	Röd gnejs
	Pegmatit
	Grönsten

TEKTONIK

	Spricka. Ca, Cl, Qz = sprickfyllnad kalcit, klorit, kvarts
	Vittrat berg
	Blockigt berg (berggrund mellan tektoniska zoner)
	<u>Krosszon</u> K1-K5 (bredd > 10 cm)

- K1 Skivigt berg (skivornas tjocklek \geq 10 cm).
 K2 Tunnskivigt berg (skivornas tjocklek < 10 cm).
 K3 Blockigt berg (blockens kantlängd \geq 20 cm).
 K4 Delvis sönderkrossat berg (blockens kantlängd < 20 cm).
 K5 Helt sönderkrossat berg.
 S1 Sekundärläkt krosszon.

Leromvandling

- L1 Lermineraliserad spricka (bredd \leq 10 cm).
 L2 Lermineraliserad spricka (bredd > 10 cm).
 L3 Zon med leromvandling i alla sprickor.
 L4 Zon med allmän leromvandling.

Vatteninläckning

- ∨ Fukt – svagt dropp.
 √ Kraftigt dropp – svagt rinnande vatten.
 √ Kraftigt rinnande vatten.

ÖVRIGT



Utfall till sprickyta.

TORBACKEN - HEDE
 SPÅRTUNNEL B
 PÅSLAG HÅLTORP
 GEOLOGISK KARTERING 436+700-750

Datum

Sign

Ritn.nr 44

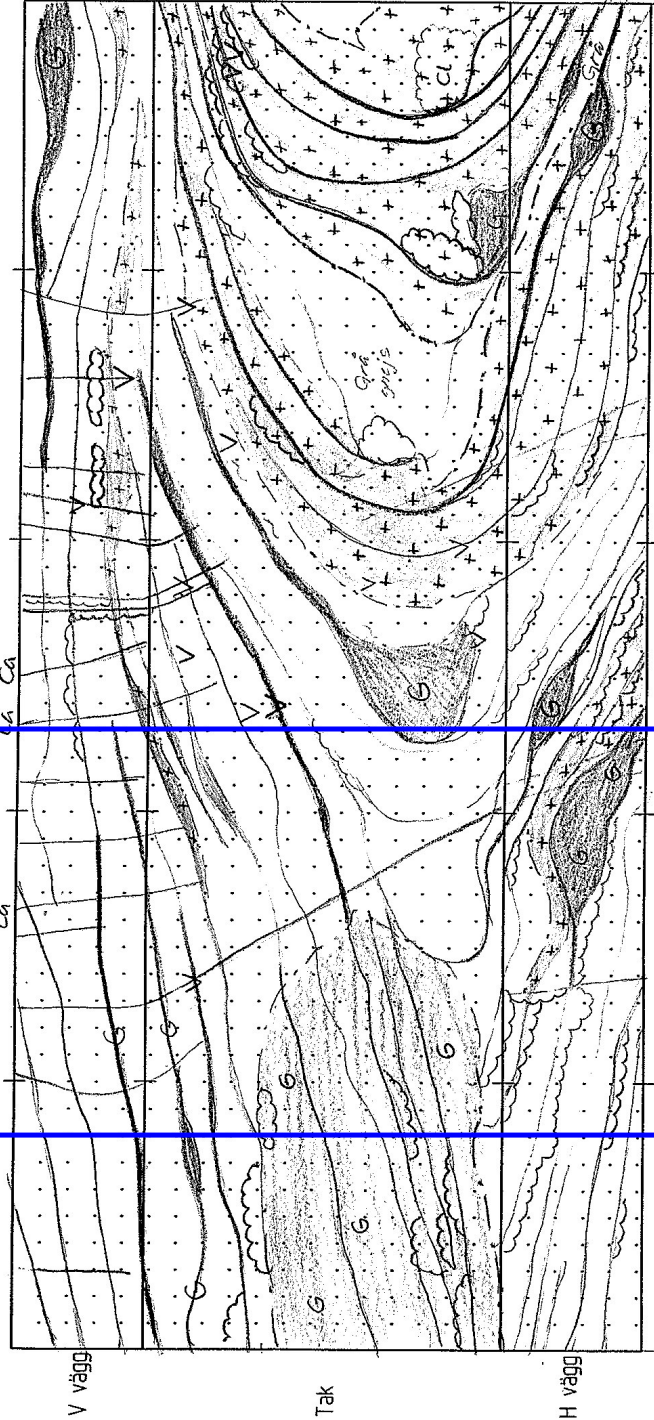
Skala 1:200

Excavation direction

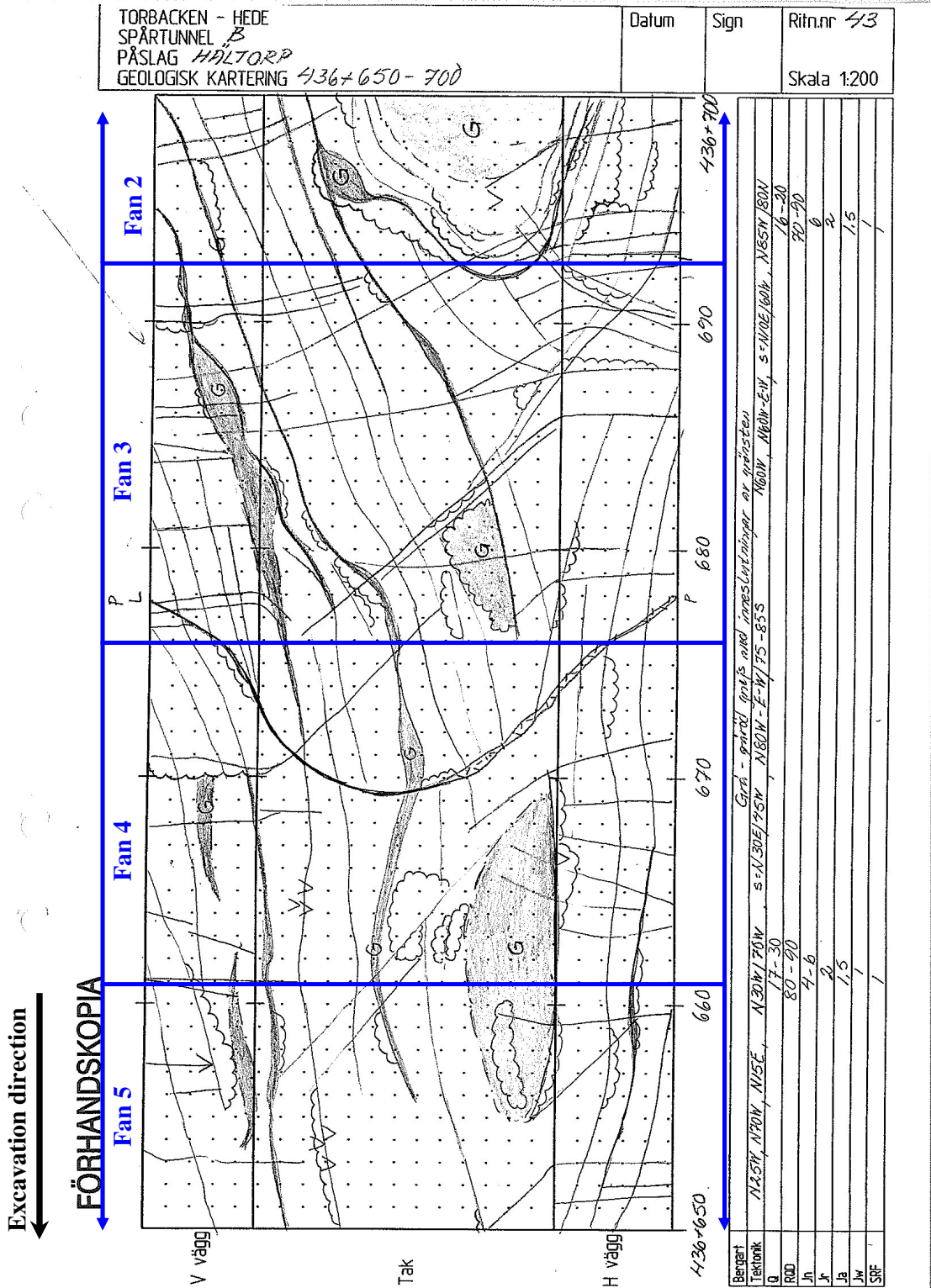
FÖRHANDSKOPIA

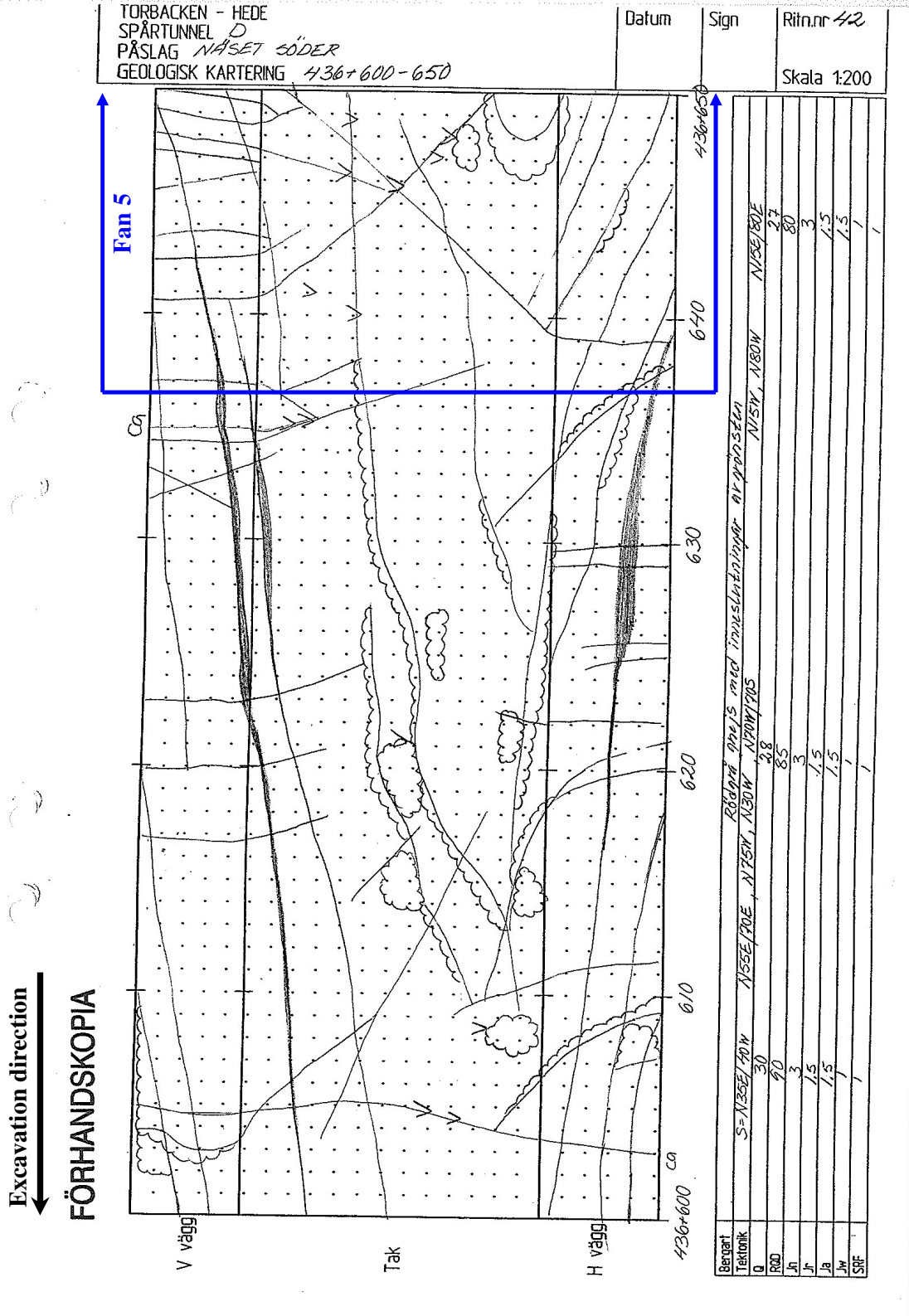
Fan 2

Fan 1

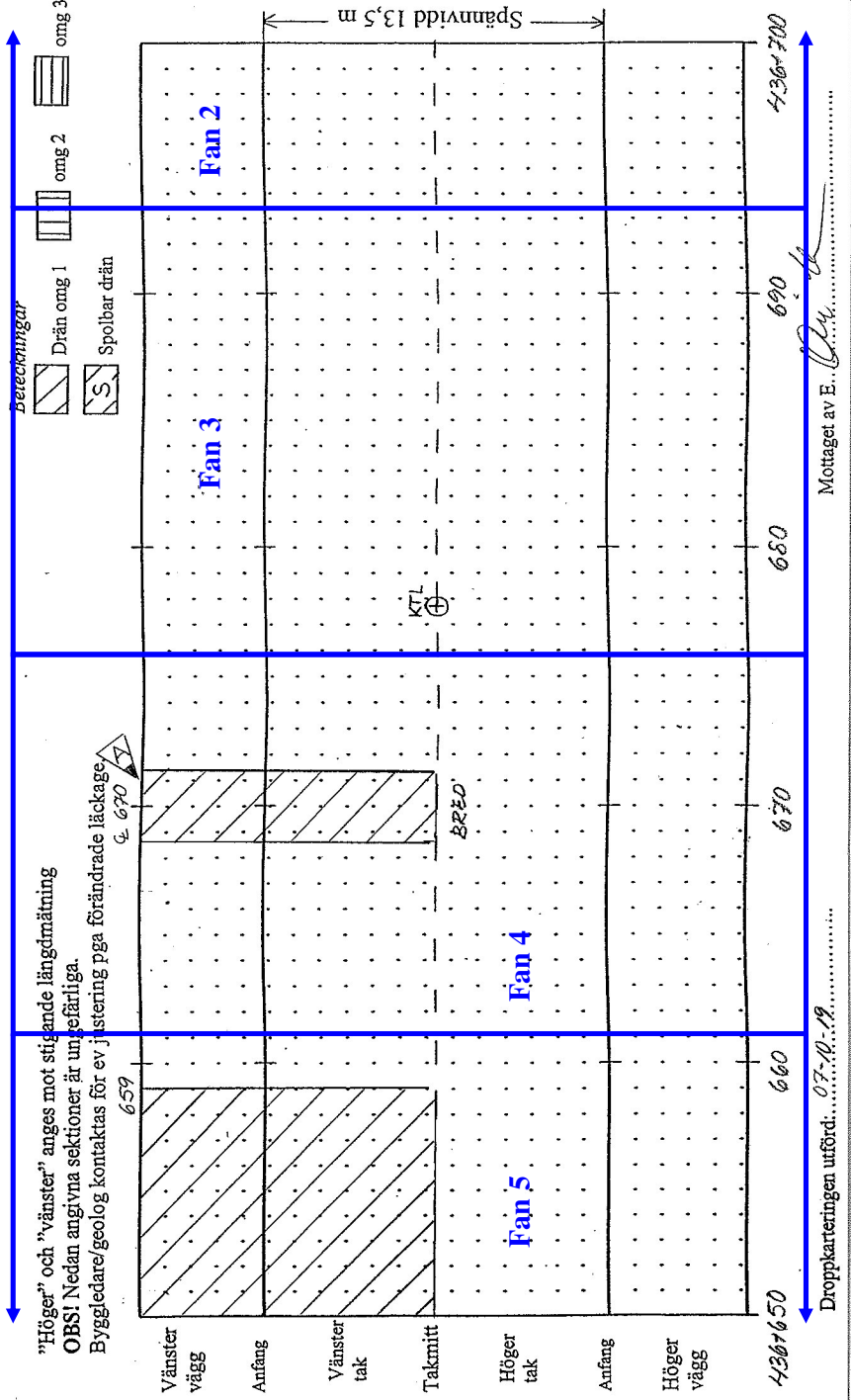


Bergart	Teckning	38	17	25	6	2	1,5	1	1	1	1
Q	Rödgrå-grå grajs med järnsulfningsar av gråsten	38	17	25	6	2	1,5	1	1	1	1
ROD	Röd och grå grajs med gråsten	85	85	85	3	2	2	1,5	1	1	1
J1		3	6	6	3	2	2	2	2	2	2
J2		2	2	2	2	2	2	2	2	2	2
J3		1,5	1,5	1,5	1,5	1,5	1,5	1,5	1,5	1,5	1,5
J4		1	1	1	1	1	1	1	1	1	1
J5		1	1	1	1	1	1	1	1	1	1
SF		1	1	1	1	1	1	1	1	1	1





TORBACKEN-HEDE, BERGTUNNEL - SPÅRTUNNEL Sid: 2(4)
 RITNING NR 43 BEST NR: 13 (omg 1)
 SKALA 1:200 DATUM: 07-09-27 Sign: MM
 SEKTION: 436/650-700 REV A 07-10-19 MM (komplettering efter utbörd efterinjicering)



TORBACKEN-HEDE, BERGTUNNEL - SPÅRTUNNEL
 BESTÄLLNING AV DRÄNER (se ritn nr 8-532 373/4062)
 SEKTION: 536 + 600 - 650

BEST NR: /3 (omg 1) Sid: / (4)

RITNING NR 42

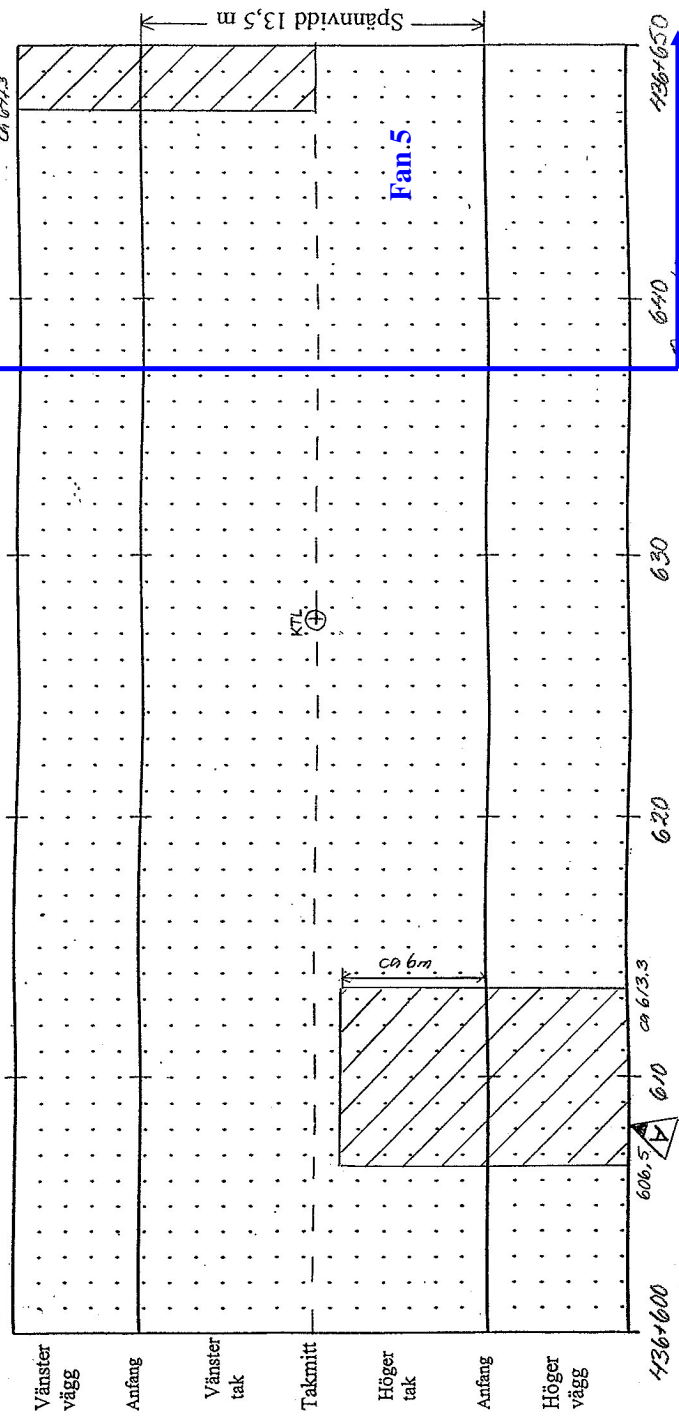
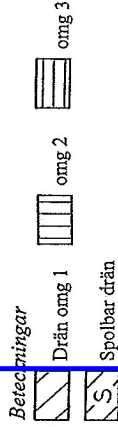
SKALA 1:200

DATUM: 07-09-27 Sign: MK

REV A 07-10-19

MK (komplettering efter utförd efterriktning)

"Höger" och "vänster" anges mot stigande längdmätning
 OBS! Nedan angivna sektioner är ungefärliga.
 Bygglédare/geolog kontaktas för ev justering pga förändrade läckage.



Mottaget av E. *[Signature]*

Droppkarteringen utförd: 07-10-19